National Technical University of Athens
School of Naval Architecture and Marine Engineering

Optimization of Ship's Bow Form
for the Added Resistance in Waves

Victor Bolbot

Diploma Thesis

Thesis Supervisor: Prof. Apostolos D. Papanikolaou
Committee Member: Associate Prof. George Zaraphonitis
Committee Member: Assistant Prof. Alexandros Ginnis

Αθήνα, Ιανουάριος 2016

Abstract

Every shipping company has a goal to reduce operational costs and increase income. One possible way to achieve that is by optimizing ship's hull in respect to calm water resistance. However, because ships seldom travel at still water conditions, it is important also to introduce the effect of the added resistance in waves.

For large ships, added resistance in waves is mainly the result of wave diffraction around the ship while the added resistance due to motions has a small contribution. The available theoretical methods at the moment find it hard to evaluate accurately the diffraction component of added resistance in short waves. This makes necessary the use of semi-empirical approach or CFD methods.

Added resistance is also important for minimization of the Energy Efficiency Design Index (EEDI). Added resistance affects the selection of suitable Sea Margin and fw correction factor, which accounts for the decrease of speed in representative sea conditions. A reduction in added resistance will affect positively the EEDI.

The development of computers during last century allowed the use of parametric models created in CAD/CAE systems for representation of hulls forms. New optimization solution techniques such as Sobol functions and genetic algorithms set up the necessary background for effective and quick optimization. All of these are present in CAESES/Friendship-Framework.

In this diploma thesis, the bow of a large tanker (KVLCC2) is optimized in terms of the added resistance in waves using CAESES/Friendship-Framework for creation of parametric model and optimization. Ship's bow is also optimized for total resistance, using Holtrop-Mennen method for estimation of calm water resistance. In the last stage, ship's bow is optimized for EEDI. The resulted maximum continuous rating of ship's main engine is compared with the minimum required power in adverse conditions.

Keywords: Added Resistance due to Waves; Added resistance in short waves; Parametric Ship Design; Hull Optimization; EEDI; CAD/CAE Systems; CAESES; Friendship-Framework; Holtrop-Mennen; Minimum Required Power in Adverse Conditions

Abstract In Greek

Ο στόχος της κάθε ναυτιλιακής εταιρείας είναι η ελαχιστοποίηση των εξόδων διαχείρησης και αύξηση των εσόδων. Ένας τρόπος να επιτευχθεί αυτό είναι η βελτιστοποήση της γάστρας ως προς την αντίσταση σε ήρεμο νερό. Ωστόσο, επειδή τα πλοία σπάνια πλέουν σε ήρεμη θάλασσα είναι σημαντικό να παρθεί υπόψην και η πρόσθετη αντίσταση σε κυματισμούς.

Για τα μεγάλα πλοία, η πρόσθετη αντίσταση σε κυματισμούς είναι κυρίως αποτέλεσμα της περίθλασης των κυμάτων γύρω άπο το πλοίο, ενώ η πρόσθετη αντίσταση λόγω των κινήσεων έχει μικρή συνιστώσα. Οι διαθέσιμες θεωρητικές μέθοδοι αυτή την στιγμή δυσκολεύονται στο να υπολογίσουν με ακρίβεια το κομμάτι της περίθλασης στα κοντά κύματα. Γι'αυτό είναι απαραίτητο να χρησιμοποιηθούν ημι-εμπειρικές μέθοδοι η μεθόδοι της υπολογιστικής υδροδυναμικής.

Η πρόσθετη αντίσταση σε κυματισμούς είναι επίσης σημαντική για την ελαχιστοποίηση του δείκτη ενεργειακής αποδοτικότητας της σχεδίασης (EEDI). Η πρόσθετη αντίσταση των κυματισμών επηρεάζει το περιθώριο ισχύος της μηχανής που επιλέγεται, καθώς και το διορθωτικό παράγοντα της πτώσης της ταχύτητας σε αντιπροσωπευτική κατάσταση θάλασσας f_w. Μείωση της πρόσθετης αντίστασης θα επηρεάσει θετικά τον EEDI.

Η ανάπτυξη των υπολογιστών κατά τον τελευταίο αιώνα επέτρεψε την χρήση των παραμετρικών μοντέλων, δημιουργημένων σε συστήματα CAD/CAE για την αναπαράσταση της μορφής της γάστρας. Νέες τεχνικές επίλυσης προβλημάτων όπως οι συναρτήσεις Sobol και οι γενετικοί αλγόριθμοι, έθεσαν τα απαραίτητα θεμέλια για αποτελεματική και γρήγορη βελτιστοποίηση. Όλες αυτές οι τεχνικές υπάρχουν στο CAESES/Friendship-Framework.

Σε αυτή την διπλωματική εργασία βελτιστοποιείται μορφή πλώρης ενός μεγάλου τανκερ (KVLCC2) ως προς την πρόσθετη αντίσταση κυματισμών χρησιμοποιώντας CAESES/Friendship-Framework για την δημιουργία παραμετρικού μοντέλου και βελτιστοποίηση. Επίσης η μορφή της πλώρης βελτιστοποιείται ως προς την συνολική αντίσταση, χρησιμοποιώντας την μέθοδο Holtrop-Mennen για την εκτίμηση της αντίστασης σε ήρεμο νερό. Σε τελευταίο στάδιο πραγματοποειίται βελτιστοποίηση της μορφής πλώρης ως προς τον δείκτη EEDI. Η επιτευχθείσα μέγιστη συνεχόμενη ισχύς της μηχανής συγκρίνεται με την ελάχιστη απαιτούμενη άπο τους κανονισμούς.

Λέξεις-κλειδιά: Πρόσθετη Αντίσταση Κυματισμών; Πρόσθετη Αντίσταση σε Κοντά Κύματα; Παραμετρική Σχεδίαση Πλοίου; Βελτιστοποίηση Γάστρας; EEDI; Συστήματα CAD/CAE; CAESES; Friendship-Framework; Holtrop-Mennen; Ελάχιστη Απαιτούμενη Ισχύς σε Δυσμενείς Καιρικές Συνθήκες

Acknowledgments

At this point, I would like to thank my thesis supervisor, Professor Apostolos Papanikolaou, who gave me the opportunity to work on such interesting and challenging topic. He provided me with valuable guidelines in order to successfully complete my thesis.

Furthermore, I would like to thank Dr. Shukui Liu for his help with gaining the necessary theoretical background on issues relevant with added resistance due to waves, supplying necessary information and valuable comments on calculation procedures and on text of diploma thesis.

My sincere thanks also go to Timoleon Plessas, who helped me with the creation of parametric model, programming of calculation procedures in CAESES and reviewing the thesis.

Also I am thankful to George Papatzanakis for providing me with the all the necessary information to initiate my thesis and for his constant willingness to help.

I would also to thank Dionisia Chroni and Nikos Fournarakis, who contributed to successful completion of my diploma thesis.

Finally, I would like to express my gratitude to my family, who incessantly support me throughout my life.

Victor Bolbot

January 2016

Contents

List Of Figures

List Of Tables

Nomenclature

Symbol	SI unit	Definition
AR	[N]	Added resistance due to waves
A_T	[m²]	Projected transverse area above the designated load condition
A_L	[m²]	Projected lateral area above the designated load condition
A_P	[m²]	Propeller area
A_R^S	[m²]	Rudder in propeller race
B	[m]	Ship beam
C	[m]	Distance from the midship section to the center of the projected lateral area (A_L); a positive value of C means that the center of the projected lateral area is located ahead of the midship section
CAD		Computer Aided Design
CAE		Computer Aided Engineering
C_B	[--]	Block coefficient
C_{Dwind}	[--]	Drag coefficient due to wind
C_L	[--]	Maximum rudder lift coefficient
C_{WP}	[--]	Water plane area coefficient
CFD		Computational Fluid Dynamics
C_{FME}	[grCO₂/gr fuel]	Conversion factor fuel oil to CO_2 for main engine
C_{FAE}	[grCO₂/gr fuel]	Conversion factor fuel oil to CO_2 for auxiliary engine
CO_2		Carbone dioxide
CPC		Center Plane Curve
d(x)	[m]	Draft at position x
Disp	[t]	Displacement
DoE		Design of Experiment
Dp	[m]	Propeller diameter
DWT	[t]	Deadweight
EEDI		Energy Efficiency Design Index
EEOI		Energy Efficiency Operational Index
fi	[--]	Correction factor to account for specific design elements

fw	[--]	Correction factor to account the decrease of speed in representative sea conditions
Fn or Fr	[--]	Froude number
FOB		Flat of Bottom
FOS		Flat of Side
GA		Genetic Algorithms
g	[m/s^2]	Gravity acceleration
GHG		Greenhouse Gases
HFO		Heavy Fuel Oil
H_s or h_s	[m]	Significant wave height
IMO		International Maritime Organization
ITTC		International Towing Tank Conference
k	[m^{-1}]	Wave number
k_1	[μm]	Initial roughness
k_2	[μm]	Final roughness
ke	[m^{-1}]	Encountering wave number
k_{yy}	[--]	Non dimensional axis gyration in lateral direction
K_{T0}	[--]	Thrust coefficient at bollard pull
K_{Q0}	[--]	Torque coefficient at bollard pull
L or L_{pp} or L_{bp}	[m]	Ship length between perpendiculars
L_{OA}	[m]	Length Overall
LCB	[m]	Longitudinal Center of Buoyancy
L_E	[m]	Length of Waterline Entrance from fore peak to 99% of maximum breadth on the waterline
LNG		Liquefied Natural Gas
LPG		Liquefied Petroleum Gas
LWT_{CSR}	[t]	Lightship of ship constructed according to Common Structural Rules
MCR	[kW]	Maximum Continuous Rating of Main Engine (ME)
n_{ME}	[--]	Number of ME
n_{MCR}	[rev/s]	Rotation speed at MCR
NSGA II		Non-dominated Sorting Genetic Algorithm II
P_{AE}	[kW]	Considered auxiliary power demanded for operation of ME

P_{ME}	[kW]	75% of MCR
r		Pearson's correlation coefficient
RANSE		Reynolds Average Navier Stoke Equations
R_{AWM}	[N]	Added resistance due to waves reflection
R_{AWR}	[N]	Added resistance due to ship motions
SEB		Stern End Bulb
SEEMP		Ship Energy Efficiency Management Plan
SF	[--]	Safety factor
SMC_{ME}	[gr/kWh]	Specific Fuel Oil Consumption of main engine
SMC_{AE}	[gr/kWh]	Specific Fuel Oil Consumption of auxiliary engine
$S(\omega)$	[m^2]	Spectrum
S	[m^2]	Wetted surface of ship
T_M	[m]	Draught at midships
T_P	[sec]	Modal wave period
t	[--]	Thrust coefficient
U	[m/s]	Ship speed
v_w	[m/s]	Wind speed
Vdesign	[m/s]	Design speed of ship
Vref	[m/s]	Reference speed of ship according to EEDI
w	[--]	Wake fraction
α	[rad]	Wave heading angle
α_{WL}	[rad]	Flare angle
ζ_α	[m]	Wave amplitude
η_0	[--]	Propeller efficiency in open water
η_R	[--]	Relative rotative efficiency
η_S	[--]	Shaft efficiency
θ	[rad]	Inclination angle of waterline segment
λ	[m]	Wave length
ρ	[kg/m^3]	Sea water density
ρ_α	[kg/m^3]	Air density
ω	[rad/s]	Wave frequency
ω_e	[rad/s]	Encounter wave frequency

1   Introduction

The main goal of a shipping company is to increase its profits by reducing the costs and increasing the income. The reduction of costs can be done at a design stage, during ships operation and recycling. But it's most logical to try to minimize the costs at the design stage. The best way to reduce operation costs at the design level is by optimizing ships hull form.

The optimization of ships hull form is also necessary due to new regulatory framework. From 2013 a new amendment has been adopted to Annex VI of MARPOL, which requires all the new-built ships from 2013 to have an Energy Efficiency Design Index (EEDI) not higher than an allowed value. The EEDI evaluates the ship efficiency by means of propulsion power and transport work. To comply with new regulations, the naval architects and ship owners have to consider new hull forms with smaller resistance.

The goal of this diploma thesis is to investigate, how performance of large ships, such KVLCC2, is affected by various sea states and based on this information to see which improvements can be made in ship's hull form, specifically in the region of bow, to reduce Added Resistance (AR) due to waves, total resistance and EEDI.

For this purpose in Chapter 2 the necessary theoretical background on issues relevant to calm water resistance and AR is presented.

Next, in Chapter 3 the components of EEDI are discussed, as well as various methods to reduce EEDI and how AR due to waves affects the EEDI.

Chapter 4 introduces parametric design, the capabilities of CAESES in parametric design and the procedure of creating a parametric model.

Afterwards, Chapter 5 refers to the optimization process in naval architecture, the parameters affecting the hydrodynamic optimization of the hull and the necessary tools that were used in optimization.

Chapter 6 presents the process of optimization, the created parametric model of KVLCC2, the calculation that were conducted and the various settings of the optimization process.

In Chapter 7 the results of optimization process and the comparison of the initial model with the optimized model are presented.

Last, Chapter 8 refers to the conclusions of the project and prospectives for future research.

2   Ship's Resistance In Waves

2.1   Decomposition of Total Resistance

According to D'Alembert paradox, integration of dynamic pressure over any body fully submerged in ideal fluid, away from free surface would give zero value. This means that, pushed in ideal water, a submarine would never stop unless helped by special break. From our experience though, we know, that it never happens, because there is friction between water and the submarine.

The friction resistance of a submerged vessel won't be the same with the resistance of a plate with same surface area running in the same fluid and same speed or as it is named equivalent skin friction, because the form of the vessel affects the flow around the body. The presence of the body causes the flow to accelerate, thus increasing the friction. This form effect, together with equivalent skin friction compose friction resistance.

The viscosity of the fluid also affects the pressure field around the body. Viscous effects such as energy losses in the boundary level, vortices and flow separation prevent an increase to stagnation pressure in the aft body as predicted in an ideal fluid theory, resulting in viscous pressure resistance.

If a vessel moves on free surface or near free surface, it creates waves moving from the ship. All the energy contained in such wave system is part of the energy generated by the ship from its propulsion. This energy is responsible for wave-making resistance. Also ship consumes energy to break it's own wave pattern. This energy is the cause for wave breaking resistance. This kind of resistance can be significant in case of blunt bow shapes. These two resistances together compose wave resistance.

Friction resistance, viscous pressure resistance and wave resistance together give the total resistance in calm water. The decomposition of calm resistance can be observed in Figure 2.1

Each part of resistance is predominant in certain range of speeds. For low speeds, friction resistance is more important. For fast ships wave resistance dominates. The relationship between resistances and speed can be also observed in Figure 2.2.

These resistances are for bare hull. The resistance of the appendages (propeller shaft, bossing, rudder etc.) should be added to the bare hull resistance in order to estimate the overall resistance in calm water. Right position and careful selection of ships appendages can significantly improve ships performance. Also because ships are moving not only in water,

but also in the air it confronts extra air resistance. Air resistance has a smaller effect in the overall resistance, but it can have significant effect in bad weather, therefore it should not be neglected. Last, but not least, because seas are seldom still, ships have to deal with resistance caused by sea waves. For fast container ships and in sea state 8 added resistance can reach even 40% of still water resistance (Politis G.K. , 2011).
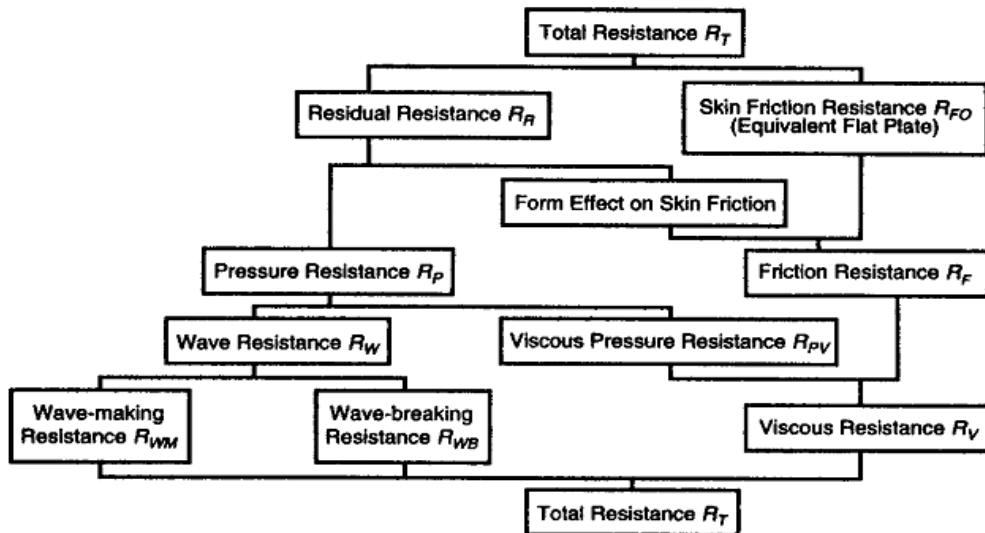
Figure 2.1: Subdivision of marine vessel resistance. (H. Schneekluth &V.Bertram, 1998)
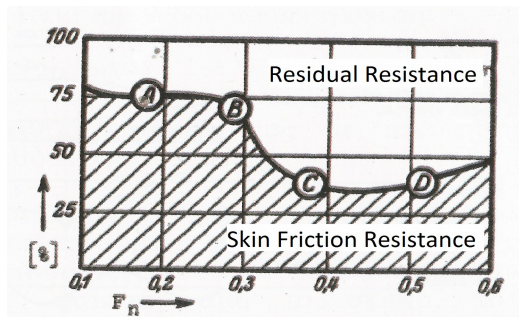
Figure 2.2: Residual and frictional resistance in % of total resistance for different Fn (Papanikolaou A., 2009)

Various other factors also affect ships resistance in calm water like ships loading and thus its trim and sinkage. In low speeds aft trim leads to an increase in resistance, while in high speeds the resistance decreases (Politis G.K., 2011). Resistance differentiates in shallow water due to change in fluid flow around the ship and in wave pattern. Usually it leads to an increase in resistance, but the results can also be opposite (Politis G.K. , 2011). Due to the fouling, the roughness of hull increases with time, leading to greater skin friction resistance. The raise in power demand can even reach 20% (Politis G.K., 2011). Near river mouth of big rivers fresh water creates a layer over salt water. Another free surface means that there is a new underwater wave pattern and consequently increase in ship resistance (Politis G., 2011).

2.2 Added Resistance (AR) in Waves

Ships seldom travel in still water conditions. As it can be inferred from Figure 2.3 there is slightly more than 11% probability that ship will encounter waves with height less than 0.5 m. In North Atlantic probability falls almost to 8% while in Northern North Atlantic even to 6%.
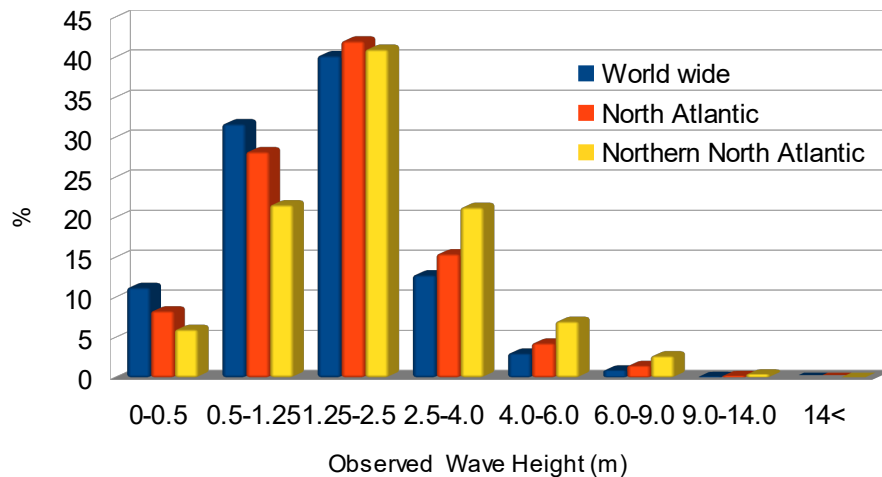
Figure 2.3: Percentage probability of a wave height (Price W.G. and Bishop R.E.D, 1974)

It's not necessary to be windy, for added resistance due to waves (AR) to occur, because waves can be coming from a storm far away from ship. If the waves come from bow (head waves to bow-quartering waves) they cause a significant AR. The increase can be greater for oblique seas. Following waves instead, may add thrust to the ship, depending on the ship speed and wave speed. In the current regulations (IMO MEPC.1 Circ. 796, 2012), only the impact of heading waves and oblique seas is examined in evaluation of AR.

According to the classical sea keeping theories, the energy dissipated by the ship, when moving in a wave field, can be attributed to three different components (Athanasoulis G.A., Belibasakis K.A.,2012). These three components are :

1. A first obtained from the integration of pressure of incident waves over the ship hull. The calculated force is also referred as Froude-Krylov force.

2. The incident waves cause the ship to move primarily in heave, pitch and secondary in roll directions. The ship motions and phase difference between incoming waves and ship motions evoke additional wave pattern consuming energy from ship. This is the radiation component.

3. The presence of ship evokes partly waves reflection and partly waves transmission. This is the diffraction component.

The common practice in regulations is to decompose AR into two components: AR due wave diffraction R_{AWR} and added resistance due to ship motions R_{AWM}. So the problem can be decomposed into two basic phenomena's, as can be seen in Figure 2.4 for steady cylinder. This is also true for an advancing ship.
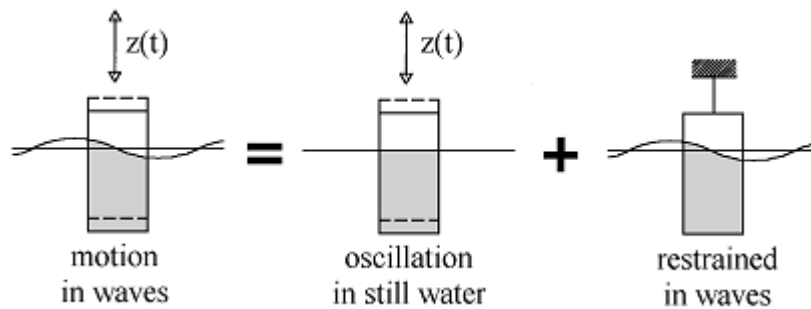
Figure 2.4: Decomposition of AR. (Journée J.M.J. and Pinkster J.,2002)

Each type of resistance dominates in different wave region. R_{AWR} is predominant in short waves (waves with length below 0.5 length of ship), while R_{AWM} in medium waves (0.5-1.5~2 length of the ship). In very long waves the ship responds following the wave motion, so there is no AR induced. This can be observed in Figure 2.5
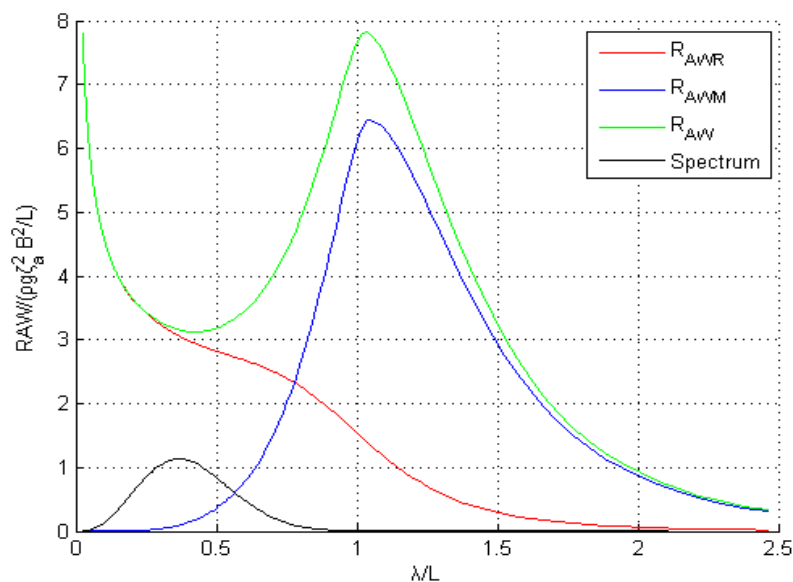
Figure 2.5: R_{AWR} and R_{AWM} for different wave lengths.

2.3   Methods to predict AR

According to Liu et al (2011), approaches to AR can be generally classified into two main categories, namely far-field and near-field. The far-field methods are based on considerations of the diffracted and radiated wave energy and momentum flux at infinity, leading to the steady AR by the total rate of momentum change. The near-field method, on the other side, leads to the AR as the steady second-order force obtained by direct integration of the hydrodynamic, steady second-order pressure acting on the wetted ship surface. The latter can be calculated exactly from first order potential functions and their derivatives.

Although expected to have similar results, this is not observed in practice, because the two methods have different physical models and neglects features of the problem, that other method take into account. Even the results of the same sea-keeping problem used for far-field and near-field method lead to different value of calculated AR (Liu et al, 2011).

In several cases, it is hard to predict accurately AR using one of the aforementioned methods, especially in short wave region. Then, it is very handy to adopt some semi-empirical approach. Semi-empirical formulas are tuned appropriately to match experimental results. Some of the formulas are result of regression analysis, while other are derived from theoretical analysis. Semi-empirical formulas are useful as a quick way to calculate AR.

The reference line for all the methods above remains towing tank tests. Every method employed has to be in a good agreement with experimental results. Towing tanks experiments are proposed by IMO and classification societies guidelines for calculation of AR (IMO MEPC.1/Circ.796, 2012).

The categorization of method's to predict AR can be seen in Table 2.1

Table 2.1: Methods to predict AR.

Far-Field Methods	**Near-Field Methods**	**Semi-Empirical Formulas**	**Towing Tank Tests**
Maruo's Gerritsima & Beukelman's	Havelock's Boese's Salvensen's RANSE	***Integrals on Waterline*** Fujii & Takahashi's Faltinsen's Liu, Papanikolaou, Zaraphonitis's ***Regression Analysis*** Jinkine & Ferdinande's STAWAVE-2	

There is a general consensus that no method from the far-field and near-field methods above can be used for accurate estimation of A.R. in all regions of speed and wave length for all hull forms (Zakaria N.M.G. and Baree M.S.,2007). Sometimes also there can be significant difference in the results among the methods, as much as 100% (Nabergoj R., Prpic-Orsic, 2007). Comparison of the results also cannot be a choice, due to diversity in results, making necessary use of modern computational tools or towing tank tests. (Zakaria N.M.G. & Baree M.S.,2007) (Nabergoj R. & Prpic-Orsic, 2007).

The far-field methods give good estimation of AR in medium and long wave lengths, catching the peak of the Figure 2.5. Maruo's method is stable in short wave region, giving however lower values in short and long waves and tends to zero as wave length tends to zero, which physically is incorrect. (Perez Arribas F., 2006). But the method calculates AR well for cruiser-stern ships without large bulbous bow (Nabergoj R., Prpic-Orsic, 2007). Gerritsima & Beukelmanns method although catches the short wave region, is unstable.(Perez Arribas F., 2006) It also doesn't predict correctly the AR of ships with small block coefficient and cruiser-stern (Nabergoj R., Prpic-Orsic, 2007). To sum up, although the far-field methods are able to estimate AR in the short wave region, but not accurately.

The near-field methods have several defects too. Boese's (or simplified pressure integration method) method overestimates the peak value (Perez Arribas F., 2006). Salvensen'a method usually overestimates the AR in short waves (Matulja D., 2011). The method fails to calculate AR in full ships, especially in bow region, because the assumption of slender ships is not applicable (Matulja D., 2011).

Semi-empirical formulas are much simpler and quicker than the above mentioned methodologies. Faltinsen's asymptotic formula has limited boundaries for application: low Froude numbers, blunt bows, short waves, with good validation results. (Liu et al 2011). However, there is a considerable difference between experimental results for slender ships and the Faltinsen's formula (Liu et al 2011). Liu et al formula is appropriate for all types of ships in short waves and wide range of speeds (Liu et al 2015). Also it takes into account parameters of ship such as draft distribution and flare angle. The comparison of Liu et al formula with experimental results for KVLCC2 can be seen in Figure 2.6. The Jinkine Ferdinande formula is the oldest and thus it doesn't cover the novel designs. STA-2 formula is a modified Jinkine Ferdinande formula, including the AR contribution in short-waves and tuned regressively to an extensive experimental data base. STA-2 is more accurate than Jinkine Ferdinande formula (Grin R., 2015).

RANSE method tends to give more accurate prediction of AR. The method deals directly with non-linear flow phenomena (Orihara H. & Miyata H., 2003), and is capable to catch the ship's hull form above waterline (Hu et al, 2014), which is important according to experimental results (Grin R., 2015). However the solution of the problem is sensitive to grid resolution (Hu et al, 2014) and requires high density grids to catch non-linear responses (Söding H. et al, 2014). One disadvantage of the method is high cost of computation. It may take hours to compute a response of ship in waves.(Azcueta R. 2004) Also RANSE methods have been so far applied to the problem of added resistance in regular head waves in a restricted range of wave frequencies (Söding H. et al, 2014).
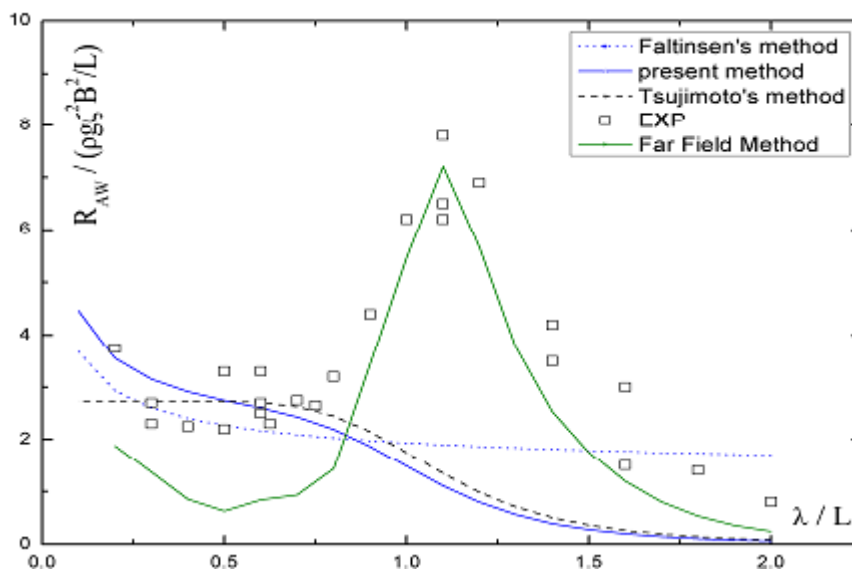
Figure 2.6: Comparison of Liu et al formula (blue color) with experimental results and other methods for KVLCC2 (Liu et al 2015)

Potential flow codes are currently the most predominant technique involved in calculation of AR because they require less computer resources achieving similar accuracy for medium and long waves with RANSE (Söding H. et. al, 2014). The method considers 3D flow field, complex ship geometry and solves the sea-keeping problem. Results from such analysis can be used either for far-field or near-field method. However, the method neglects non-linear effects such as wave-breaking and hull shape above the stationary waterline (Söding H. et al., 2014).

Experiment in towing tanks is the most reliable method from physical point of view as it deals directly with all non-linear phenomena. It requires 3-4 experiments at different Fn to define AR in short waves, taking approximately 4 hours (IMO MEPC.1/Circ.796, 2012).

However towing tank experiments for AR require a special arrangement, so as not to restrain surge motion. In addition, another disadvantage is that AR computed as average longitudinal force over time is small compared to the amplitude of force variations leading to errors even exceeding the average force itself. Furthermore, the method is sensitive to the quality of wave generation and wave measurement, especially in short waves, because AR depends on wave amplitude square (Söding H. et. al, 2014).

To sum up, the accuracy of prediction of AR in medium and long waves increases with computational effort. Thus, for quick results, the most suitable method is semi-empirical formulas. Better estimation can be achieved with far-field and near-field methods. In case where the most accurate results are needed, it is necessary to use either RANSE methods or experimental results from model tests in towing tanks.

The situation is different in short waves. The far-field and near-field methods do not approach the short waves region correctly. The accuracy of measurement of AR in short waves in towing tank tests is also low due to the very small measured value of AR. So the best way to estimate AR in short waves may be by using semi-empirical formula, which has good agreement with experimental results such as the formula of Liu et al (2015).

2.4   AR in short waves

As it can be observed in Figure 2.7 AR differentiates over wave lengths. Dimensionless AR has zero value for long waves, reaches peak at wave length equal approximately to ships length, and has constant value for short waves.
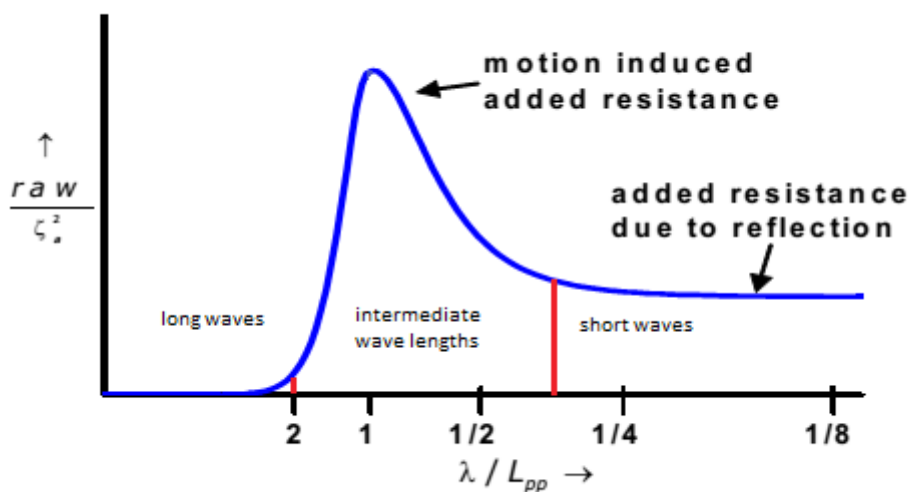
Figure 2.7: Distinction of wave length regions. (Grin R., 2015)

For long waves ($\lambda/L\sim2\text{-}3$) the wave length is too big, the ships is mowing with the wave, so the ships responses hydrostatically and there is almost no AR. In the intermediate wave lengths ($\lambda/L\sim0.5\text{-}2$) the ships motions are significant, causing R_{AWM}. In the short wave region, ship motions diminish and waves are totally diffracted at ships hull. Thus R_{AWR} is significant in short wave region. (Grin R., 2015)

For large ships, like KVLCC2, R_{AWR} is predominant in calculation of EEDI. As it can be seen in Figure 2.8 the dimensionless R_{AWR} has the same amplitude with R_{AWM}. But because the representative sea conditions, defined in MEPC.1/Circ.796, are placed in region of short waves the impact of each part is different. As it can be seen in Figure 2.9. R_{AWR} is greater almost in all range of wave lengths. In fact, more than 95% of AR is owed to wave reflection. The AR here is calculated with Liu et al (2015) simplified formula as presented in appendix C. The ship data used is presented in Table 2.2.
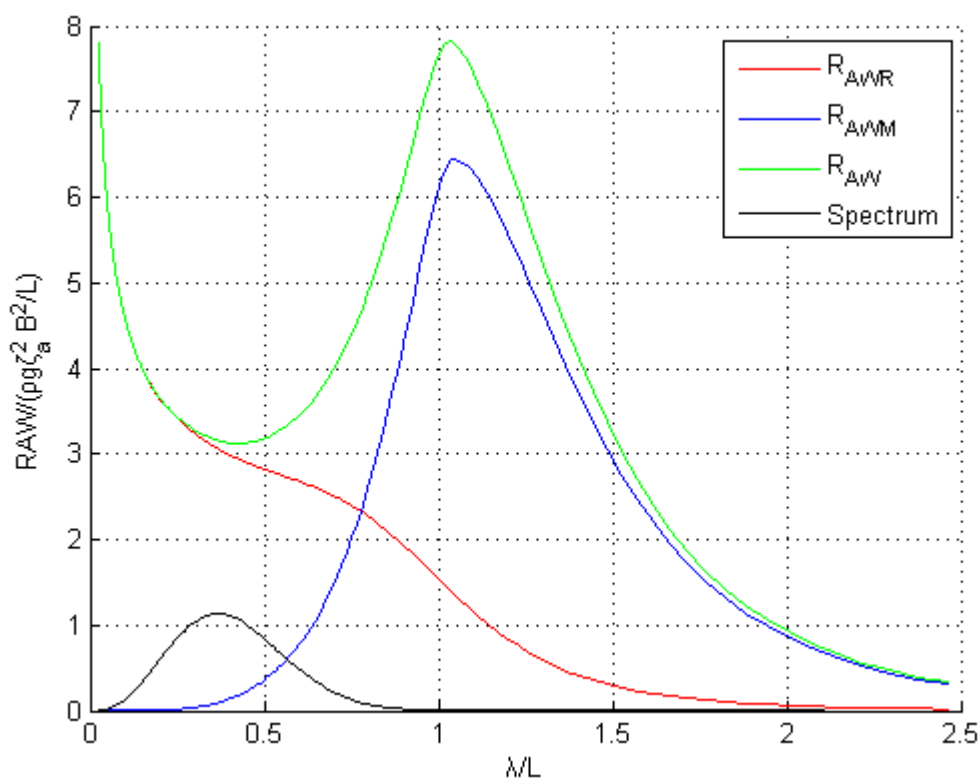
Figure 2.8: The non-dimensional AR of KVLCC2.
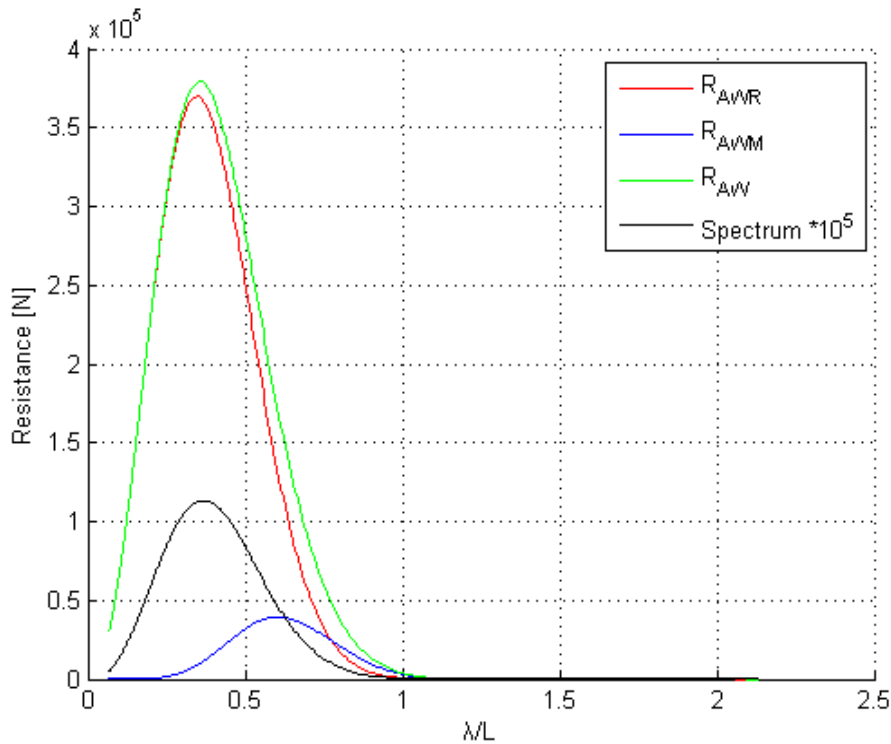
Figure 2.9: AR of KVLCC2 for each wave length.

Table 2.2: Data of KVLCC2 (Simman workshop, 2008)

Ship parameters	Value	Units
L_{pp}	320	[m]
B	58	[m]
C_B	0.8096	[--]
V	15.5	[kn]
L_E	60	[m]
Tm	20.8	[m]
k_{yy}	0.25	[--]

Of course the ship has to travel also in sea states different from the EEDI spectrum. But the probability of encountering short waves is very high. By using the probabilities of sea states proposed by S. Bales (1982), it's it obvious that R_{AWR} contributes more than 80% of AR during ship operation in North Atlantic. The trend changes only slightly with speed. Thus it is very important to consider the effect of R_{AWR} in ship design. The AR, R_{AWR}, R_{AWM} for each state are calculated using simplified Liu-Papanikolaou's formula as described in Appendix B. The average AR is weighted sum of AR at different sea states. The analytical calculation procedures, sea states and their probabilities are available in Appendix A.
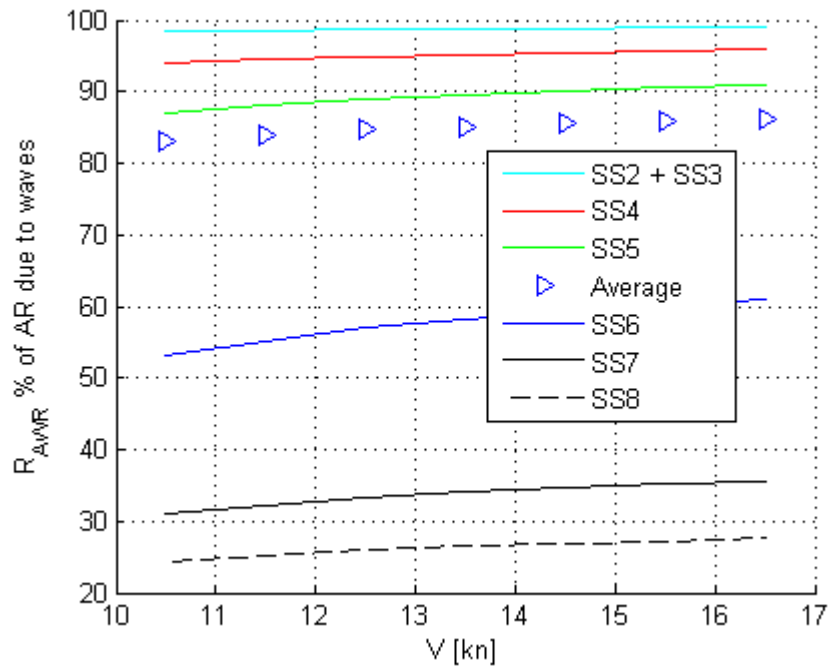
Figure 2.10: R$_{AWR}$ in % of AR for different sea states (SS) and speeds.
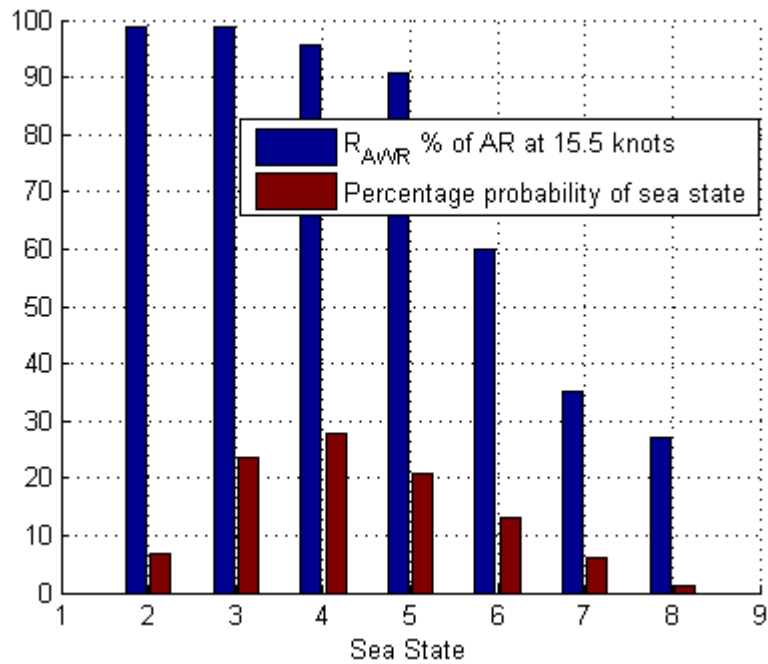
Figure 2.11: R$_{AWR}$ in % of AR for V=15.5 knots and % probability of Sea States.

3   The Energy Efficiency Design Index (EEDI)

3.1   Introduction to EEDI/EEOI

In the end of 80s it became evident that there is correlation between increasing concentrations of carbon dioxide (CO_2) and global warming. This lead to Kyoto Protocol in 1997, an international agreement with binding targets for greenhouse gas (GHG) emissions reductions from industrialized countries. Shipping emissions were also included in national targets. According to IMO research in 2009 international shipping is estimated to have emitted 870 million tonnes or 2.7% of total annual anthropogenic emissions of CO2 in 2007. In the absence of regulations to control CO_2 emissions, it would increase by a factor of 2.4-3.0 by 2050 (IMO 2009)

This made necessary the introduction of regulations to improve energy efficiency of ships. In 2011 technical measures for new ships and operational reduction measures for all ships were adopted, the first ever mandatory global GHG reduction regime for an entire industry sector. The adopted measures add to MARPOL Annex VI (Resolution MEPC.203(62)) a new Chapter 4 entitled Regulations on energy efficiency for ships, making the Energy Efficiency Design Index (EEDI) mandatory for new ships and the Ship Energy Efficiency Management Plan (SEEMP) mandatory for all ships. In January 2013 EEDI and SEEMP entered into force.

EEDI represents theoretical emissions of CO_2 per ship's capacity -mile. So the smaller is EEDI, the more energy efficient is the design. For ship designs it's required to have EEDI smaller than values proposed by reference line. For the most of the ships the reference line was reduced by 10% in 2015, and is going to be reduced further 10% in 2020 and again in 2025 as can be seen in Figure 3.1. The designer is free to use the most economical solution to meet the regulation requirements. Currently the EEDI regulation apply to oil tankers, bulk carriers, gas carriers, general cargo, container ships, refrigerated cargo and combination carriers. Formulas for EEDI for other types of ship are under research.

SEEMP has the goal to assist shipping companies to improve energy efficiency of their fleet cost effectively by supplying relevant tools. Energy Efficiency Operating Index (EEOI) is an example of such a tool. EEOI represents actual CO2 emissions per cargo transferred and distance sailed. In comparison with EEDI, EEOI varies with ships speed, environmental conditions, distance of ballast voyage, hull and propeller fouling, etc. In order to avoid environmental impacts its value is usually averaged over number of voyages.
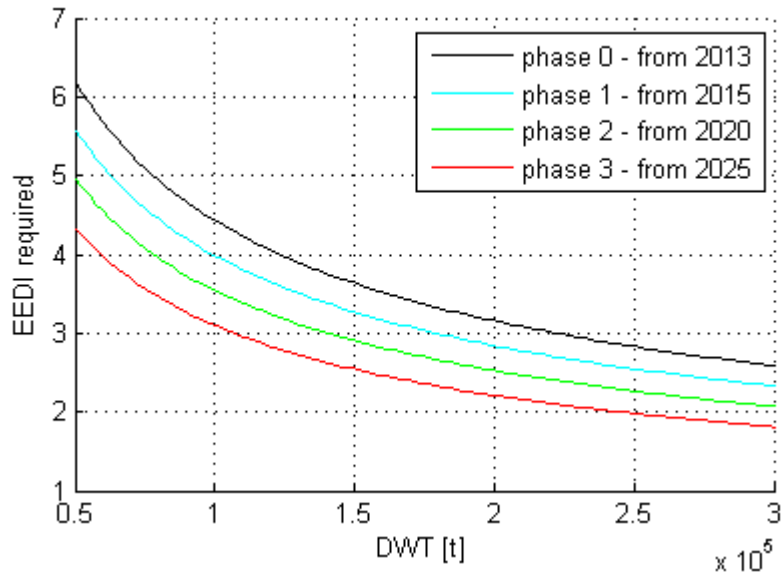
Figure 3.1: EEDI reference line for tankers during different phases.

3.2   About the components of EEDI

The attained Energy Efficiency Design Index is calculated as following:

Main engine(s) CO$_2$ emissions

$$EEDI_{attained} = \left\{ \left(\prod_{j=1}^{n} f_j \right) \left(\sum_{i=1}^{n_{ME}} P_{ME(i)} \cdot C_{FME(i)} \cdot SFC_{ME(i)} \right) \right.$$

Auxiliary engine(s) CO$_2$ emissions

$$+ \left(P_{AE} \cdot C_{FAE} \cdot SFC_{AE} \right) + \left(\left(\prod_{j=1}^{n} f_j \cdot \sum_{i=1}^{n_{PTI}} P_{PTI(i)} - \sum f_{eff(i)} \cdot P_{AEeff(i)} \right) C_{FAE} \cdot SFC_{AE} \right)$$

(3.1)

CO$_2$ emission reduction due to
Innovative technology(s)

$$- \left. \left(\sum_{i=1}^{n_{eff}} f_{eff(i)} \cdot P_{eff(i)} \cdot C_{FME} \cdot SFC_{ME} \right) \right\} \cdot \frac{1}{f_i \cdot f_l \cdot f_w \cdot f_c \cdot Capacity \cdot v_{ref}}$$

Transport work

Main Engine(s) CO_2 Emissions

Main Engine(s) CO_2 emissions are calculated as following:

$$\left(\prod_{j=1}^{M} f_j \right) \left(\sum_{i=1}^{n_{ME}} C_{FME_i} \cdot SFC_{ME_i} \cdot P_{ME_i} \right) \tag{3.2}$$

where:

- f_j is correction factor for specific ship designs.

- C_{FME_i} is conversion factor fuel oil to CO2, depending on the fuel types.

- SFC_{ME_i} is specific fuel oil consumption of the main engine at 75% of Maximum Continuous Rating (MCR).

- P_{ME} is 75% of MCR_i of the main engine. If there is a shaft generator installed, the value of MCR_i is reduced according to EEDI regulations.

- i represents each installed engine.

- n_{ME} is number of installed main engines.

Auxiliary Engine(s) CO2 Emissions

Auxiliary engine(s) CO_2 emissions are found as following:

$$C_{FAE} \cdot SFC_{AE} \cdot P_{AE} \tag{3.3}$$

where:

- C_{FAE} is conversion factor fuel oil to CO_2, as for main engine. If engines with different fuel types are installed, C_{FAE} should be the weighted average.

- SFC_{AE} is weighted average among SFCAE(i) of all respective auxiliary engines i at 50% load.

- P_{AE} is the considered auxiliary power demanded for operation of the main engine(s) and is calculated as a share of the installed main engine power according to EEDI regulations.

<u>Auxiliary Engine(s) CO_2 Emissions Correction</u>

Carbon emissions for auxiliary engines are corrected for shaft motors, innovative electrical energy efficient technology and design restrictions due to ice class as following:

$$\left(\prod_{j=1}^{M} f_j \cdot \sum_{i=1}^{nPTI} P_{PTI(i)} - \sum f_{eff(i)} P_{AEeff(i)} \right) C_{FAE} \cdot SFC_{AE} \tag{3.4}$$

where:

- f_j is correction factor for specific ship designs such as ice class.

- $P_{PTI(i)}$ is 75% of the rated mechanical power of the shaft motor(s) divided by the weighted efficiency.

- $f_{eff(i)}$ is availability factor for each innovative technology.

- P_{AEeff} is the auxiliary power reduction due to innovative technology.

<u>CO_2 Emissions Reduction due to Innovative Technology(s)</u>

If technologies are installed which reduce the main engine power the following term can be applied:

$$\sum_{i=1}^{n_{eff}} f_{eff(i)} \cdot P_{eff(i)} \cdot C_{FME} \cdot SFC_{ME} \tag{3.5}$$

where:

- $f_{eff(i)}$ is availability factor for each innovative technology.

- Peff is 75% of the main engine power reduction due to mechanical energy efficiency technologies.

- C_{FME} is conversion factor fuel oil to CO_2.

- SFC_{ME} specific fuel oil consumption, as for main engine at 75% of MCR.

Transport Work

Transport work is calculated as following:

$$f_i \cdot f_l \cdot f_w \cdot f_c \cdot \text{Capacity} \cdot v_{ref} \tag{3.6}$$

where:

- f_i is correction factor to account for ship specific design elements which reduce the capacity.

- f_l is correction factor for general cargo ships.

- f_c is cubic capacity correction factor for chemical tankers.

- f_w is correction factor to account the decrease of speed in representative sea conditions.

- V_{ref} is ships speed at EEDI conditions (engine output 75% of MCR and calm water).

3.3   Ways to Reduce EEDI

There are different ways to reduce EEDI:

1. By using technologies that have direct impact on the speed-power curve of a vessel and thus cannot be separated from overall performance of the ship. MCR of the propulsion plant is usually selected by calculating the necessary propulsion power for desired speed in calm water and by adding an extra power margin for adverse weather conditions. If any of the two components is reduced, then the MCR is reduced, thus, improving the EEDI. This can be achieved by using e.g. low friction coating, by using better anti fouling, by doing bare hull form optimization, by using low resistance rudders, by optimizing propeller design or fitting propulsion improving devices, like Moewes ducts etc. and by reducing AR due to waves.

2. By using technologies that reduce the propulsion power (excluding generation of electricity). These technologies can be switched off or their use is limited to certain ambient conditions. Hull air lubrication system is one type of such system with potential reduction in resistance of about of 5-10% (Kawabuchi et.al.2011). In ambient conditions with strong winds can be used sails, Flettner-Rotor systems and kites.

3. By using technologies that generate efficiently part of the required electrical power. Waste heat recovery system uses the energy of exhaust gases to heat water and through Rankine cycle produce electricity. Photo voltaic cells convert directly energy of sunlight to electricity during day.

4. By using fuels with low carbon content. LNG has 11.7% lower C_{FME} than HFO, while LPG 3.7%. LNG also has energy density of 53.6MJ/kg, while HFO 43MJ/kg, so the specific fuel consumption is lower for LNG. (Natural Gas, Engineering Toolbox) All this together makes LNG a possible mean for reduction of CO_2 emissions.

5. By reducing service speed of ship as discussed in the next chapter.

3.4   Impact of Slow Steaming

Slow steaming is practice of traveling at lower speed than usual. Ships required power for propulsion is proportional to cubic of speed, so even a small reduction in speed can reduce the propulsion power significantly, and consequently reduce bunkering costs. It was introduced in 2007, when the oil prices doubled in one year period (from 350$ per tone HFO in July 2007 to 700$ in July 2008). (Lloyd's Register, 2008). During the next years many ships decreased their operational speed from 20-25 to 14-18knots. In Ulysses project it was proposed to reduce even to 5-6knots. (H. Psaraftis, 2011) (Transport research innovation portal, 2013).

The obvious benefit of slow steaming is reduced operational costs. According to Wartsilla, fuel consumption can reach 41% of initial by changing cargo ship speed from 27 knots to 18 knots at the cost of an additional week's sailing time on Asia-Europe routes (Wiesman, 2010). Decrease in fleet speed, also means that more time is needed to transfer cargo, so more ships can be employed. Reduction of fuel consumption means that CO_2 emissions will be reduced, so there is an improvement in EEDI and EEOI, as is proved next.

The formula for calculation of EEDI (3.1) can be simplified as following.

$$EEDI = \frac{b_e * 0.75 * MCR * C_{FME}}{Capacity * V_{ref}}$$
(3.7)

The required power is proportional to cubic of speed.

$$MCR = c * V^3$$
(3.8)

So the EEDI is analogous to square of speed.

$$EEDI \sim \frac{b_e * 0.75 * V_{ref}^2 * C_{FME}}{Capacity}$$
(3.9)

The EEOI is calculated as following:

$$EEOI = \frac{Fuel_{consumed} * C_{FME}}{Cargo_{transported} * Distance_{sailed}} \qquad (3.10)$$

By deriving with time:

$$EEOI = \frac{\partial Fuel_{consumed}/\partial t * C_{FME}}{Cargo_{transported} * V} \qquad (3.11)$$

Rate of fuel consumption is analogous to propulsion power, so it's analogous to cubic of speed. So in final:

$$EEOI \sim \frac{V_{ref}^2 * C_{FME}}{Cargo_{transported}} \qquad (3.12)$$

That's a simplified assessment, but it clearly shows a trend that lower reference speed results in lower MCR and thus EEDI and EEOI. However there is a limit in speed reduction. For existing ships operating in lower speed means that they are going out of region of high propeller efficiency. Furthermore specific fuel consumption is optimized for ranges of engines output 70-85% of MCR, so going out of this region means higher specific consumption. The hull form of the ship is optimized for certain range of speed, so decreased speed means lower hull efficiency. Last, but not least smaller engine output results in smaller exhaust gas energy. That results in smaller output of waste heat recovery system, making necessary an extra fuel consumption for auxiliary systems.

For new and existing ships, it's necessary to have minimum propulsion power in order to maintain adequate maneuverability in adverse conditions. According to IMO MEPC 64/4/13 & MEPC 64/INF.7 the ship should be able to keep course in waves and winds from any direction and keep advance speed of at least 4 knots in waves and wind from any direction. These guidelines were issued in 2012 and amended in the 2013 Interim Guidelines. The new amendments however are in potential conflict with progressively enhancing EEDI requirements, demand the use of model tests for simplified assessment level, use the minimum propulsion curves that do not reflect the real physics of the problem and discourage the development/implementation of innovative propulsion and steering concepts, contradicting the reasoning of EEDI introduction. To address the above challenges was launched a new European research project called SHOPERA (Energy Efficient Safe SHip OPERAtion) (2013-2016), funded by the European Commission in the frame of FP7. SHOPERA is developing suitable numerical methods and software tools and is conducting systematic case studies, which will enable the development of improved guidelines. (Papanikolaou et al, 2015)

3.5   Influence of AR on EEDI

AR affects in two different ways EEDI index. First, it affects sea margin of a ship and thus the MCR. Secondly, it is involved in calculation of fw correction factor.

According to ITTC sea margin is: " The margin which should be added to the estimation of the speed power relationship of a newly built ship in ideal weather conditions to allow for the operation of the ship in realistic conditions. In practice it doesn't mean that the ship must meet full speed in all weather conditions, but that it can sustain it's service speed over a realistic percentage of conditions". So the sea margin reflects the necessity to spent extra energy to overcome AR in waves, AR in winds and increase in resistance due to fouling.

The fw correction factor reflects the expected speed decrease during ship operation. For a representative sea condition, both AR in waves and winds is calculated for various speeds and based on that a curve of dependence between speed and power output in representative conditions is drawn. Then for the power equal to engine output at EEDI conditions, a reduced speed Vw is found. This speed divided by Vref gives fw factor.

AR is important especially for slow steaming. From Figure 3.2 can be inferred that AR as % of total resistance decreases with increase in speed. This can be explained by the fact that calm water resistance is analogous to square of speed and while AR due to waves seems to be proportional to speed in methods employed. This trend can be observed also in Figure 3.3. The sea margin depends on the ratio of total resistance over calm resistance. The greater the ratio the greater is the sea margin. The increase of AR as % of total resistance in low speeds reveals that sea margin in % of continuous service rating should be also increased in low speeds. Furthermore from Figure 3.4 it can be observed that reduction of reference speed affects negatively the fw correction factor. However, this change is small (only -3% for 2 knots reduction) and practically is unimportant.

Here calm water resistance was estimated using Holtrop and Hollenbach method, the AR in waves was calculated using simplified Liu-Papanikolaou method as described in Appendix B, AR due to winds using method proposed by ITTC as described in Appendix C, while fouling increase was set to 5% of calm water resistance.

Concluding, by reducing AR, it's possible to reduce sea margin and increase fw and consequently improve Energy Efficiency Design Index.
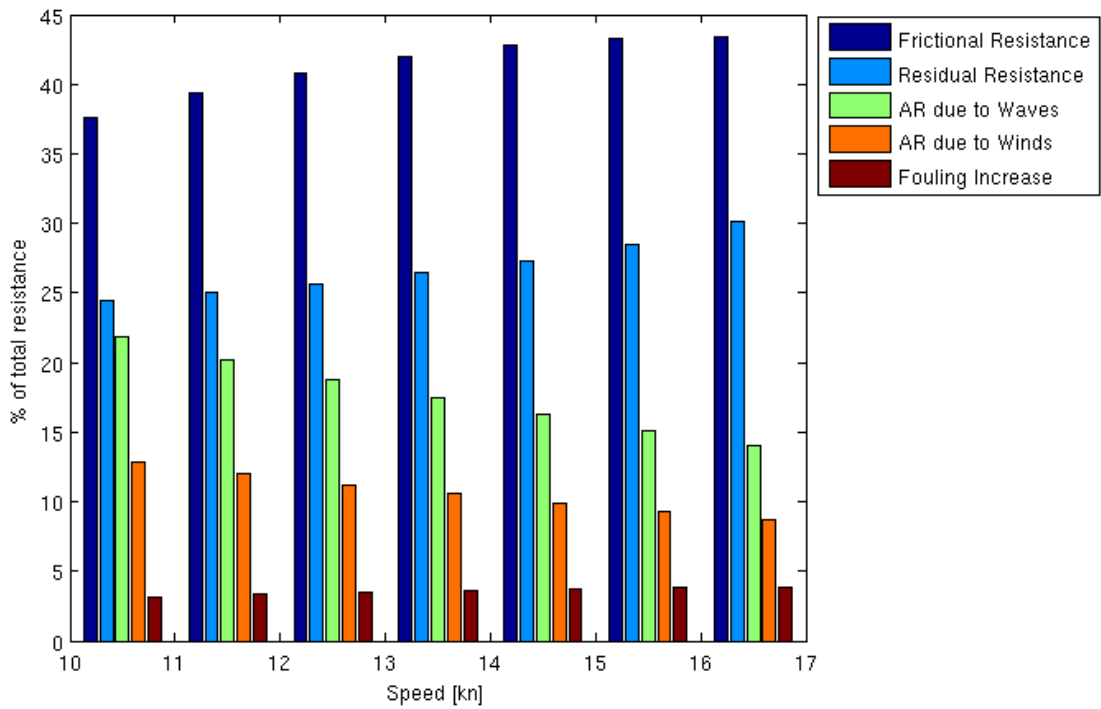
Figure 3.2: AR in % of total resistance for KVLCC2
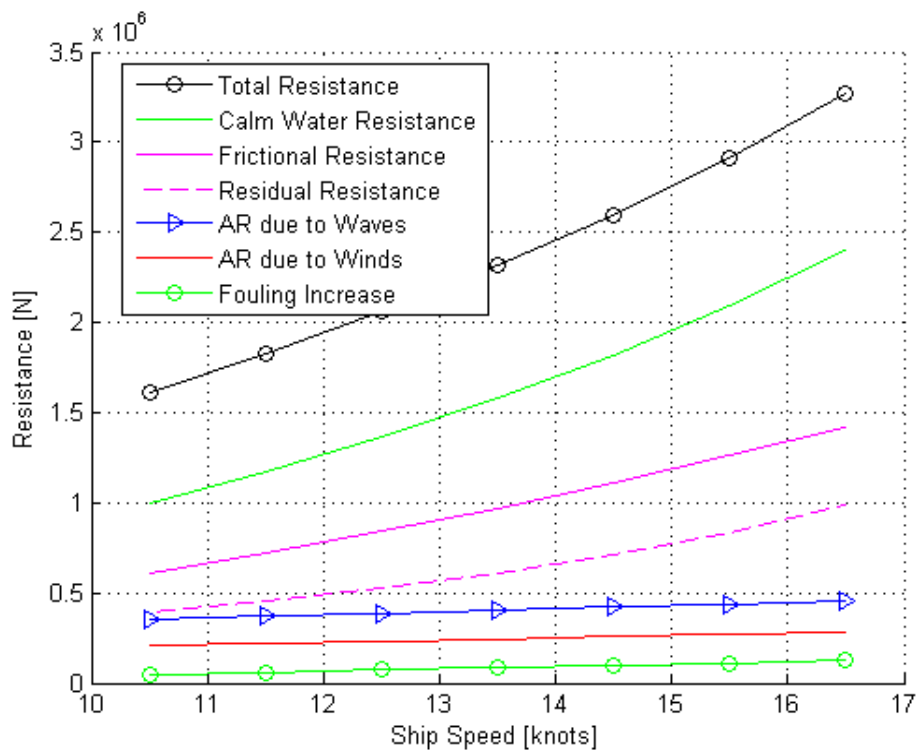
Figure 3.3: Components of total resistance for KVLCC2
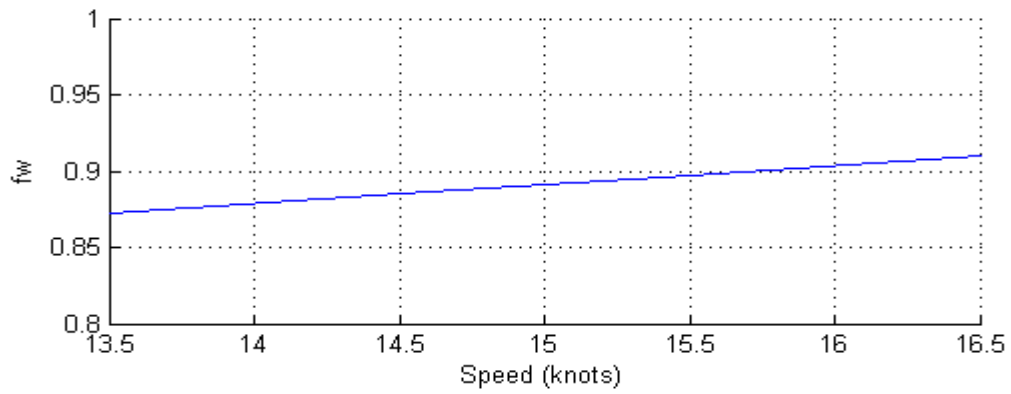
Figure 3.4: fw for different speeds for KVLCC2

4   Parametric Ship Design - The Caeses S/W Framework

4.1   Introduction

Computer-aided Design (CAD) is "the use of computer systems to aid in the creation, modification, analysis, or optimization of a design" (Narayan et al, 2008).

Traditionally, the invention of the 3 dimensional CAD is attributed to a French engineer, Pierre Bezier (Arts et Metiers ParisTech, Renault). After his mathematical work concerning surfaces, he developed UNISERF, between 1966 and 1968, to ease the design of parts and tools for the automotive industry. Then, UNISURF became the working base for the following generations of CAD software. (Flutterby, Wikipedia, 2015)

Today CAD is used in many fields. It's used in automotive, aerospace, industrial and architectural design, prosthetics, computer animation, advertising, technical manuals and of course shipbuilding and ship design. CAD systems are involved in design and fairing of 2D curves like sections, waterlines, buttocks, in design and fairing of 3D curves, in design of 3D model of ships hull, in determination of machinery spaces, in hydrostatic calculations, in resistance calculations, ship strength studies etc. Special application of CAD systems is parametric modeling (Kaklis, 2011).
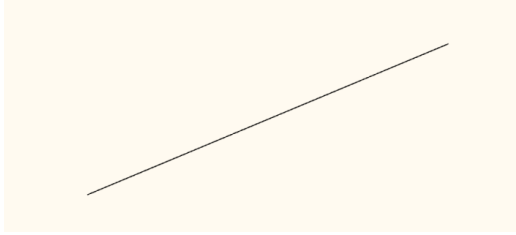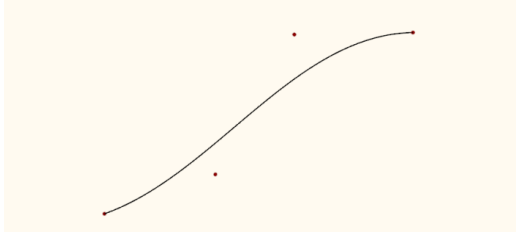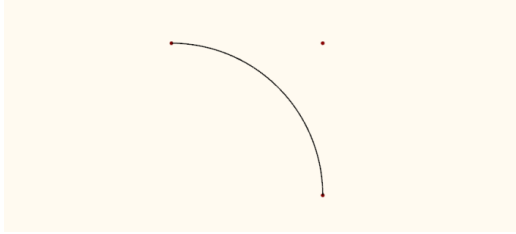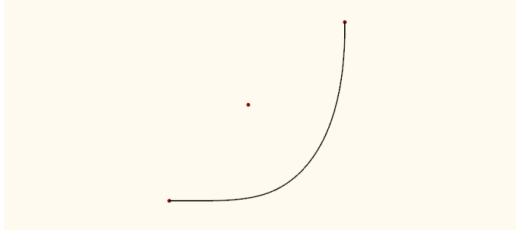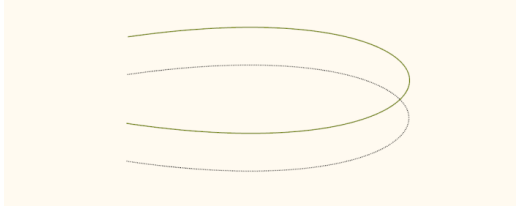
Parametric modeling is creation of design with use of parameters. If any parameter is changed, then the model is changed. In several occasions relationship between parameters and design can be very complex. Therefore, the relationships are given with the help of suitable codes or functions. The parametric modeling has a lot of advantages. It's much easier to make changes to a parametric model whereas in a non-parametric model any possible change might need to rebuild the model from the beginning. Thus it provides a whole range of possible solutions and makes it's possible to add constraints to the model which can be used easily in optimization processes.
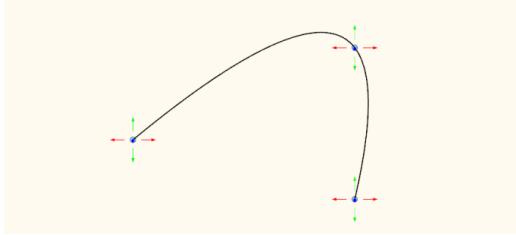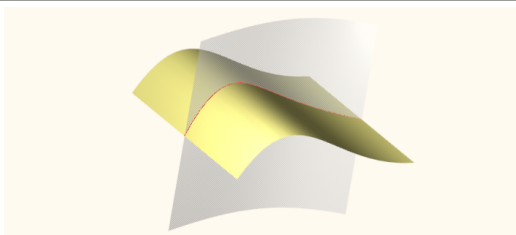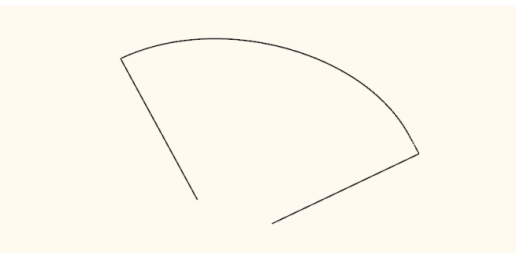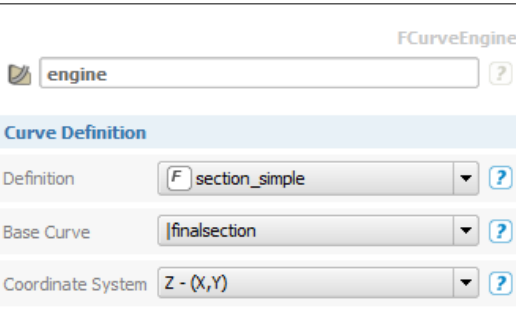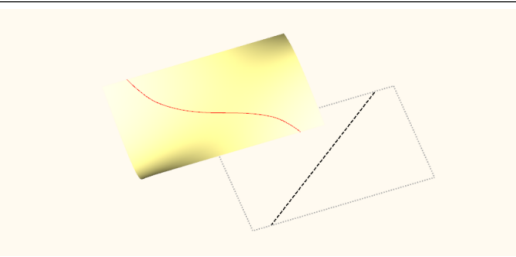
The CAESES® is a CAD system that emphasizes on parametric modeling and problems solved with use of Computational Fluid Dynamics. CAESES® is an evolved version of Friendship-Modeller, presented by Harries in 1998 and is result of extensive research at Technical University of Berlin (Makris, 2015). CAESES® is capable of creating 3D geometries with use of a number of design parameters, adding constraints, importing and exporting geometries of different types, connecting to CFD packages, receiving results of CFD simulations and performing optimization.

4.2   Curves Definitions in CAESES s/w Framework

CAESES® uses more than 20 curve definitions for parametric design. Here are briefly discussed only the curves that were used in project (CAESES documentation , 2015).

Table 4.1: Curves used for parametric design.
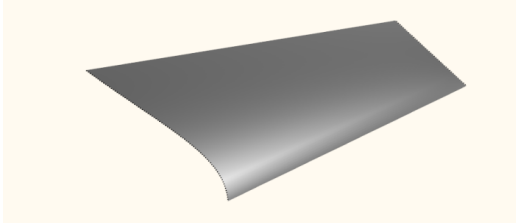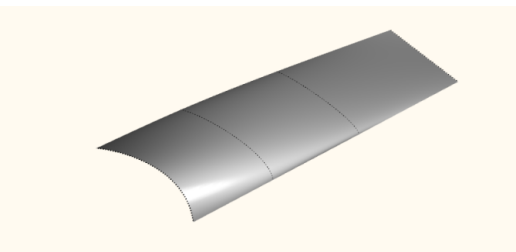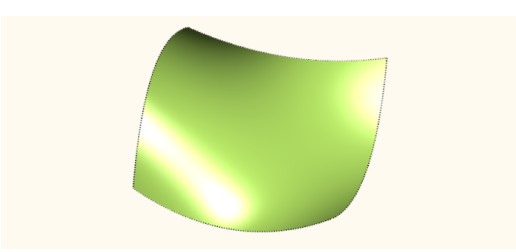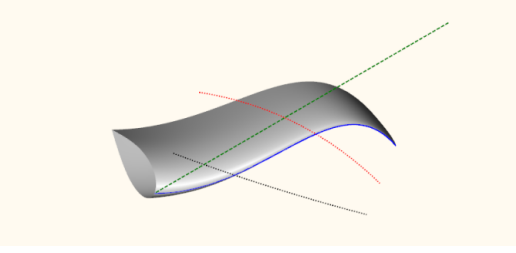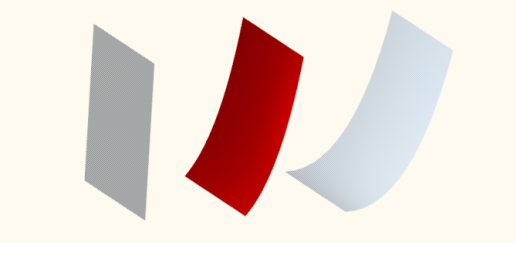
	• FLine**:** This simple curve type is defined by a vector-based start and end position.
	• FBSplineCurve: This is B-Spline (short for Basis-Spline) curve defined by its degree and a set of control points.
	• FNurbsCurve: This is a NURBS curve (short for Non Uniform Rational B-Spline) defined by its degree, a set of weighted control points and a knot vector. The control points of type FVector3 affect the curve progression of the NURBS curve.
	• FSpline: This is a fairness-optimized curve of CAESES. In terms of a specified principal plane (2D) it allows to set the starting and terminating positions with their tangents as well as settings for the curve's area and centroid values.
	• FImageCurve: This type represents an image of an arbitrary curve (serving as source) along with one or more specified transformations.

	• FInterpolationCurve: This curve interpolates a set of given 3D points.
	• FIntersectionCurve: This entity represents an intersection curve between a parent surface and either another surface or a plane.
	• FPolyCurve: A polycurve puts together a set of single curves and can then be adressed with a single parameter interval.
	• FCurveEngine: The curve engine combines a "template" curve definition with a continuous description of this definition.
	• FSurfaceCurve: This curve represents a curve on a parametric surface where the underlying domain curve must be defined in the parameter domain of the surface.

4.3   Surfaces Definitions in CAESES s/w Framework

CAESES® uses 17 surfaces definitions for parametric design. In Table 4.2 are briefly presented only the surfaces that were used in project (CAESES documentation, 2015).

Table 4.2: Curves used for parametric design.

	• FRuledSurface: A ruled surface is a linear surface between two arbitrary curves (lines, circles, ellipses, B-Spline curves, NURBS curves, ...).
	• FLoftedSurface: This type is a surface between two or more arbitrary curves (lines, circles, ellipses, B-Spline curves, NURBS curves, ...), also known as skinning
	• FCoonsPatch: The Coons patch is a type of surface that is defined via four boundary curves.
	• FMetaSurface: This type of surface definition lets the user design its own surface parameterizations based on arbitrarily complex curve descriptions defined in FcurveEngine.
	• FInterspaceSurface: An interspace surface is the result of the linear interpolation of two point based surfaces.

4.4   Parametric Hull Form

The parametric ship design usually starts with setting the goal of the optimization process. Whether it is for the optimization of the AR in waves, calm water resistance, air resistance, strength analysis, suitable evaluation criteria are determined along with the necessary constrains. The next step is the determination of the desired design variables. The design variables can be global, affecting the whole design (length of ship, beam of ship, C_B, etc.) or local, affecting specific regions of design. Design parameters must be directly or indirectly involved in the evaluation criteria or constrains. This is the background of a parametric model.

Afterwards, like in conventional CAD, the Center Plane Curve (CPC), Flat Of Bottom (FOB), Flat Of Side (FOS), design waterline and deck are determined. After the basic lines, surfaces are created, with special treatment in difficult areas such as bulb or stern tube, according to the desired shape of sections and desired parameters. The last step is the evaluation of the range of parameters that give feasible models. If the range is not the one desired, the process starts again.

Usually it requires more than one iteration to reach the desired parametric model. The difficulty hides in the requirement to reach smooth surfaces and connections. While for conventional model that's straightforward, it's not for parametric model, because it's necessary to predict the behavior of parametric model and verify that the model works properly and provides realistic results. Without adequate experience that's not easy. This makes the creation of parametric model the most difficult part of optimization process.

In this project, the iterations were performed with increasing number of parameters. During the first iteration the hull of the reference vessel was created (KVLCC2). In the next iteration the first parameter was introduced. After ensuring that the model works properly with one parameter, the second parameter was introduced. Then the feasibility of the design for extreme and intermediate values for both parameters was checked. If the results were unfeasible, the model changed appropriately. The procedure continued for the third, fourth, etc. parameter. After the introduction of the last parameter, the whole range of possible solutions was evaluated using Sobol functions and the feasibility of all designs, was checked. After that, the procedure was terminated.

The algorithms for the creation of parametric model can be observed in Figure 4.1 and 4.2.
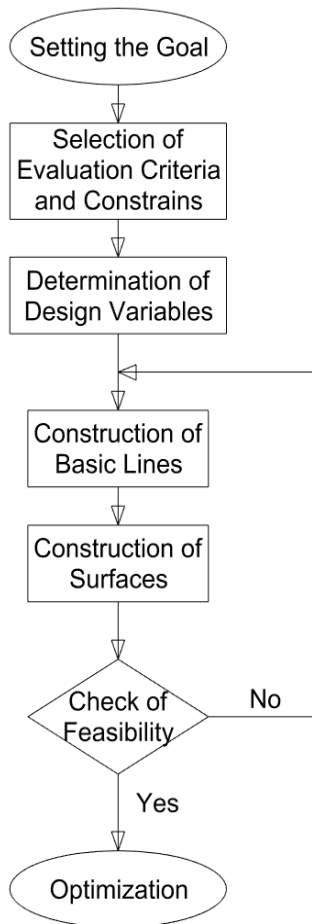
Figure 4.1: Algorithm for creation of parametric model.
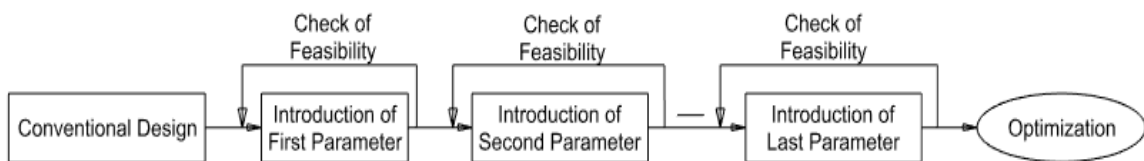
Figure 4.2: Algorithm of iterations for parametric model.

5   Ship's Design Optimization

5.1   Introduction

Optimization is the selection of a best element (with regard to some criteria) from some set of available alternatives (Wikipedia, 2015). In the simplest case, an optimization consists of maximizing or minimizing a real function by systematically choosing input values from within an allowed set and computing the value of the function (Wikipedia, 2015). More generally, optimization includes finding "best available" values of some objective function given a defined domain (or a set of constraints), including a variety of different types of objective functions and different types of domains (Wikipedia, 2015).

Optimization is an activity strongly connected with human nature (Nowacki, 2003). Our ancestors had to find the best weapon for hunting, the best way to cultivate crops, the best place to rest in order to survive in difficult environment. However, Greeks were the first to solve optimization problems related to their geometrical studies using scientific approach. 300 BC Euclid considers the minimal distance between a point and a line, and proves that the square has the greatest area among the rectangles with given total length of edges. In the medieval ages only few separate optimization problems were investigated. In 17th century, I. Newton and G.W. Von Leibniz created mathematical analysis that forms the basis of calculus of variations. In 19th century were presented the first optimization algorithms and optimization became the integral part of economic theory. After the World War II the field of algorithmic research expanded as electronic calculation developed. In the 80s of the last century, increased efficiency of computers lead to greater popularity of heuristic algorithms for global optimization. (Mitrikitti, 2015)

Today optimization is used in mechanics, economics, electrical engineering, operations research, control engineering, geophysics, petroleum engineering and of course ship design. Optimization leads to reduction in construction and operations costs, engineering time, increased safety and profits. Optimization is a necessary tool for every engineering problem.

5.2   Optimization in Naval Architecture

Traditional approach to ship design was more art than science. It required naval architects, with good background in various fundamental and specialized scientific and engineering subjects and experience. The designs were strongly attached to the previous, while the new designs were evaluated through a process of trial and error, often over the course of decades (A. Papanikolaou, 2009).

Since the middle 1960s, however, advance of computer hardware and software together with development of computer-aided design allowed the introduction of optimization to ship design. By using parametric hull forms, ships hulls can be optimized for least resistance in calm water and best sea-keeping behavior. Ships midship/structural design can be optimized for least steel weight. As time passed, the computer and hardware tools have evolved enough to be able to optimize ship in a holistic way, or by addressing and optimizing several and gradually all aspects of ship's life, at the stages of design, construction, operation and recycling.(A. Papanikolaou, 2009).

There are, in principle, two methods of approaching optimization problems (H. Schneekluth &V.Bertram, 1998):

1. Direct search approach

   Solutions are generated by varying parameters either systematically in certain steps or randomly. The best of these solutions is then taken as the estimated optimum. Systematic variation soon becomes prohibitively time consuming as the number of varied variables increases. Random searches are then employed, but these are still inefficient for problems with many design variables.

2. Steepness approach

   The solutions are generated using some information on the local steepness (in various directions) of the function to be optimized. When the steepness in all directions is (nearly) zero, the estimate for the optimum is found. This approach is more efficient in many cases. However, if several local optima exist, the method will 'get stuck' at the nearest local optimum instead of finding the global optimum, i.e. the best of *all* possible solutions. Discontinuities (steps) are problematic; even functions that vary steeply in one direction, but very little in another direction make this approach slow and often unreliable.

Very often it's necessary to optimize for more than one objective. It's also referred in literature as 'multi-criteria optimization'. Then it's understood as approximating or computing all or representative set of Pareto optimal solution. (Wikipedia) Pareto optimal solution, is a state of allocation of resources in which it is impossible to make any one individual better off without making at least one individual worse off. (Wikipedia) In other words, it's impossible to improve one objective without degrading the achievement of other (Priftis, 2015).

Multi-objective optimization can be easily transformed to one criteria optimization. There are two methods to achieve that (H. Schneekluth &V.Bertram, 1998):

1. One criterion is selected and the other criteria are formulated as constraints.

2. A weighted sum of all criteria forms the optimization objective. This is an 'optimum compromise'. The selection of weights is quite arbitrary.

5.3 Hull Form Optimization

A special problem during ship design is hull form optimization. Usually, this is done with respect mainly to calm water resistance or propulsion power and secondly with respect to behavior in waves. Obviously, the goal is to reduce calm water resistance and ship motions and/or AR in waves.

In order to reap real benefits from hull optimization, it is necessary to define properly ships operational profile. Ships travel at different drafts. For instance tankers travel loaded with oil from Persian Gulf to Europe, and with empty cargo holds from Europe to Persian Gulf. This incurs great difference in operational drafts, as can be seen in Figure 5.1. Ships also travel at different speeds as can be seen in Figure 5.2 and due to the practice of slow-steaming the most probable operational speed is shifted to lower speeds. Thus it's impractical to optimize only for design conditions. It's necessary to optimize ships hull for several conditions (i.e. 4 x speeds and 3 x draughts)(Fradelos, 2015). For realistic optimization of hull shape it is also necessary to predict correctly the sea states, that the ship will encounter. This can be done by assuming sea route and finding the most probable sea states on this sea route. For instance optimization of AR can be performed for R_{AWM}, while the most probable sea states induce mostly R_{AWR}.
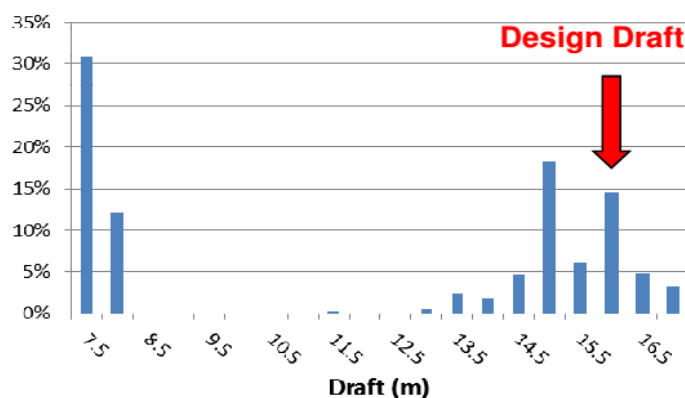
Figure 5.1: The probability of tanker draft during operation.(Fradelos, 2015)
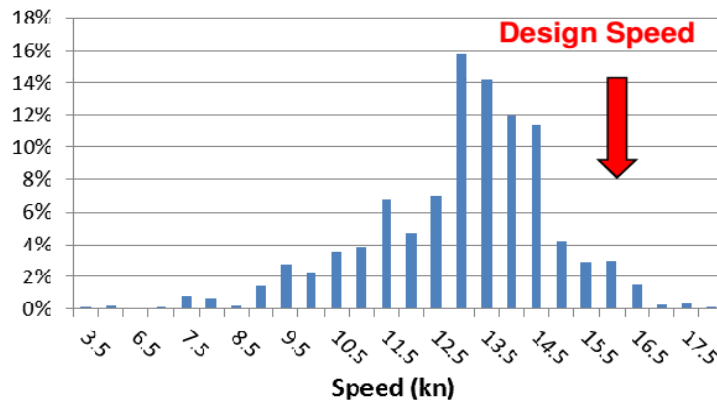
Figure 5.2: The probability of tanker speed during operation.(Fradelos, 2015)

During hull optimization it's necessary to consider superposition of transverse wave pattern: bow wave pattern, fore shoulder wave pattern, aft shoulder pattern, stern wave pattern. Also it's desirable to achieve good flow at aft shoulders of ship and to avoid flow separation at stern. Furthermore it's necessary to achieve favorable flow to propeller and rudder to improve propulsion. Last but not least, it's important to constrain wetted surface, because resistance is linear to wetted surface, especially for ships operating at low Froude numbers (Papanikolaou 2014).+

One of the most important area of hull for optimization is bulb. Bulb is a protruding surface under design waterline at the fore peak (Figure 5.3). The significance of bulb is that it reduces wave resistance by superposition two wave patterns to cancel out the effect of both, as can be seen in Figure 5.3. The optimization of bulb can reduce resistance even 8%, without changing main dimensions (Fradelos, 2015). Unfortunately, bulb works well only under specific conditions (speed, draft) and for specific ship. For different speed and draft the results can be opposite. That's why it's necessary to know exactly the operational profile.
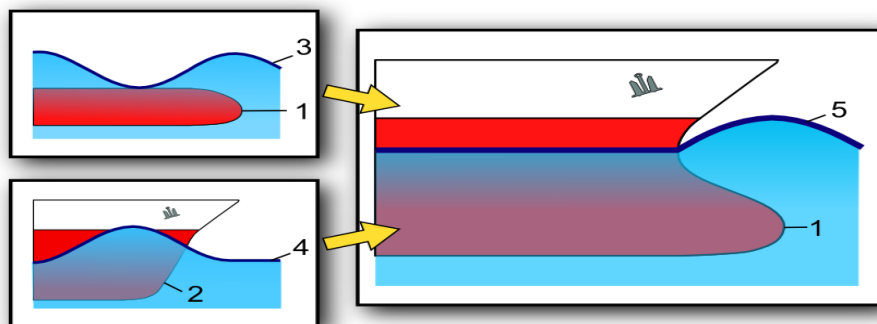
Figure 5.3: The effect of bulb. (Passy's World of Mathematics, 2015)

Another important parameter in hydrodynamic optimization at bow of ship is length of entrance of section area curve. This length of entrance defines the position of forward shoulder of ship. The correct position of forward shoulder is important in order to achieve superposition of bow wave pattern with shoulder.

At stern a special area of consideration is Stern End Bulb (SEB). SEB is a bulb-shaped structure which can be installed at the stern end of a ship to reduce both wave-making and eddy-making resistance. (The Free Dictionary). The optimization at SEB is claimed to offer a reduction in resistance in the range of 5% to 7% (Karafiath, 2011).

Other factors also affect resistance in calm water such a position of LCB, length of parallel body, section area curve distribution, the shape of sections at stern and bow, waterplane coefficient C_{WP}. For optimization of propulsion power it's necessary to introduce the impact of appendages on resistance, on wake fraction and thrust deduction (Papanikolaou 2014).

AR in waves is concentrated primary at the bow region (Guo, Steen 2011). Hull shape at stern has only a small impact on R_{AWM}, while R_{AWR} is created at the bow around waterline. In this way the parameters affecting the waterline at the bow, such as waterplane coefficient C_{WP}, length of entrance of waterline L_E, entrance angle of waterline, have great impact on AR. Also other parameters such as flare angle and hull shape beneath and above waterline like bulb and stem shape affect the AR. For instance straight stem seems to affect positively AR. (Lee J. et al 2015).

Last but not least, during hull optimization it's necessary to take into account other design constrains. For instance for containers, the number of containers, that can be loaded in such design, for tankers cargo hold capacity, EEDI of design, construction costs and recycling, maneuverability of design, safety issues. All these factors combined can lead to a viable and eco-friendly solution.

5.4   Design of Experiment (DoE)

The Design of Experiment (DoE) is receiving possible solutions by uniformly distributing design variables. The DoE is used before optimization in order to obtain better monitoring of possible solutions and to find the relationship between design variables and evaluation criterias.(Wikipedia, 2015) DoE is an expample of direct search approach.

A useful tool for the DoE are Sobol sequences. Sobol sequences are quasi-random low-discrepancy sequences introduced by the Russian mathematician I.M. Sobol in 1967. These sequences use a base of two to form successively finer uniform partitions of the unit interval,

and then reorder the coordinates in each dimension (Sobol 1967). As it can be seen in Figure 5.4 Sobol sequence covers the space more evenly than a pseudo random source.
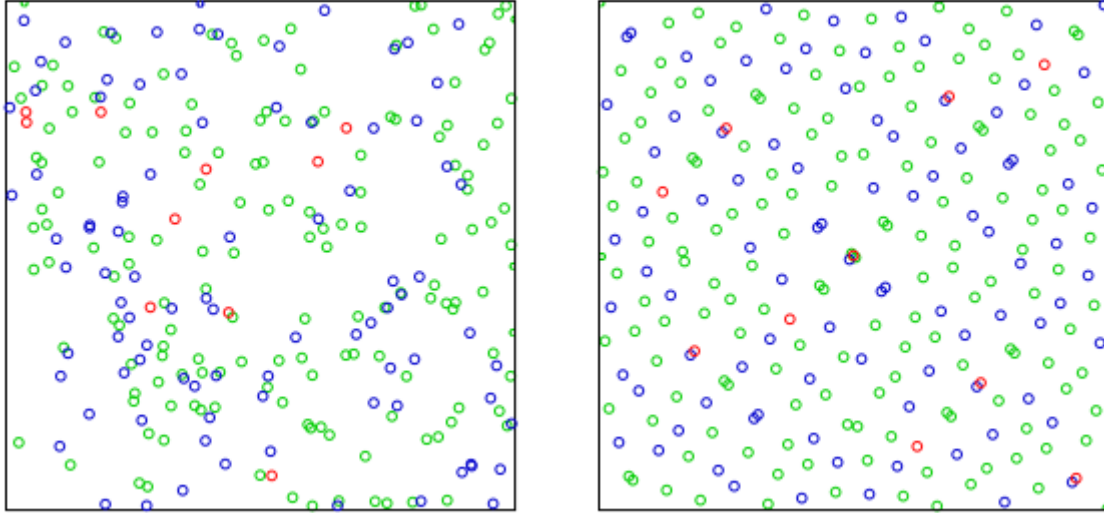
Figure 5.4: Comparison of Sobol(right) with pseudo random source (left). (Wikipedia,2015)

In CAESES® the DoE is performed by using ready Sobol design engine.

5.5   Genetic Algorithms (GA)

Genetic Algorithm (GA) is a search heuristic, that mimics the process of natural selection. This heuristic is routinely used to generate useful solutions to optimization and search problems. GA belong to the larger class of evolutionary algorithms which generate solutions to optimization problems using techniques inspired by natural evolution, such as inheritance, mutation, selection, and crossover.(Wikipedia) GA is kind of steepness approach to optimization.

The GA are performed as following (Malhotra et al 2011):

1. [Start] Generate random population of chromosomes, that is, suitable solutions for the problem.

2. [Fitness] Evaluate the fitness of each chromosome in the population.

3. [Selection] Select two parent chromosomes from a population according to their fitness. Better the fitness, the bigger chance to be selected to be the parent.

4. [Crossover] With a crossover probability, cross over the parents to form new offspring, that is, children. If no crossover was performed, offspring is the exact copy of parents.

5. [Mutation] With a mutation probability, mutate new offspring at each locus.

6. [Accepting] Place new offspring in the new population.

7. [Replace] Use new generated population for a further run of the algorithm.

8. [Test] If the end condition is satisfied, stop, and return the best solution in current population.

9. [Loop] Go to step 2.

The idea of using GA appeared in the middle of 20th century. In 1950, Alan Turing proposed a "learning machine" which would parallel the principles of evolution. In 1957, the Australian quantitative geneticist Alex Fraser published a series of papers on simulation of artificial selection of organisms with multiple loci controlling a measurable trait (Mitchel, 1996) . Genetic algorithms became popular through the work of John Holland in the early 1970s, and particularly his book Adaptation in Natural and Artificial Systems (1975). During the next years, dramatic increase in computational power of computers allowed wide use of new algorithms. (Wikipedia). Its applications cover a wide range of science, engineering and management fields: from CAD to process controllers, from bioinformatics to economics.

In CAESES® the GA are performed by using ready Non-dominated Sorting Genetic Algorithm II (NSGA II) design engine.

6 Optimization Case Study

6.1 Definition of the Optimization Problem

Conventional hull form optimization always involve calm water resistance as an objective. It's very rational, because fuel costs are by far the largest operating costs. But, as it was shown in chapter 2, ships seldom travel in calm water conditions. Thus, it's important to include effects of AR in hull form optimization.

The objective of this diploma thesis is to perform hull form optimization of KVLCC2 in the region of bow with criteria the AR in waves and secondary to optimize for total resistance by changing the local hull parameters. Another objective is optimization for different angles of waves heading, in order to understand what is the impact of course direction on ship design. Last, by using some simplifications, optimization of bow form with respect to EEDI is performed.

The aim of this thesis is to examine the impact of the hull form at the bow in the AR for a certain vessel, at a specified draft and speed. As mentioned in chapter 5.3, a more comprehensive analysis would require to examine also different drafts and speeds. The sea states of possible routes were simplified to EEDI spectrum.

It was shown in chapter 3, that for large ships, like KVLCC2, R_{AWR} contributes the most to AR. That's why the R_{AWR} will be calculated with the use of the most complicated formula, derived by Liu, Papanikolaou and Zaraphonitis (2015) as presented in Appendix B. The R_{AWM} is calculated using less complicated formula, while calm water resistance is estimated with Holtop method. All the calculation procedures are analytically described in chapter 6.3 and relevant appendixes.

The only constrain used in ships optimization was that for displacement (not to be lower than certain value). Other constrains, such as minimum propulsion power in adverse conditions, were introduced simply as an observable parameter. Their significance for the optimization process is discussed in chapter 7 and 8.

Based on that, the parameters for optimization problem were selected. Since AR is concentrated at bow, as was referred in chapter 5.3, all the parameters were selected in the bow region: There is one parameter for stem profile, one parameter for waterline entrance angle, two parameters affecting the area of waterline and one parameter for flare angle, affecting all bow sections. The developed parametric model is discussed in the following chapter.

6.2   Description of Parametric Model of KVLCC2

6.2.1   The Constant Part of KVLCC2 Model

The constant part of hull was constructed like in a conventional design. In the begging, all the design lines were created by interpolating available points for FOS, FOB, profile, and sections using available CAESES function. Then, these curves were faired to reach satisfying level of smoothness. In CAESES this was perfomed by substituting the initial FInterpolationCurves with FSplines merged in FPolyCurves or FBSplines. This was also necessary in order to free the parametric model from loading .txt file every time during initialization and to reduce computational time for optimization problems. In this way "skeleton" of aft part and parallel body of ship was created as can be seen in Figure 6.1. The two waterlines at the region of tube were approximated by using the available information from neighboring sections.
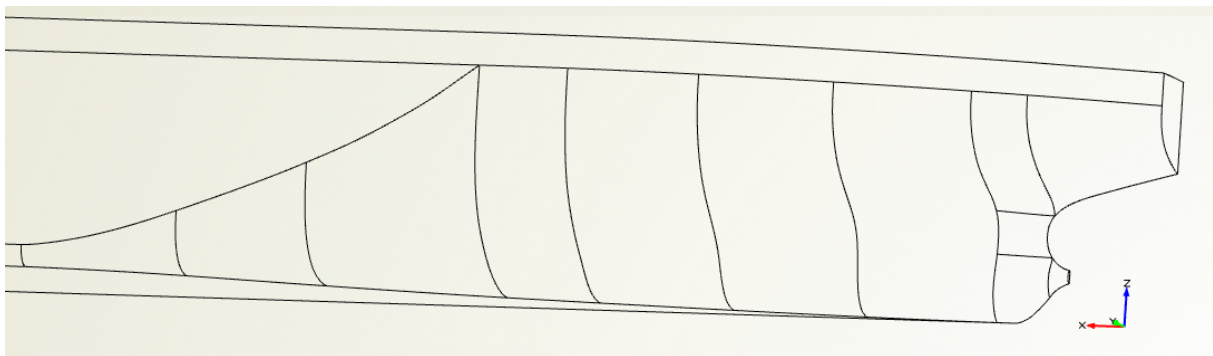
Figure 6.1: Lines used for aft of the ship.

As soon as these lines were created, the surfaces was created using FRuledSurfaces, FCoonsPatches, FLoftedSurfaces. The result can be seen on Figure 6.2. The surface was not totally smooth, especially in tube region. However this was neglected, because it in no way affects the calculations.
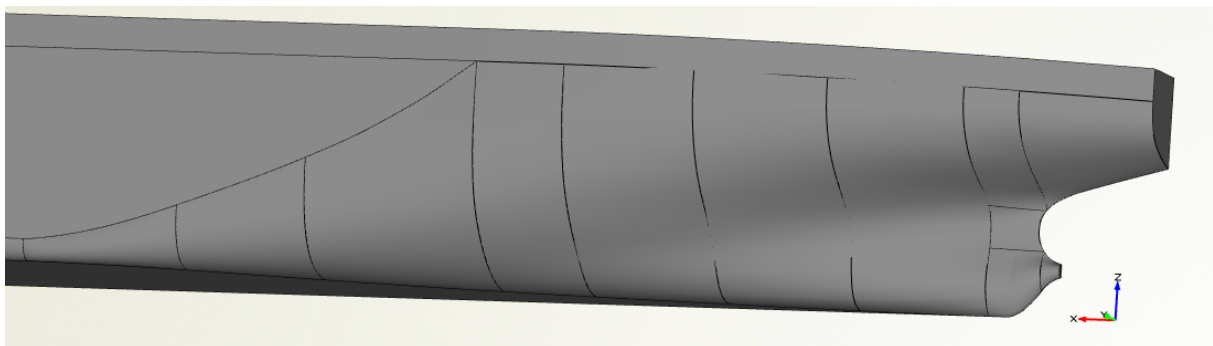
Figure 6.2: Generated surfaces at aft of ship.

6.2.2   The Parametric Part of KVLCC2 Model

At first stages in bow region the process was the same: import of points, interpolation of them by FInterpolationCurve, replacement with FSplines merged in FPolyCurves or FBSplines. Afterwards in specific hull areas design parameters were introduced as following:

<u>Stem</u>

The idea was to evaluate all possible stems between the initial and leadge bow (straight line at the end of bulb) as can be seen in Figure 6.3. For this reason, a FRuledSurface between leadge bow and the initial stem was created. By selecting the correct domain for FSurfaceCurve it's possible to take curve on Surface, interpolated between the leadge bow and initial stem, as can be seen in Figure 6.3. Zero value corresponds to initial bow, one to leadge stem and intermediate values to intermediate stems.
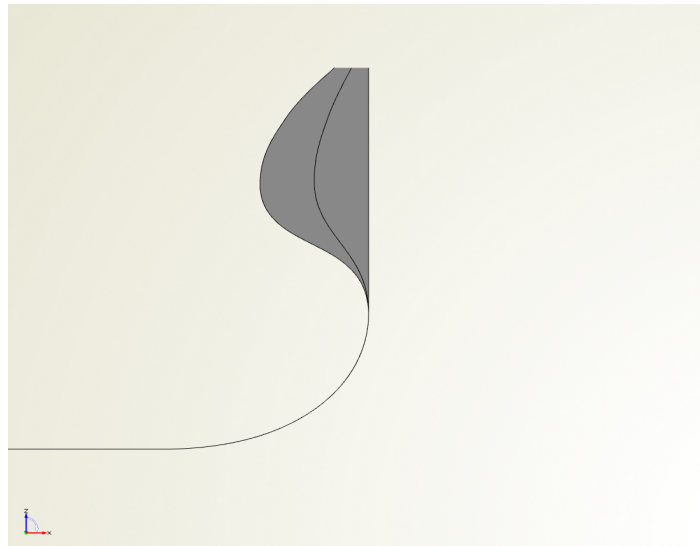
Figure 6.3: Interpolated stem.

<u>Waterline</u>

Waterline is represented by FBSplineCurve using 5 control points (Figure 6.4). The first point on the right is attached to the stem and every change of stem also affects waterline. The line connecting the first and second control point is tangent to the curve. This property of B-spline curves allows by defining the second point to define also angle of entrance of waterline and reverse, by defining the angle of entrance the position of second point is also defined. In the model, waterline entrance angle fluctuates between 50º and 70º.

For the third and fourth point the initial values were selected in order to assess in the best way the initial waterline curve. Then other two parameters, allowing their transfer were

introduced. One parameter allowed movement in x-axis for the third and fourth control point, 10 meters backward and 5 meters forward form the initial position. The another allowed till 1 meter movement in y-axis for the third point from initial position into outside direction. How these parameters affect the waterline can be seen on Figure 6.4. With orange is initial waterline, while with black after changing the parameters.

Figure 6.4: Design waterline.

In order to achieve smoothness of the surfaces created in the next steps, the waterlines above design waterline and waterline just beneath were sensitive to changes of the waterline. In other words, they were parameterized too, with suitable correction coefficients. This can be observed on Figure 6.5. With orange is new waterline, with black the changed. Also a correction was applied to account for change of stem. This correction was found empirically.
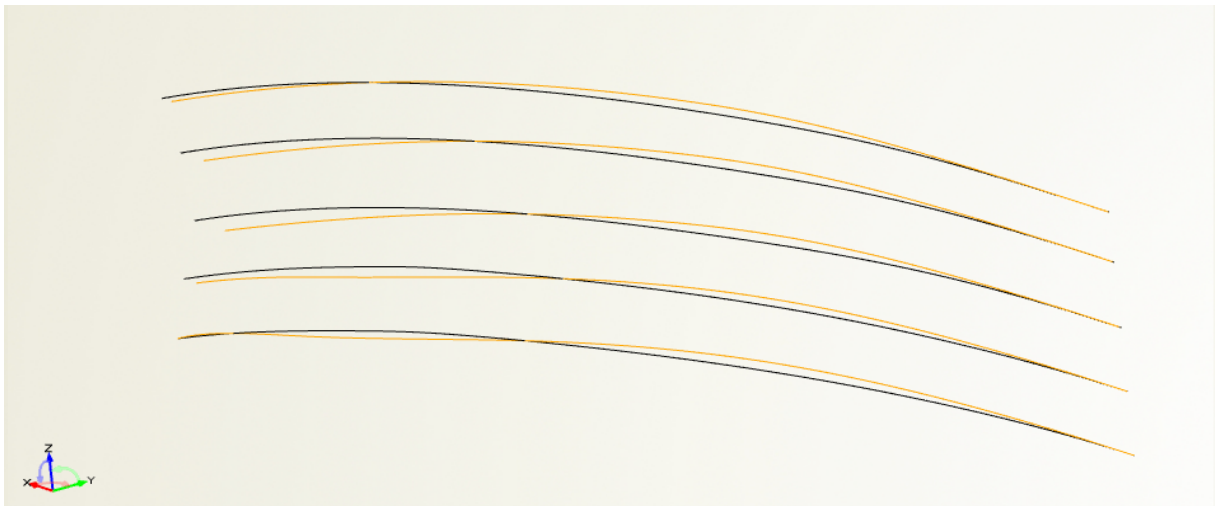
Figure 6.5: The parameterized waterlines and deck.

<u>Surfaces</u>

The resulting surfaces can be seen on Figure 6.6. The lowest part of ships bow was constructed with use of mixture of FMetaSurfaces, FConsPatches, FLoftedSurfaces. This part remained steady in every change of design parameters. The intermediate part consists of FMetaSurface (the lowest of the marked with orange colour) and two FConsPatches at the region of bulb. The up part consist of two different FMetaSurfaces: one at the fore peak and another between FOS and the first one (also marked with orange colour).
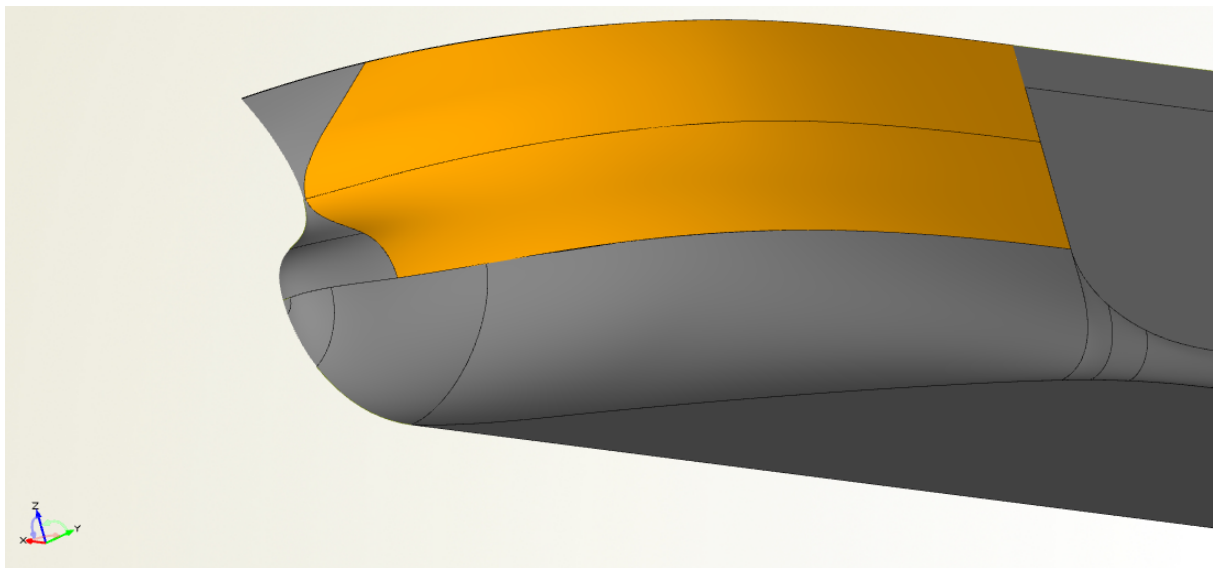
Figure 6.6: The bow of the ship.

The two FMetaSurfaces above were marked with the same colour, because they are important for optimization problem. The lowest of the two receives as input the waterlines down, intermediate (not seen in the figure 6.6) and up position as well as flare angle down and up. The flare angles were measured from the initial ship. The up flare angle of the lowest surface affects directly the problem of optimization. That's why this angle is parameterized. The parameter introduced here allowed evaluation of flare angle between maximum flare angle allowing smooth representation of the hull and straight walls as can be seen in Figure 6.7. The initial section is represented with black colour, the section with maximum flare angle with blue and the section with straight walls with purple. The orange horizontal line shows the position of waterline. The values for the flare angle parameter change between -1 for maximum flare angle and 0.99 for straight walls.

The up surface is constructed to have smooth connection with the previous one for every value of flare angle.
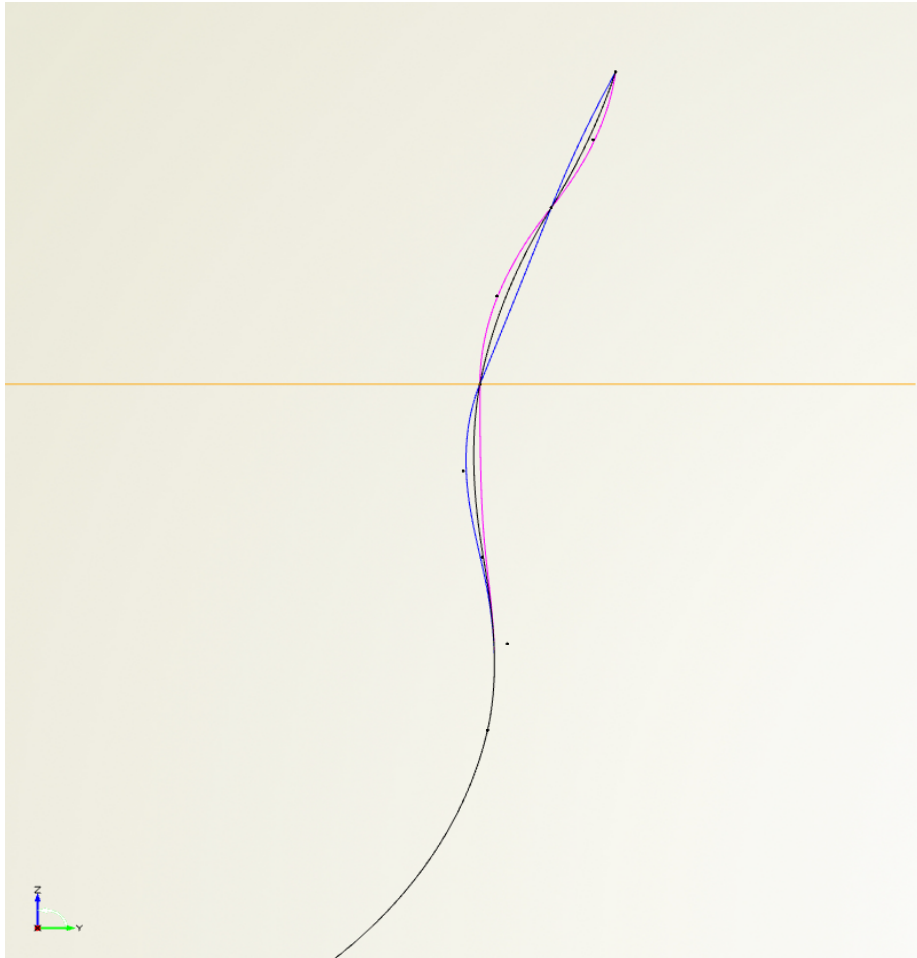
Figure 6.7: Various shapes of sections.

As it can be seen in Table 6.1 the deviation of created parametric model from the real model of KVLCC2 is very small. The difference in LCB % seems to be great, however in absolute values the difference is also small.

Table 6.1: Comparison of parametric model with initial KVLCC2.

	Initial Parametric Model of KVLCC2	Real Model of KVLCC2	% difference
Displacement [m^3]	310370	312622	-0.72
Wetted Surface [m^2]	27729	27194	1.97
C_B	0.8040	0.8098	-0.72
LCB (%) fwd+	3.19	3.48	-8.33
LCB [m]	170.19	171.14	-0.56

6.3 Calculation Procedures

The optimization is performed for R_{AWR} in different headings, for total resistance and for EEDI. Below are analyzed calculation procedures for each type of optimization. All the calculations were performed in CAESES by creating relevant features.

6.3.1 Optimization for R_{AWR} for Different Headings

R_{AWR} is calculated as in appendix C using EEDI spectrum for headings of 0°, 20° and 45°. The EEDI spectrum is defined as:

$$S(\omega; H; T) = \frac{As}{\omega^5} \exp\left(\frac{Bs}{\omega^4}\right)$$

$$As = \frac{Hs^2}{4\pi}\left(\frac{2\pi}{Tz}\right)^4 \qquad Bs = \frac{1}{\pi}\left(\frac{2\pi}{Tz}\right)^4 \qquad Tz = 0.920\,T$$

(6.1)

The significant height (H_s) and mean wave period (T) are equal to 3m and 6.7sec according to EEDI regulations.

All the necessary input (flare angle distribution, waterline, C_B, draft distribution, etc.) is automatically loaded to feature, specially programmed to calculate R_{AWR}.

6.3.2 Optimization for Total Resistance

The total resistance is decomposed as:

$$R_{total} = R_{calmwater} + AR_{waves} + AR_{wind} + AR_{fouling}$$

(6.2)

- $R_{calmwater}$ is calculated using Holtrop Method according to Appendix B. All the necessary input is created by CAESES and so every change in ships hull form is automatically transfered to Holtrop feature in CAESES.

- AR_{waves} is calculated as sum of R_{AWR} and R_{AWM}. R_{AWR} and R_{AWM} are calculated according to Appendix B for EEDI spectrum.

- AR_{wind} is found according to Appendix C using Beaufort 6 for wind speed definition. Wind speed for Beaufort 6 is taken equal to 12.6 m/s. For the estimation of AR_{wind} the parameters from similar ship were used as described in Table 6.2.

- $AR_{fouling}$ is estimated as 5% of calm water resistance according to Appendix D for 5 years between docking and assuming use of traditional antifoulings.

Table 6.2: Necessary input for estimation of AR due to wind.

A_T [m^2]	1216.4
A_L [m^2]	3532.6
L_{OA} [m]	332
B [m]	58
C [m]	-18.7

All the symbols are defined in nomenclature and in Appendix C.

6.3.3   Optimization for EEDI

EEDI is calculated assuming that there are no innovative technologies applied. Thus it can be expressed as:

$$EEDI = \frac{P_{ME}*C_{FME}*SFC_{ME}+P_{AE}*C_{FAE}*SFC_{AE}}{f_i*f_w*V_{ref}*DWT} \tag{6.3}$$

- The P_{ME} is found as 75% of MCR

- MCR is estimated as

$$MCR = SHP*SF \tag{6.4}$$

where

- SHP is power required for propulsion at calm water conditions and calculated as following:

$$SHP = \frac{V_{design}*R_{calmwater}}{PC} \tag{6.5}$$

- V_{design} is 15.5 knots=7.9732m/s,

- $R_{calmwater}$ is calm water resistance estimated with Holtrop at 15.5 knots

- PC is propulsion coefficient and is calculated as:

$$PC = \frac{1-t}{1-w}\eta_0\eta_R\eta_S \tag{6.6}$$

- The thrust deduction t, relative rotative efficiency η_R and wake fraction w are calculated using Holtrop-Mennen method. Efficiency of propeller in open water η_0 is assumed to have constant value of 0.66, while shaft efficiency is assumed to be 0.99.

- SF is safety factor representing Sea Margin. Here a simplification is made that it can be calculated as ratio of total resistance over calm water resistance at 15.5 knots. The total resistance is calculated as sum of calm water resistance, AR due to waves for Sea State represented by EEDI spectrum, AR due to winds for Vwind=12.6m/s and fouling increase 5% of calm water resistance.

- C_{FME} is set 3.114 for heavy fuel oil.

- SFC_{ME} is 155 gr/kWh according to project guide for WARTSILA X82.

- P_{AE} is found using EEDI guidelines as

$$P_{AE} = 0.025\text{MCR} + 250 \qquad (6.7)$$

- C_{FAE} is set 3.206 for diesel oil.

- SFC_{AE} is 210 gr/kWh for Watrsila Auxpac 16 at 50% load of MCR.

- The f_i correction factor is found as:

$$f_i = 1 + \left(0.08 \frac{LWT_{CSR}}{DWT_{CSR}}\right) = 1 + \left(0.08 \frac{Displ - DWT_{CSR}}{DWT_{CSR}}\right) \qquad (6.8)$$

- Displacement is found as:

$$Disp = 1.026 * Volume \qquad (6.9)$$

- Volume is directly computed in CAESES using FSectionGroup and FHydroComputation connection.

- DWT is estimated using regression analysis formula for tankers (Papanikolaou, 2014).

$$DWT = \frac{Disp - 4773.95}{1.1213} \qquad (6.10)$$

- V_{ref} is speed of ship at calm water conditions and engine output of 0.75MCR. Assuming that power is proportional to cube of speed and for calm water conditions the relationship between V_{design} and V_{ref} is

$$V_{ref} = V_{design} \left(\frac{0.75\,MCR}{SHP}\right)^{(1/3)} \qquad (6.11)$$

- Practically V_{design} and V_{ref} have the same values.

- The right determination of f_w requires calculation of AR using directional spectrum. Here a simplification is made, that AR due to waves can be estimated using only head

waves. For two speeds $V_1 = V_{ref} - 1.5$ knots and $V_2 = V_{ref} - 1$ knot total resistance except fouling increase is estimated. Using PC this can be translated into power. Assuming that the power is linear to speed in this small region, by using linear interpolation or extrapolation it's possible to calculate the reduced speed V_w. Then $f_w = V_w / V_{ref}$.

- The required EEDI is calculated as:

$$EEDI_{required} = 1218.80 \, DWT^{-0.488} \qquad (6.12)$$

The minimum required power for propulsion power is calculated following the guidelines of appendix F. The relevant input can be seen in Table 6.3. The propulsion parameters were estimated using Holtrop method. Ship particulars were loaded directly in CAESES to the relevant feature.

Table 6.3: Data for evaluation of maneuverability.

Hs [m]	5
n_{MCR} [rpm]	75.263
K_{Q0}	0.03133
K_{T0}	0.3117
Dp [m]	9.86
C_L	1.31
$A_R{}^S$ [m^2]	82.275

6.4   Settings for DoE and GA

The optimization is performed in two stages.

Firstly is conducted a DoE using Sobol functions in order to examine design space and the response of parameters to the change of the model parameters. In this case, for every optimization 100 variants of the model were created. This number allows to provide reasonable value of Pearson's correlation coefficient r. For instance, if there is no linear correlation between correlation parameters at all (r=0), then 80% of the time Pearson's relation coefficient will fall between -0.13 and 0.13. (Graham, 2015) The design variables, including both the base model's and the extreme values are presented in Table. 6.4

The next step is finding of the optimum solution using GA. In this case NSGA II algorithm is used. In every optimization case a number of 32 variations was used for a generation. Ten generations were used to find the most suitable case. In each case a constrain for displacement was used. For EEDI calculation also a constrain requiring that attained EEDI is smaller than required EEDI. The requirement for minimum propulsion power was used as an additional calculated parameter, not as constraint. The constraints used are presented in Table. 6.5. After the best solution is found by using GA, the final optimized hull is explored using trends found by Sobol functions near by the solution proposed by GA.

Table 6.4: The boundaries of design variables.

Design variable	Min. Value	Base Model Value	Max. Value
Flare angle parameter	-1	0	0.99
Dx for 3rd and 4th waterline control point	-10	0	5
Dy for 3rd waterline control point	0	0	1
Waterline entrance angle	50°	62.2°	70°
Parameter for leadge bow	0	0	1

Table 6.5: The constrains used.

Constrain	Value
$EEDI_{attained}/EEDI_{required}$	<1
Volume [m^3]	>308000

7 Results

7.1 Introduction

In this chapter are presented the results of the optimization problem defined in 6.1, that were produced using parametric model discussed in 6.2, following calculation procedures presented in 6.3 and taking into account the settings and constrains of the optimization problem as referred in 6.4. First, the relevant calculation for the base model are presented. Next are presented the graphs showing the relationship between design variables and optimized parameters. Last the result of optimization problem is presented and compared with the Base Model (BM).

7.2 Base Model (BM)

The particulars of the Base Model (BM) can be seen in Table 7.1. The results of the calculation are presented in Table 7.2. The bow shape of BM can be seen in Figure 7.1.

<p align="center">Table 7.1: The particulars of BM.</p>

L_{BP} [m]	320.00
B [m]	58.00
T_M [m]	20.80
LCB [% L_{BP} from midship]	3.19
C_B	0.8040
Displacement [m^3]	310370
Wetted surface [m^2]	27729
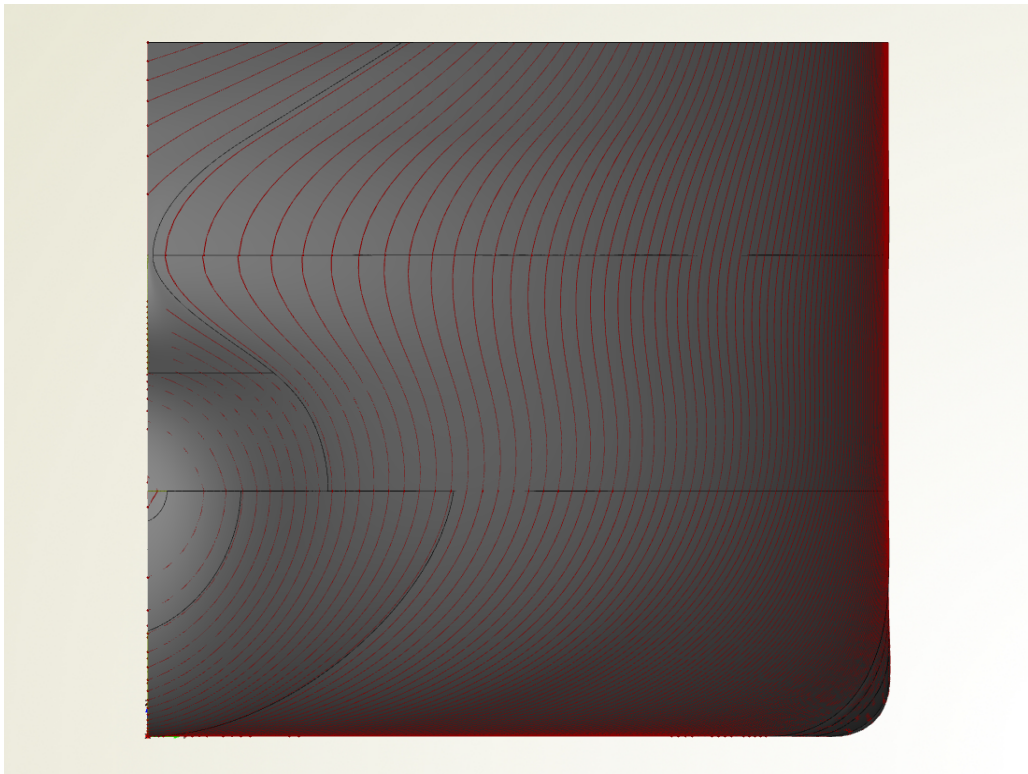
Figure 7.1: Initial bow of KVLCC2.
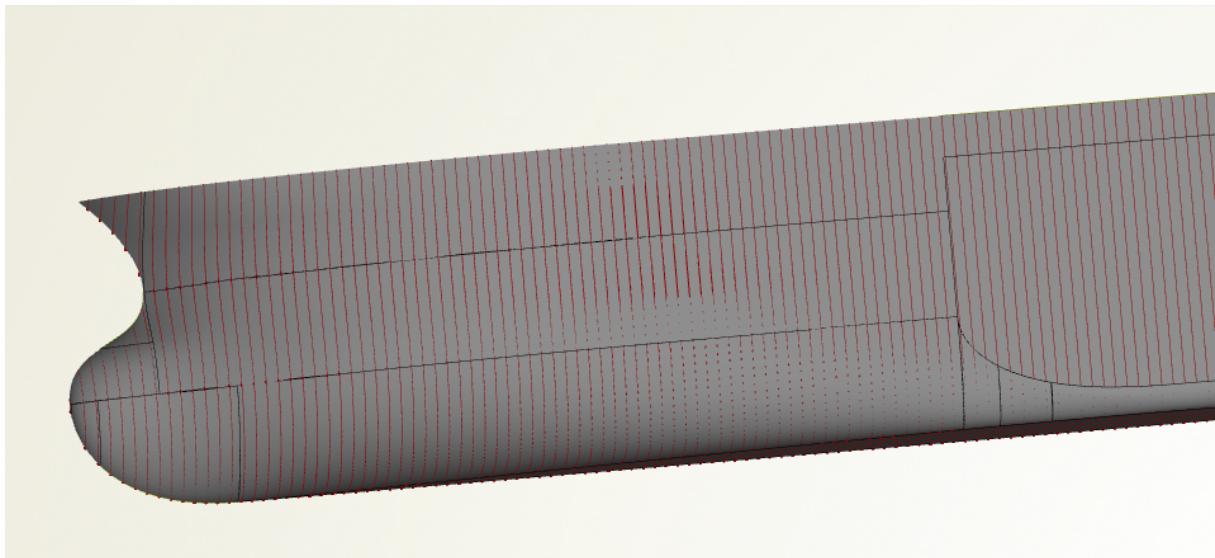
Figure 7.2: Initial bow of KVLCC2.

Table 7.2: Results for BM.

R_{AWR} for head waves [kN]	395
R_{AWR} 20º angle of waves [kN]	419
R_{AWR} 45º angle of waves [kN]	437
Total Resistance [kN]	2960
$EEDI_{attained}$	2.65
$EEDI_{required}$	2.67
$EEDI_{attained}/EEDI_{required}$	0.99
MCR [MW]	27.57
MCRmin (regression curves) [MW]	24.20
MCRmin (SHOPERA) [MW]	25.08
DWT [t]	279739

The MCR of KVLCC2 here is higher than that estimated for VLCC by MAN (2013), although MAN also used Holtrop-Mennen method for estimation of resistance. The MCR for VLCC with similar speed and DWT is around 25MW, while for the BM here 27.57MW. The difference can be explained by different relationship between SHP and MCR in this diploma thesis and in MAN publication. MAN assumes a sea margin of 15% of SHP and an additional engine margin of 10% i.e. a service rating of 90% SMCR, including 15% sea margin. This results in ratio between SHP and MCR calculated as following:

$$\frac{MCR}{SHP} = \frac{(1.15\,SHP/0.9)}{SHP} = 1.278 \qquad (7.1)$$

In this diploma thesis the ratio between MCR and SHP is equal to the ratio of total resistance at 15.5knots and calm water resistance at 15.5 knots. For the BM it's value is 1.371. By using the ratio between SHP and MCR equal to the 1.278 the MCR of BM would be 25.6 MW, closer to the values proposed by MAN. So this difference between MAN results and results of diploma thesis can be justified by more conservative approach to sea margin.

7.3 DoE

7.3.1 DoE of R_{AWR} in Different Headings
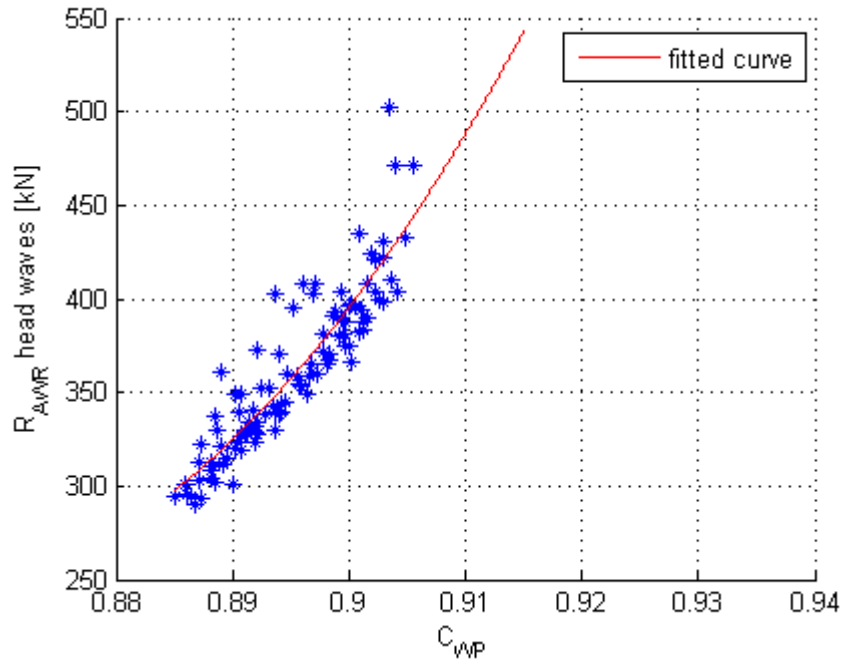
Figure 7.3: R_{AWR} in head waves for different C_{WP}.
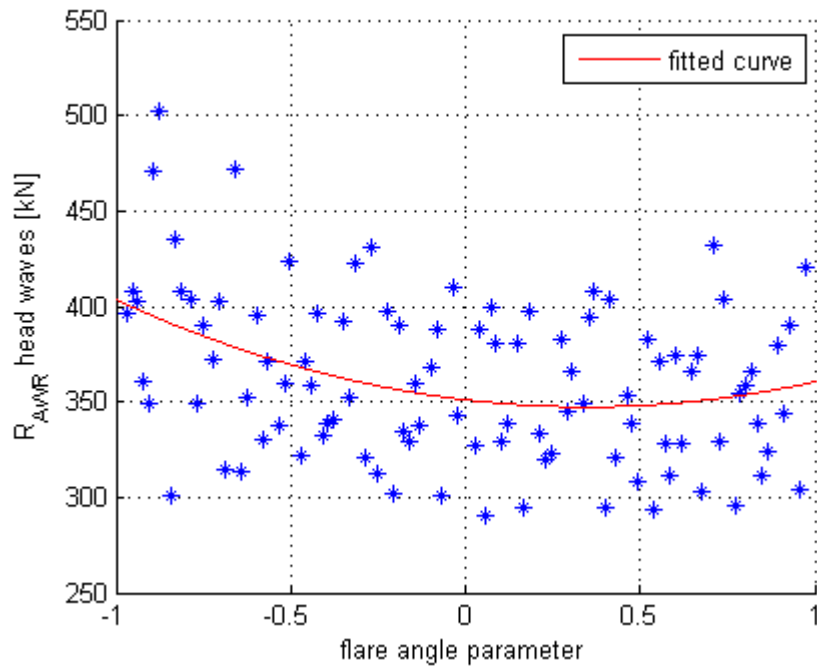
Figure 7.4: R_{AWR} in head waves for different flare angle between maximum (-1) and straight walls(1).
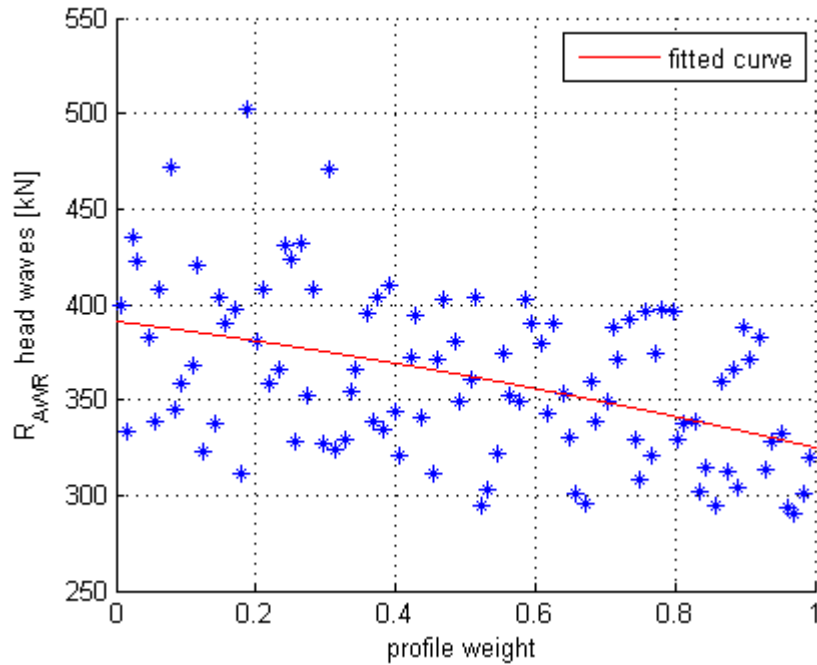
Figure 7.5: R$_{AWR}$ in head waves for different stem profile between initial (0) and leadge (1).
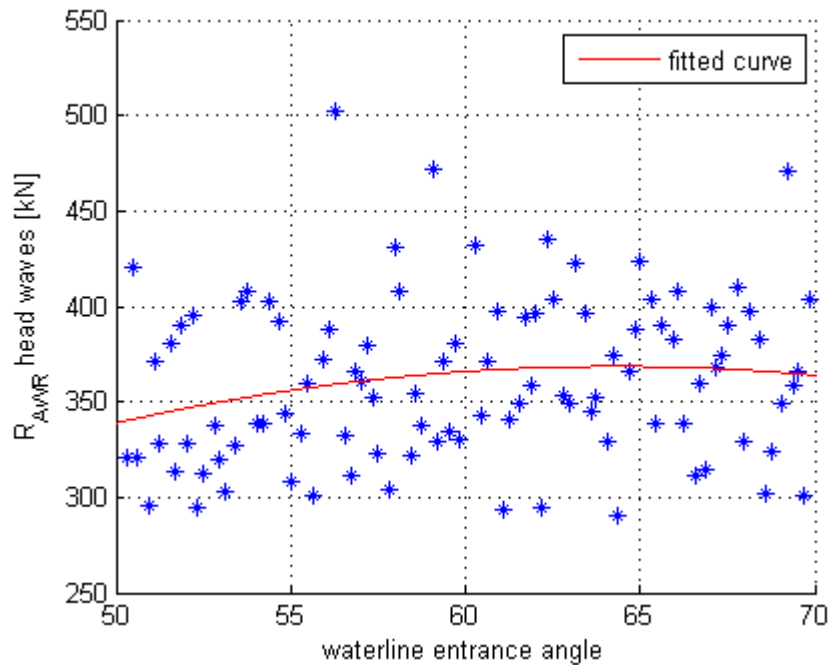
Figure 7.6: R$_{AWR}$ in headwaves for different waterline entrance angle.
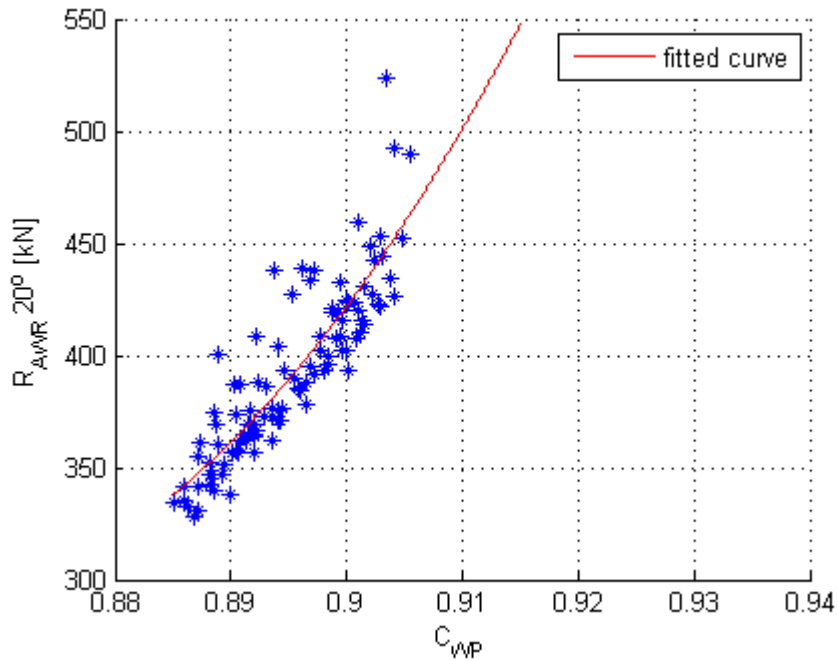
Figure 7.7: R$_{AWR}$ (20º) for different C$_{WP}$.
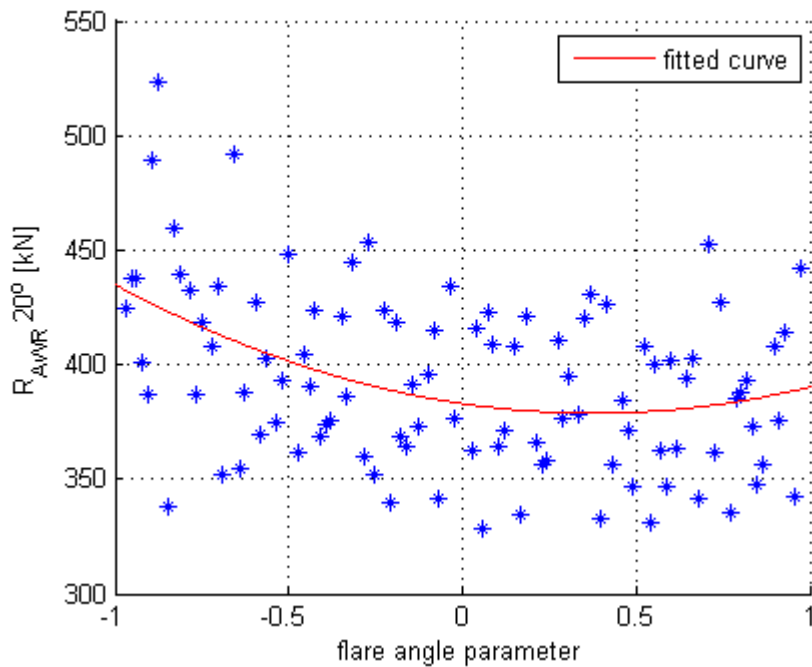
Figure 7.8: R$_{AWR}$ (20º) for different flare angle between maximum (-1) and straight walls(1).
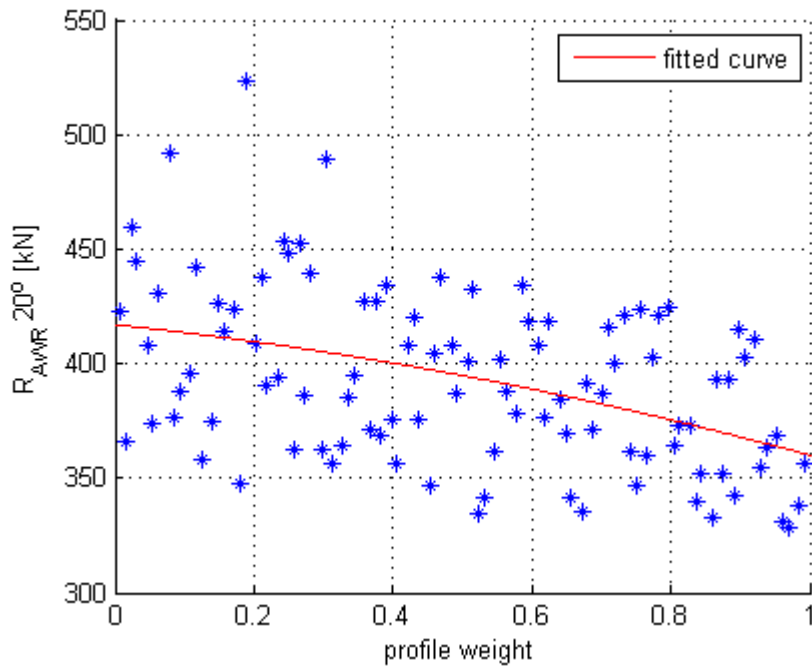
Figure 7.9: R_AWR (20º) for different stem profile between initial (0) and leadge (1).
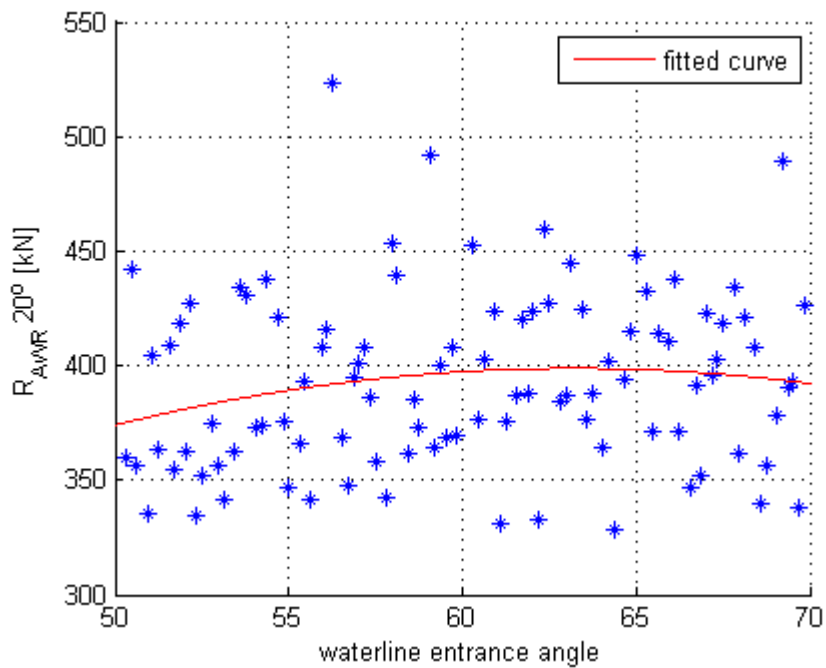
Figure 7.10: R_AWR (20º) for different waterline entrance angle.
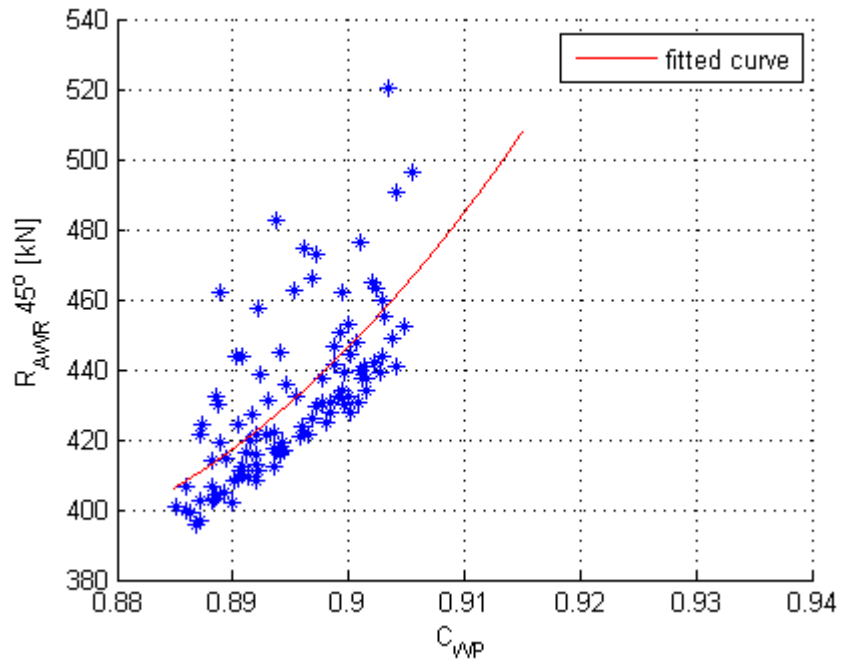
Figure 7.11: R$_{AWR}$ (45º) for different C$_{WP}$.
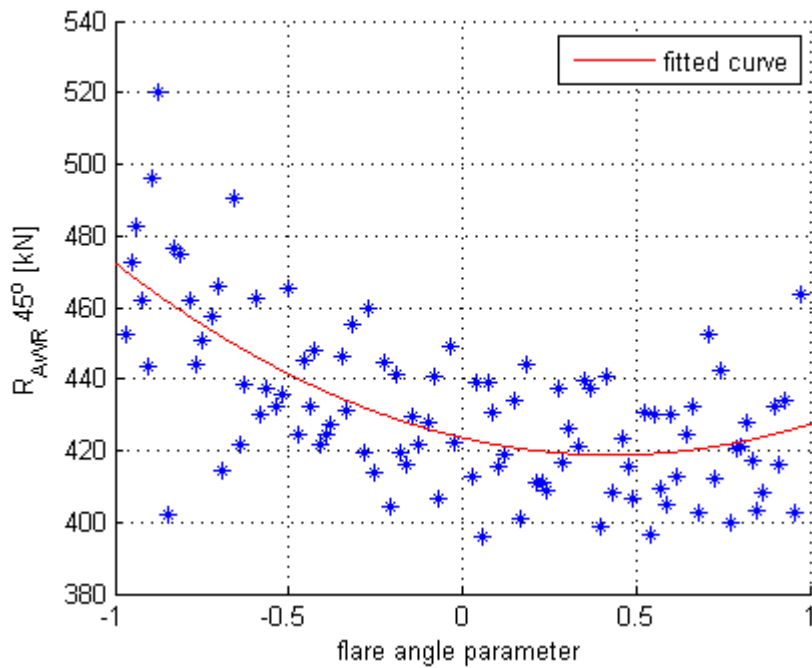
Figure 7.12: R$_{AWR}$ (45º) for different flare angle between maximum (-1) and straight walls(1).
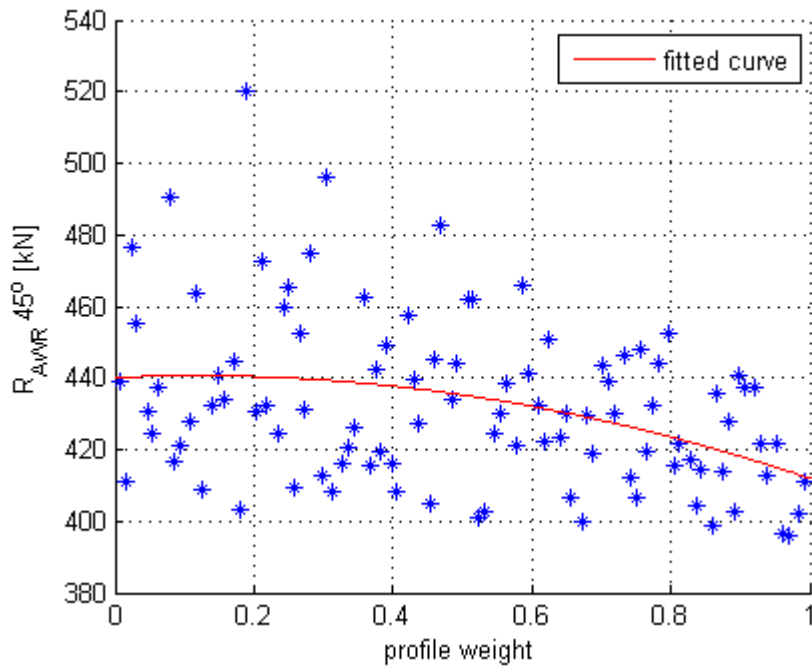
Figure 7.13: R$_{AWR}$ (45º) for different stem profile between initial (0) and leadge (1).
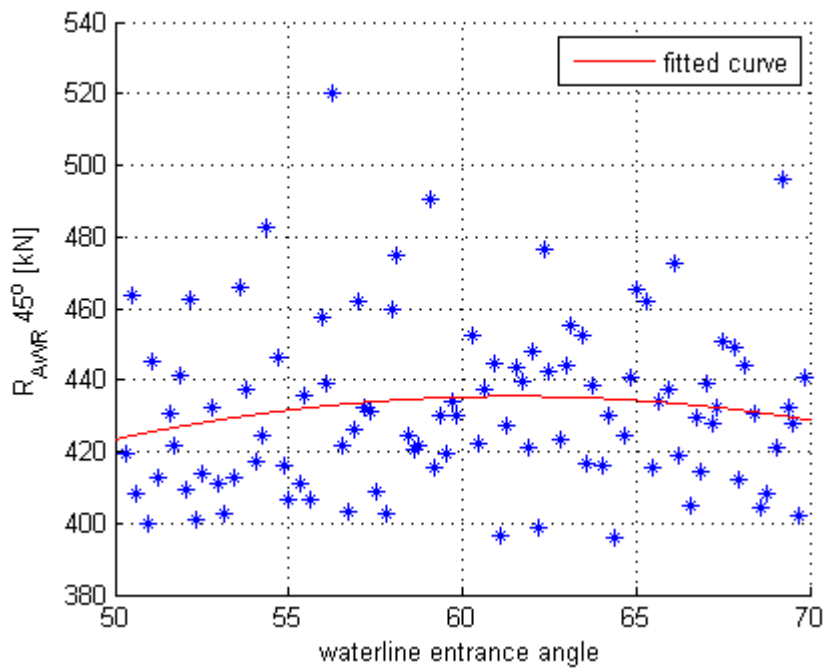
Figure 7.14: R$_{AWR}$ (45º) for different waterline entrance angle.

7.3.2   DoE for Total Resistance
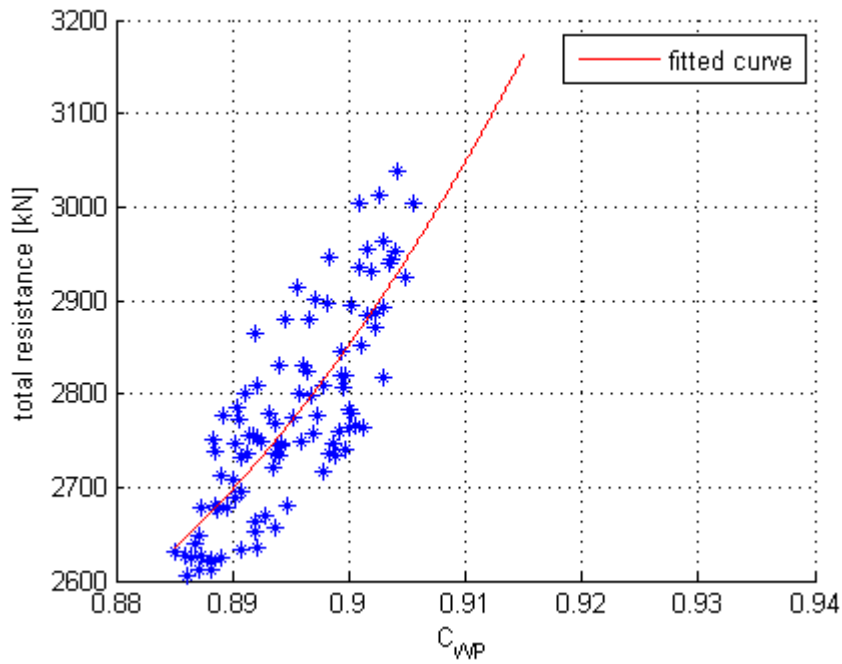
Figure 7.15: Total resistance for different C$_{WP}$.
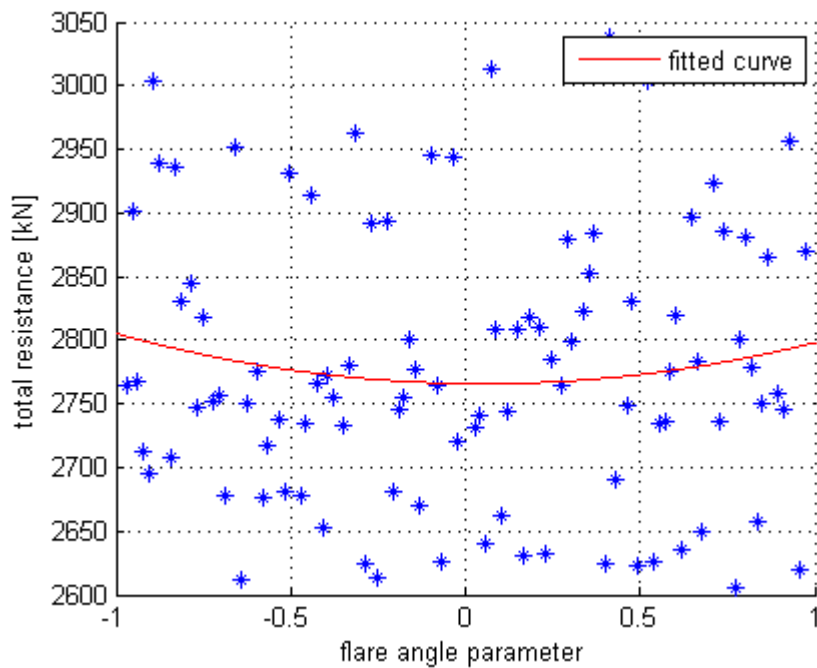
Figure 7.16: Total resistance for different flare angle between maximum (-1) and straight walls(1).
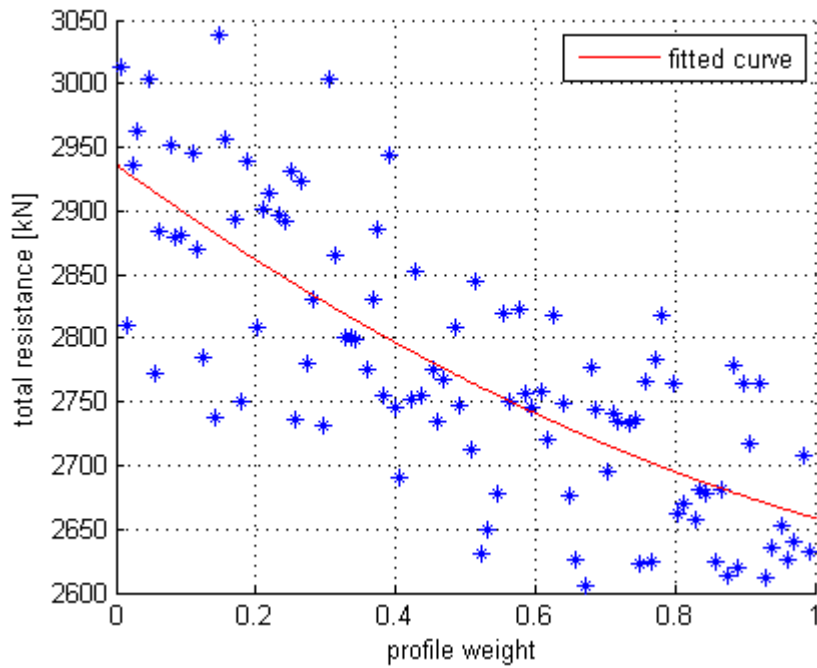
Figure 7.17: Total resistance for different stem profile between initial (0) and leadge (1).
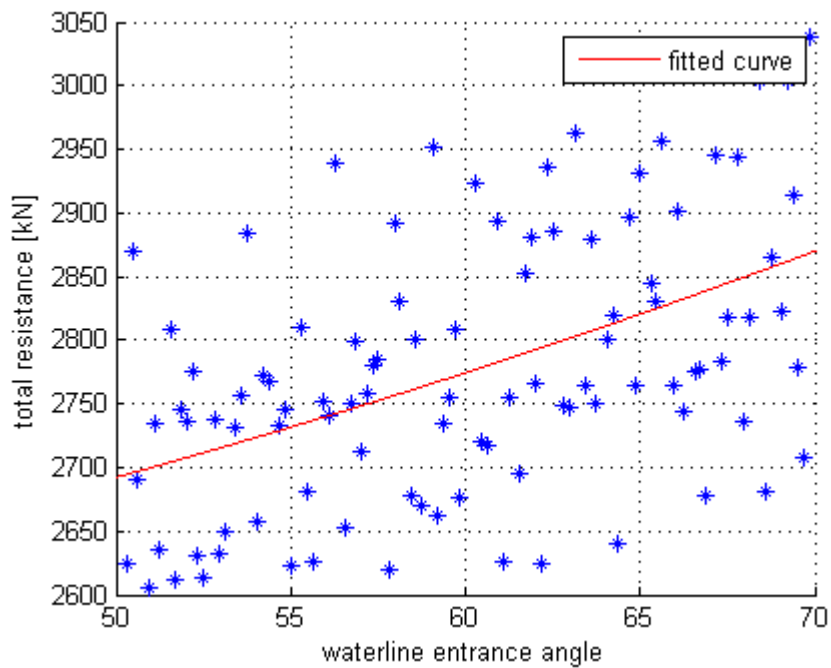
Figure 7.18: Total resistance for different waterline entrance angle.
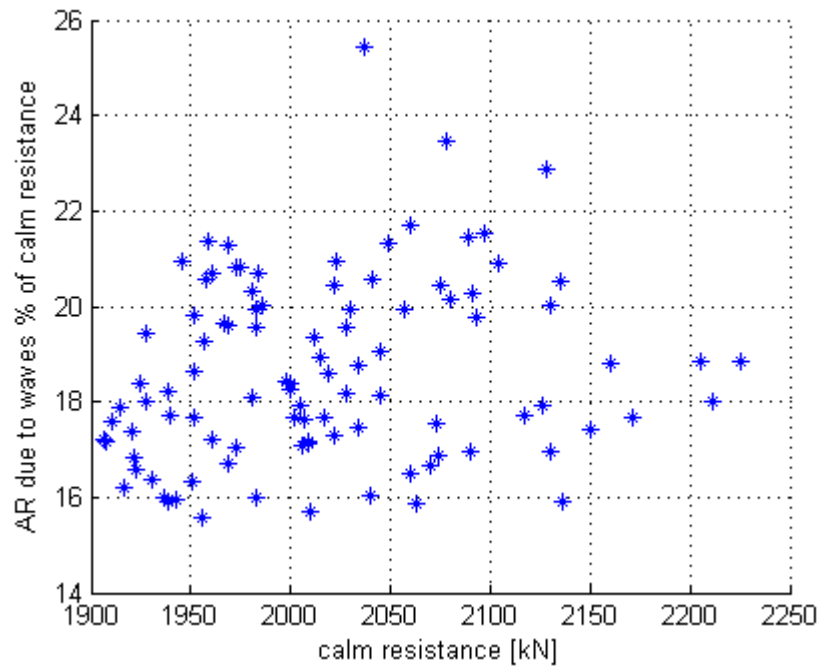
Figure 7.19: Relationship between calm resistance and AR due to waves in % of calm resistance.

7.3.3   DoE for EEDI
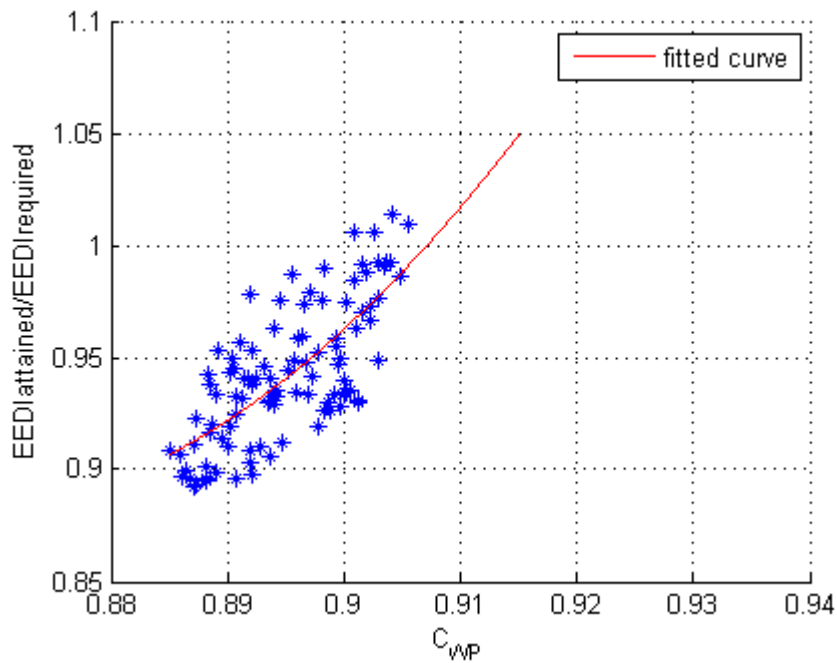
Figure 7.20: EEDI for different C$_{WP}$.
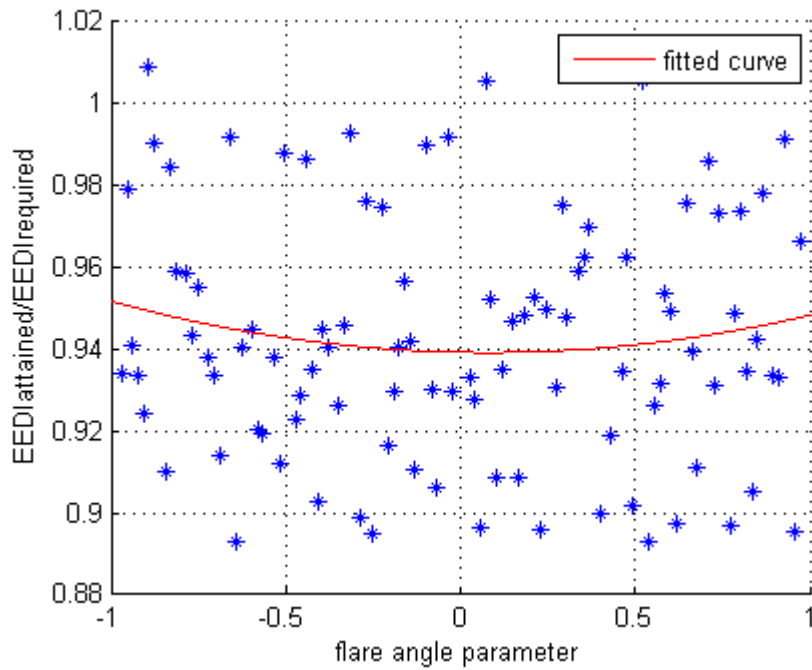
Figure 7.21: EEDI for different flare angle between maximum (-1) and straight walls(1).
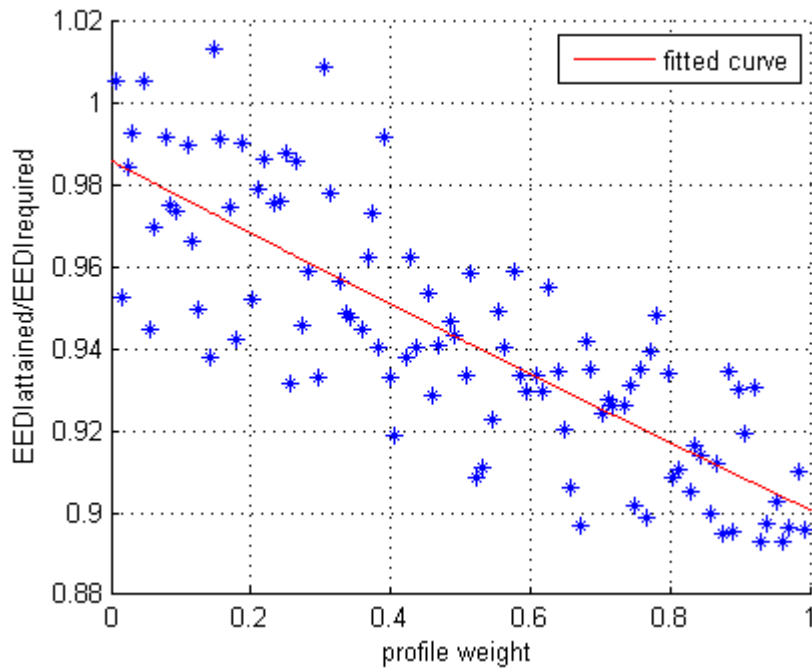
Figure 7.22: EEDI for different stem profile between initial (0) and leadge (1).
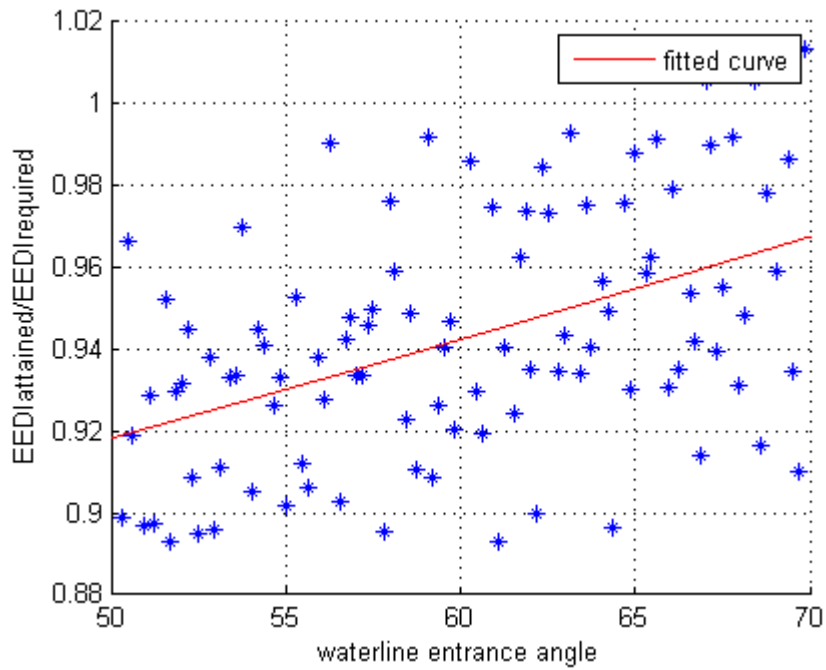
Figure 7.23: EEDI for different waterline entrance angle.
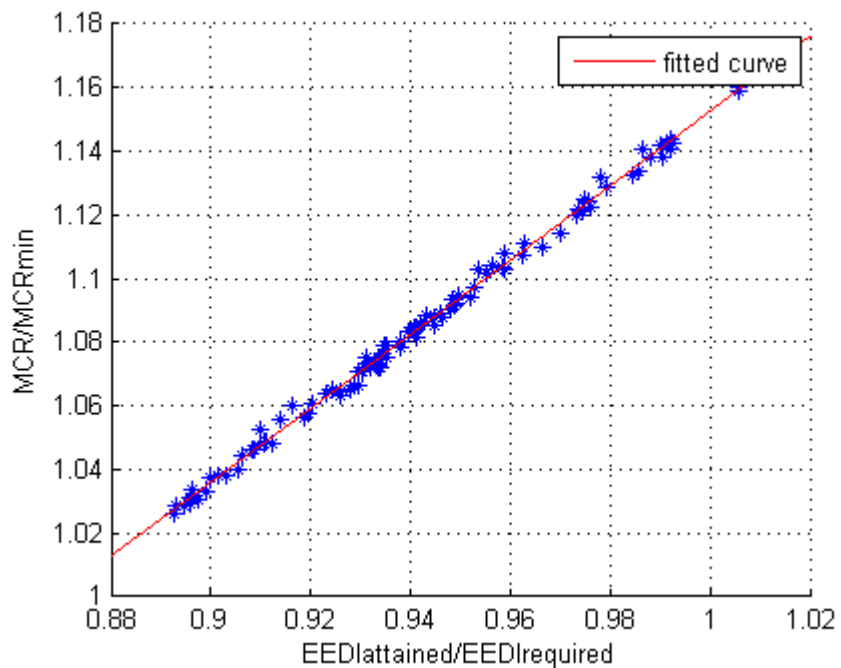
Figure 7.24: Relationship between requirement for minimum propulsion power and EEDI.
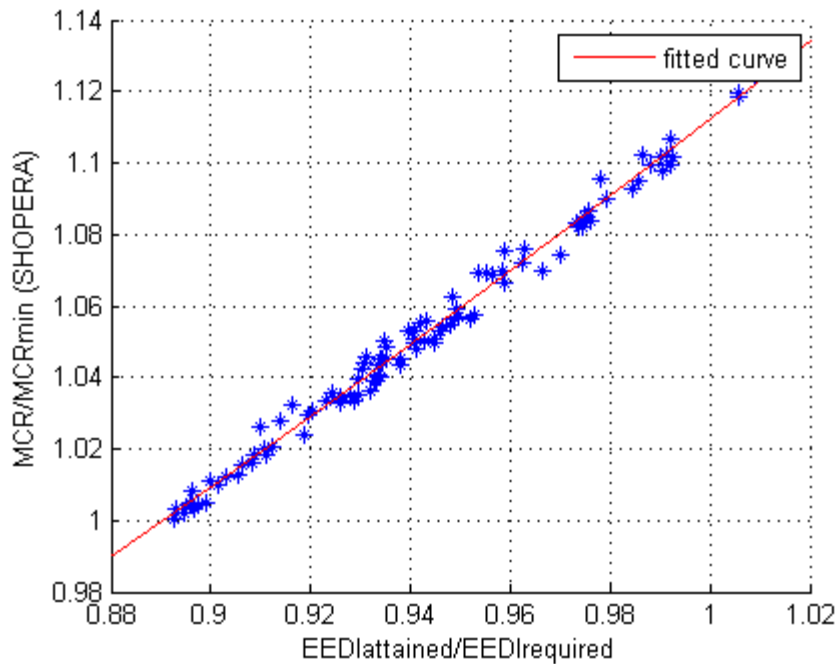
Figure 7.25: Relationship between requirement for minimum propulsion power according to SHOPERA and EEDI.

7.4   Comments on DoE

The results of application of Pearson's correlation coefficient between design variables and optimized parameters with standard error can be seen in Table 7.3. The interpretation of these parameters, using the guidance suggested by Evans (1996) can be seen in Table 7.4. The formula for Pearson's correlation coefficient, why it's justifiable to apply it here, the verbal characterization of correlation coefficients according to Evans (1996), as well as formula for standard error for correlation coefficient are presented in Appendix F.

Table 7.3: Pearson's correlation coefficient between design variables and optimized parameters.

	R_{AWR} head waves	R_{AWR} 20°	R_{AWR} 45°	Total Resistance	EEDI
Cwp	0.90±0.04	0.87±0.05	0.68±0.07	0.80±0.06	0.73±0.07
Flare angle parameter	-0.29±0.10	-0.34±0.10	-0.56±0.08	-0.02±0.10	-0.03±0.10
Stem profile parameter	-0.44±0.09	-0.43±0.09	-0.35±0.09	-0.76±0.07	-0.81±0.06
Waterline angle of entrance	0.16±0.10	0.13±0.10	0.06±0.10	0.48±0.09	0.47±0.09

Table 7.4: Interpretation of Pearson's correlation coefficient between design variables and optimized parameters.

	R_{AWR} head waves	R_{AWR} 20º	R_{AWR} 45º	Total Resistance	EEDI
Cwp	Very Strong Positive Correlation	Very Strong Positive Correlation	Strong Positive Correlation	Very Strong Positive Correlation	Strong Positive Correlation
Flare angle parameter	Weak Negative Correlation	Weak Negative Correlation	Moderate Negative Correlation	Very Weak Negative Correlation	Very Weak Negative Correlation
Stem profile parameter	Moderate Negative Correlation	Moderate Negative Correlation	Moderate Negative Correlation	Strong Negative Correlation	Very Strong Negative Correlation
Waterline angle of entrance	Very Weak Positive Correlation	Very Weak Positive Correlation	Very Weak Positive Correlation	Moderate Positive Correlation	Moderate Positive Correlation

It can be observed from the graphs and Pearson's correlation coefficients that for every optimization case with respect to R_{AWR}, independently from heading, the trends are as following: for smaller C_{WP} and leadge bow profile at stem the R_{AWR} is smaller. The waterline entrance angle seems not to affect the R_{AWR}. Flare angle is of lower significance according to Pearson's correlation coefficient. But, as can be deducted from graphs, the relationship between flare angle and R_{AWR} also is not linear. The correlation between flare angle and R_{AWR} seems to be increasing with the increase of angle of attack (from head waves to quartering seas), while the correlation between the other design variables and R_{AWR} decreases from head seas to quartering seas.

Total resistance seems to be strongly connected with C_{WP}, stem profile and waterline entrance angle. Flare angle affects insignificantly the total resistance. The correlation between calm resistance and AR in % of calm resistance was low ($r = 0.19 \pm 0.09$, very weak positive correlation according to Evans, (1996)). It can be concluded that reduction in calm resistance will not always result in reduction of AR as % of calm resistance.

Behavior of EEDI is similar to behavior of total resistance: smaller C_{WP}, leadge stem profile, sharper waterline results in better EEDI. The possible reduction of EEDI exceeds 10% of required value. The possible optimized designs seem no to overcome the IMO's requirement for minimum propulsion power. This can be also observed for the requirement for minimum propulsion power according to SHOPERA. However it's obvious that this requirement creates a border for further EEDI reduction through hull optimization.

7.5   Optimization's Result

The optimization with GA revealed that for three cases there was one common solution. The particulars of solution can be observed in Table 7.5 and Table 7.6 and the relevant results in Table 7.7. Bow shape can be seen in Figure 7.25 and Figure 7.26. The last generation of each optimization can be found in Appendix G.
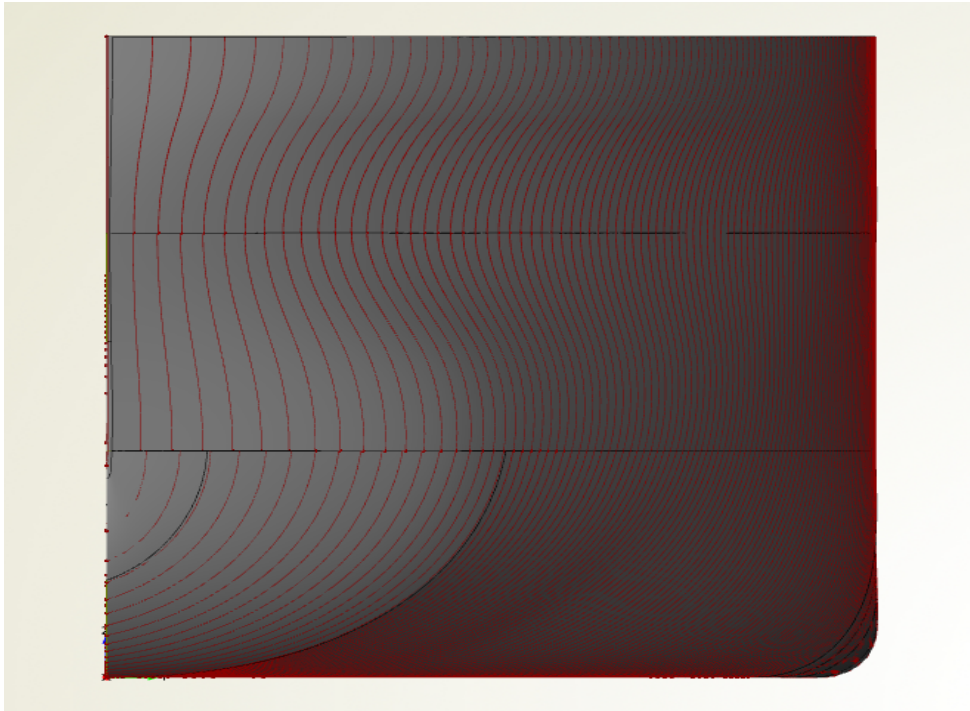
Figure 7.26: Bow of optimized ship.
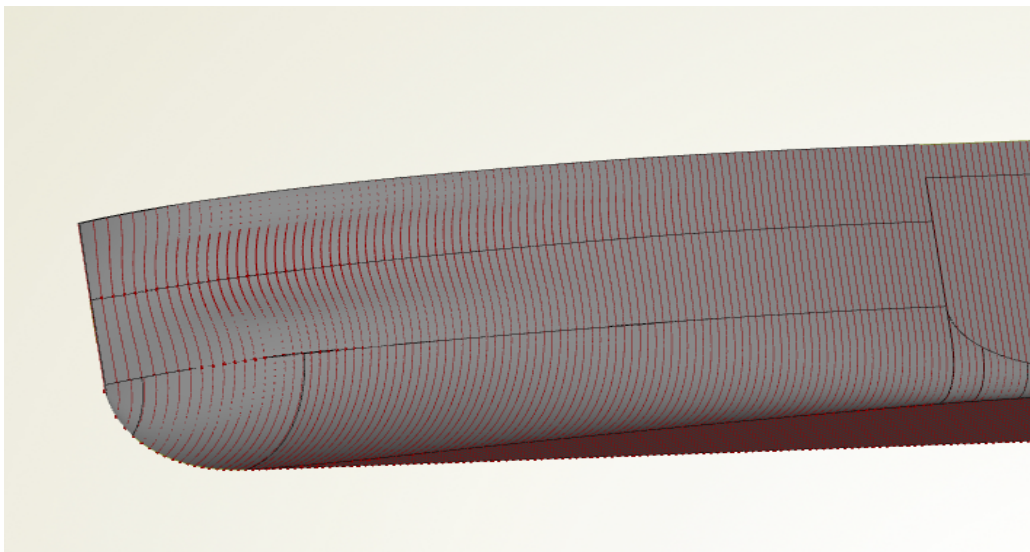
Figure 7.27: Bow of optimized ship.
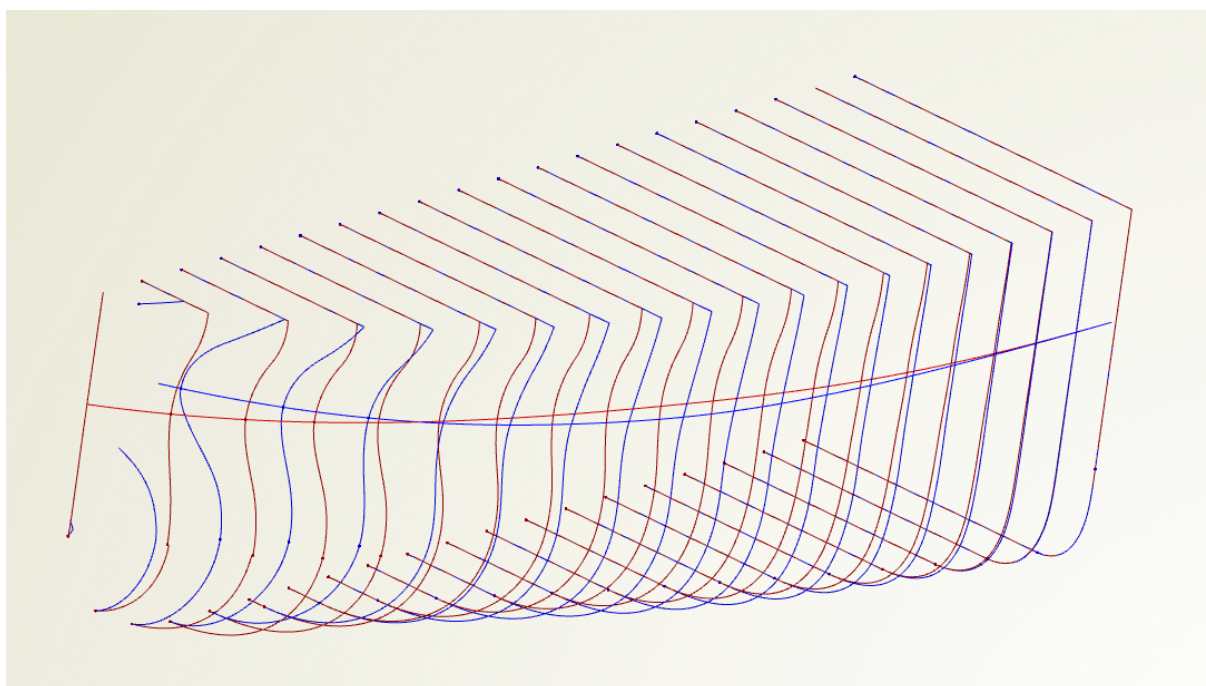
Figure 7.28: Comparison of bow shapes for initial (blue) and optimized (red) model.

Table 7.5: The particulars of optimized model.

L_{BP} [m]	328.00
B [m]	58.00
T_M [m]	20.80
LCB [% L_{BP} from midship]	1.82
C_B	0.7819
Displacement [m³]	309417
Wetted surface [m²]	27737

Table 7.6: The variables of optimized model.

Design variable	Min. Value	Optimized Model Value	Max. Value
Flare angle parameter	-1	0.99	0.99
Dx for 3rd and 4th waterline control point	-10	5	5
Dy for 3rd waterline control point	0	0	1
Waterline entrance angle	50°	50°	70°
Parameter for leadge bow	0	1	1

Table 7.8: Results for optimized model.

	Value	% Reduction comparing with BM
R_{AWR} for head waves [kN]	255	-35.44
R_{AWR} 20° angle of waves [kN]	300	-28.40
R_{AWR} 45° angle of waves [kN]	360	-17.62
Total Resistance [kN]	2543	-14.09
EEDI$_{attained}$	2.34	-11.70
EEDI$_{required}$	2.68	0.38
EEDI$_{attained}$/EEDI$_{required}$	0.8726	-12.12
MCR [MW]	24.24	-12.44
MCRmin (regression curves) [MW]	24.14	-0.25
MCRmin (SHOPERA) [MW]	24.73	-1.40
DWT [t]	278867	-0.31

The reduction in total resistance is mainly the result of reduction of bulb resistance (-201 kN), AR in waves (-140 kN) and change in form factor (-47 kN). It is obvious that this design is on borderline on passing the requirement for minimum MCR. It passes the IMO's regression curve, but fails to pass requirement proposed by SHOPERA

8   Conclusions

Through this work it was shown how important is the prediction of AR in waves and especially of the component due to wave diffraction. It was demonstrated that for large ships, such as KVLCC2, this component contributes much more than AR due to ship motions. Thus it's important to introduce this impact during ships bow optimization and holistic optimization.

Based on this concept, a number of variants of VLCC based on KVLCC2 were evaluated. It was shown that a small change in C_{WP} can significantly improve the AR due to waves. It was also shown that vertical wall design can improve the performance in waves in terms of added resistance for ships of such size. Also based on this research it was discovered that vertical stem is advantageous, because of sharpening the waterline, not only for better wave-breaking. All in all, leadge stem profile seems to be the more advantageous for R_{AWR}.

Also, it was proved that vertical stem and sharpening the waterline is beneficial for total resistance. This is in good agreement with experimental results (Lee et al. 2015).

It was also shown that such a design is better from EEDI perspective and can offer significant reduction in EEDI. However, it becomes obvious that hydrodynamic optimization is meeting the border of minimum power requirement. This makes obvious the necessity of new methods for evaluation of minimum power requirement, and designs, that except better EEDI retain adequate maneuverability in adverse conditions.

The future work would be to seek for new designs that compromise these two requirements. It would be also interesting to evaluate the total resistance by using more sophisticated tools, such as RANSE. Another aspect that could be improved in future work is the more correct prediction of sea margin, based on real sea route and more accurate estimation of propulsion coefficient. Another issue, that was neglected here and could be done in future research is introduction of variations in drafts and speeds. A more holistic approach would also take into account all the changes in ship design and the relevant impact on transferred cargo, trim, ships construction cost and required freight rate. It would be also interesting, to see what would be the results of such optimization process on ships with constrained dimensions such as a container ship or gas tanker.

9   References

http://www.engineeringtoolbox.com/fuels-higher-calorific-values-d_169.html   December 2015

http://encyclopedia2.thefreedictionary.com/stern+end+bulb December 2015

https://en.wikipedia.org/wiki/Computer-aided_design#2D.2F3D_modellingDecember 2015

https://en.wikipedia.org/wiki/Design_of_experiments December 2015

https://en.wikipedia.org/wiki/Genetic_algorithm December 2015

https://en.wikipedia.org/wiki/Mathematical_optimization#cite_note-1 December 2015

https://en.wikipedia.org/wiki/Pareto_efficiency#Weak_Pareto_efficiency December 2015

https://en.wikipedia.org/wiki/Sobol_sequence#cite_note-Sobol67-1 December 2015

http://www.mitrikitti.fi/opthist.html December 2015

http://www.natural-gas.com.au/about/references.html December 2015

http://www.ncss.com/wp-content/themes/ncss/pdf/Procedures/PASS/Pearsons_Correlation_Tests-Simulation.pdf
December 2015

https://www.nmri.go.jp/center_project/eedi_project_team/sub/eedi.html December 2015

http://passyworldofmathematics.com/mathematics-of-ships-at-sea/ December 2015

www.simman2008.dk/KVLCC/KVLCC2/kvlcc2_geometry.html December 2015

http://www.statstutor.ac.uk/resources/uploaded/pearsons.pdf December 2015

http://www.transport-research.info/project/ultra-slow-ships December 2015

Antonopoulos G. (2015). 'On the EEDI and minimum propulsion power: A case study on the interim guidelines for determining minimum propulsion power to maintain the maneuverability of ships in adverse conditions', Master thesis, National Technical University of Athens.

Alexandersson M. (2009). 'A study of methods to predict added resistance in waves', KTH Centre for Naval Architecture, Stockholm, Sweden.

Arsham   H.   (1994).   'Statistical   thinking   for   managerial   decisions', http://home.ubalt.edu/ntsbarsh/Business-stat/opre504.htm

Athanasoulis G.A., Belibasakis K.A.(2012). 'Ships dynamics', National Technical University Publications, Athens (available in Greek language).

Azcueta R. (2004). 'Steady and unsteady RANSE simulations for littoral combat ships', 25th Symposium on Naval Hydrodynamics, St. John's, Newfoundland and Labrador, Canada.

Bales S. (1982). 'Designing ships to the natural environment', 19th Technical Symposium, Association of scientists and engineers of the naval sea systems commands.

CAESES documentation (2015). CAESES documentation browser> Basics>Geometry

DNV GL (2013). 'Additional rules and guidelines – Energy Efficiency', Rules for classification and construction.

Evans JL (1996). 'Straightforward statistics for the behavioral sciences', Brooks/Cole Publishing Company.

Havelock T.H. (1940). 'The pressure of water waves upon a fixed obstacle', Proceedings of the Royal Society of London, Vol.175. A. pp 409-421

Havelock T.H. (1942). 'The drifting force on a ship among waves', The London, Edinburgh, and Dublin Philosophical Magazine and Journal of Science, Vol 33,Iss. 221 pp 467-475

Holtrop J. and Mennen G.G.J. (1982) 'An approximate power prediction method', International Shipbuilding Progress', Vol. 29 No.335

Holland J. (1975). ' Adaptation in natural and artificial systems', MIT PRESS.

Hollenbach I. (1999). 'Estimating resistance and propulsion for single-screw and twin-screw ships in the preliminary design', 10th International conference on computer applications in shipbuilding, 7-11 June 1999.

Hu Changhong, Takashi Mikami, Koutaku Yamamoto (2014). 'Prediction of added resistance in short waves by CFD simulation', 29th Intl. Workshop on water waves and floating bodies, Osaka, Japan.

Fraser A. (1957). 'Simulation of genetic systems by automatic digital computers I Introduction', Aust. J. Biol. Sci. 10: 484-491

Graham H. (2015). 'Correlation interpretation handout', Research Skills One Internet page

Grin R. (2015). 'On the prediction of wave added resistance with empirical methods', Maritime Research Institute Netherlands (Marin), Wagenigen, The Netherlands.

Guo B., Steen S. (2011), 'Evaluation of Added Resistance of KVLCC2 in Short Waves', Journal of Hydrodynamics 23(6):709-722, Elsevier Publishers.

IMO (2009). 'Second IMO GHG Study 2009'

IMO MEPC 64/4/13, "Consideration of the Energy Efficiency Design Index for new ships – Minumum propulsion power to maintain the maneuverability in adverse conditions", submitted by IACS, BIMCO, INTERCARGO, INTERTANKO and OCIMF, 2012.

IMO MEPC 64/INF.7, "Background information to document MEPC 64/4/13", submitted by IACS, 2012

IMO MEPC.1 Circ. 796 (2012). "Interim Guidelines for the Calculation of the coefficient fw for decrease in ship speed in a representative sea condtion for trial use".

International Marine Coatings (2004), 'Hull roughness penalty calculator',

ITTC, (2012), 'Recommended Procedures and Guidelines, Speed and Power Trials, Part 2 Analysis of Speed/PowerTrial Data', 7.5-04 -01 -01.2, Effective Date 2012, Revision 00

ITTC, (2008), 'Recommended Procedures and Guidelines, Testing and Extrapolation Methods, Propulsion, Performance, Predicting Powering Margin', Analysis of Speed/PowerTrial Data', 7.5-04 -01 -01.2, Effective Date 2008, Revision 01

Jinkine V. ,Ferdinande V. (1974). 'A method for predicting the added resistance of fast cargo ships in head waves', International Shipbuilding Progress, Vol 21, No 238

Journée J.M.J. and Pinkster J. (2002), 'Introduction to ship hydrodynamics', Delft University of Technology, Delft, Holland

Kaklis P. D. (2011). 'CAD/CAM systems for design and construction of ships', National Technical University Publications, Athens (available in Greek language).

Karafiath G. (2011). 'Stern end bulb for energy enhancement and speed improvement', 11th International Conference on Fast Sea Tansportation FAST, Honolulu, Hawaii, USA.

Kawabuchi M., Kawakita C., Mizokami S., Higasa S., Kodan Y., Takano S. (2011). 'CFD Predictions of Bubbly Flow around an Energy-saving Ship with Mitsubishi Air Lubrication System', Mitsubishi Heavy Industries Technical Review, Vol. 48 No. 1

Lee J., Park DM. , Kim Y., (2015), 'Experimental study on the added resistance of modified KVLCC2 hull forms with different bow shapes', Journal of Engineering for the Maritime Environment

Liu S. and Papanikolaou A. (2015). 'Fast approach to the estimation of added resistance of ships in head waves', Ocean Engineering, Vol. 112. pp. 211-225, DOI: 10.1016/j.oceaneng.2015.12.022.

Liu S., Papanikolaou A. and Zaraphonitis G. (2015). 'Practical approach to the added resistance of a ship in short waves', Proc. 25th International Ocean and Polar Engineering Conference, Kona, Hawaii, USA.

Liu S., Papanikolaou A. and Zaraphonitis G. (2011). 'Prediction of added resistance of ships in waves', Ocean Engineering, **38**(2011) 641-650.

Loyd's Register (2008). 'Container Ship Focus'

Makris D. (2015). 'Parametric modeling and optimization of hydrodynamic performance of Ro-Ro ship', Master thesis, National Technical University of Athens. (Available in Greek)

Malhotra R., Singh N. & Singh Y. (2011). 'Genetic Algorithms: Concepts, Design for Optimization of Process Controllers', Computer and Information Science Vol. 4, No. 2

MAN, (2013). 'Propulsion trends in tankers', MAN Diesel & Turbo.

Matulja D., Sportelli M., Guedos Soares C., Prpic-Orsic J. (2011). 'Estimation of added resistance of a ship in regular waves', Brodo Gradnja, **62**(2011)3, 259-26

Mitchell, M. (1996). 'An introduction to genetic algorithms, MIT Press, Cambridge.

Nabergoi R., Prpic-Orsic (2007). 'A Comparison of different methods for added resistance prediction', 22nd IWWWFB, Plitvice, Croatia.

Narayan L., Mallikarjuna R., Sarcar M. (2008). 'Computer Aided Design and Manufacturing', Prentice Hall of India, New Delhi.

Nowacki (2010). 'Five decades of computer-aided ship design', Computer-aided design , 42(11):956

Papanikolaou A., Zaraphonitis G., Bitner-Gregersen E. & Shigunov V., Moctar O. El, Guedes Soares C., Reddy D.N. Sprenger F. (2015), 'Energy efficient safe ship operation (SHOPERA)', 12th International Marine Design Conference IMDC2015, Tokyo, Japan.

Papanikolaou A. (2009), 'Holistic Ship Design Optimization', Computer-Aided Design (42):1028 – 1044, Elsevier Publishers.

Papanikolaou A.(2014). 'Ship Design : Methodologies of Preliminary Design.' Springer

Perez Arribas F. (2006). 'Some methods to obtain the added resistance of a ship advancing in waves', Ocean Engineering 34 (2007) 946 – 955

Price, W.G. and Bishop, R.E.D (1974). Probabilistic theory of ship Dynamics, Chapman and Hall Publications, London.

Politis G.K. (2011). 'Ships resistance', Notes of lecture "Ships resistance and propulsion", National Technical University of Athens Publications.

Priftis A. (2015). 'Parametric desing and multi-objective optimization of a 6,500 TEU container ship, Master thesis, National Technical University of Athens.

Psaraftis H. (2011), 'The economic and environmental dimensions of slow-steaming', Laboratory for Maritime Transport, School of Naval Architectuer and Marine Engineering, National Technical University of Athens, Athens, Greece.

Rebull M.S. (2014). 'Powering a vessel in a seaway', Universitat Politècnica de Catalunya, Barcelona, Catalonia.

Sedgwick Ph. (2012). 'Pearson's correlation coefficient', Centre for Medical and Healthcare Education, St. George's, University of London, Tooting, London, UK

Schneekluth H., Bertram V. (1998). Ship design for efficiency and economy, 2nd ed. Butterworth Heinemann Publications.

Sobol I. (1967). 'Distribution of points in a cube and approximate evaluation of integrals', U.S.S.R Comput. Maths, Math. Phys. 7:86-112 (in English)

Soding H., Shigunov V., Schellin T.E., Moctar el Ould, Walter S. (2012). 'Computing added resistance in waves - rankine panel method vs RANSE method', Numerical Towing Tank Symposium , Duisburg, Germany

Wartsila (2015). 'Ship power business white paper VLCC propulsion'.

Wartsila (2014). 'Wartsila auxpac product guide', Wartsila Generating Sets.

Wiesman A. (2010). 'Slow steaming – a viable long-term option?', Wartsila Technical Journal, February 2010.

J. Willsher (2001). 'The effect of biocide free foul release systems on vessel performance', SHIP EFFICIENCY, 1st International Conference, Hamburg, October 8-9 , 2001

Zakaria N.M.G. and Baree M.S. (2007). 'Alternative methods on added resistance of ships in regular head waves', The Institution of Engineers**69**(4)

Appendix A Annual Sea States For Evaluation Of AR Due To Waves In North Atlantic

Table A.1: Annual sea states occurrences in the open ocean North Atlantic. (Bales, 1982)

Sea State Number	Significant Wave Height (m) Hs_i		Percentage Probability of Sea State	Modal Wave Period (s) Tp_i	
	Range	Mean		Range	Mean
0 - 1	0- 0.1	0.05	0	-	-
2	0.1-0.5	0.3	7.2	3.3 -12.8	7.5
3	0.5-1.25	0.88	22.4	5.0-14.8	7.5
4	1.25-2.5	1.88	28.7	6.1-15.2	8.8
5	2.5 – 4	3.25	15.5	8.3-15.5	9.7
6	4 – 6	5	18.7	9.8-16.2	12.4
7	6 – 9	7.5	6.1	11.8-18.5	15
8	9 – 14	11.5	1.2	14.2-18.6	16.4
>8	>14	>14	<0.05	18.0-23.7	20

The AR is calculated as following

$$AR = \sum AR_i * p_i \qquad (A.1)$$

$$AR_i = 2 \int \frac{S_i(\omega)}{\zeta_\alpha^2} * (R_{AWR}(\omega) + R_{AWM}(\omega)) d\omega \qquad (A.2)$$

Where:

- AR_i is AR for every spectrum $S_i(\omega)$

- p_i is probability of each spectrum $S_i(\omega)$

- R_{AWR} and R_{AWM} are calculated using Liu et al simplified formula.

The spectrum $S_i(\omega)$ is calculated as following:

$$Si(\omega) = \frac{5}{16} Hs_i \frac{\omega_{pi}^4}{\omega^5} \exp\left(-\frac{5}{4}\left(\frac{\omega}{\omega_{pi}}\right)^{-4}\right) \qquad (A.3)$$

Appendix B Calculation Of AR Due To Waves

The AR due to waves is decomposed into two parts:

$$AR = R_{AWR} + R_{AWM} \qquad (B.1)$$

Calculation of R_{AWR}

R_{AWR} is calculated as following:

$$R_{AWR}(a) = 2 \int \frac{S_{(\omega)}}{\zeta_a^2} * R_{AWR}(\omega, a) d\omega \qquad (B.2)$$

The $R_{AWR}(\omega)$ for different headings and wave frequency is calculated according to Liu et al (2015) as

$$R_{AWR}(\omega) = \int_L \vec{F}_n \sin\theta \, dl \qquad (B.3)$$

where L is non-shadowed region as can be seen in Figure C.1

The F_n of each segment is calculated as:

$$\vec{F}_n = \frac{1}{2} \rho g \zeta_a^2 sec\, \alpha_{WL} \alpha_d \left(\frac{0.87}{C_B}\right)^{cos\alpha(1+n\sqrt{Fn})} \left\{ \sin^2(\theta+\alpha) + \frac{2\omega U}{g}[1 - cos\theta \cos(\theta+\alpha)] \right\}$$

$$(B.4)$$

where:

$$a_d = \frac{\pi^2 I_1(k_e d)}{\pi^2 I_1(k_e d) + K_1^2(k_e d)} \qquad (B.5)$$

$$k_e = \frac{\omega_e^2}{g} \qquad (B.6)$$

$$\omega_e = \omega + \frac{\omega^2}{g} V \cos(a) \qquad (B.7)$$

Here α_{WL} is flare angle as defined in Figure C.2, d=min[$T_M *cos\alpha_{WL}$, d(x)], α is heading angle (α=0 for head waves). The n factor is selected 4 to match experimental data. I_1 and K_1 are modified Bessel functions of first order and of first and second kind respectively, ω wave frequency.
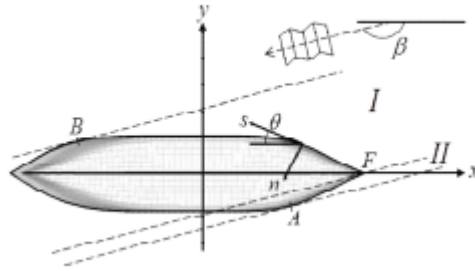
Figure B.1: The integration region according to method of Liu et al (2015)
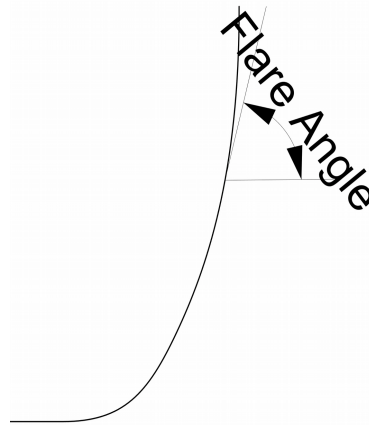
Figure B.2: Definition of flare angle

Calculation of R_{AWR} (simplified method)

$$R_{AWR} = \frac{2.25}{2} \rho\, g\, B\, \zeta_\alpha^2\, a_d \sin^2 E \left(1 + 5\sqrt{\frac{L_{pp}}{\lambda}}\, Fn\right) \left(\frac{0.87}{C_B}\right)^{1+4\sqrt{Fn}}$$ (B.8)

where:

$$E = atan\left(\frac{B}{2\,L_E}\right)$$ (B.9)

L_E is length of entrance of waterline, a_d is defined as in C.5.

Calculation of R_AWM

R_AWM is calculated as following:

$$R_{AWM} = 2 \int \frac{S_{(\omega)}}{\zeta_\alpha^2} * R_{AWM}(\omega) d\omega \tag{B.10}$$

The $R_{AWM}(\omega)$ for different headings and wave frequency is calculated according to Liu et al (2015) as:

$$R_{AWM} = 4\rho g \zeta_\alpha^2 B^2 / L_{pp} \bar{\omega}^{b1} \exp\left[\frac{b_1}{d_1}(1-\bar{\omega}_1^d)\right] a_1 a_2 \tag{B.11}$$

where:

$$a_1 = 60.3 \, C_B^{1.34} \left(\frac{0.87}{C_B}\right)^{(1+Fn)} \tag{B.12}$$

$$\alpha_2 = \begin{cases} 0.0072 + 0.1676Fn & for \, Fn < 0.12 \\ Fn^{1.5} \exp(-3.5Fn) & for \, Fn \geq 0.12 \end{cases} \tag{B.13}$$

$$\bar{\omega} = \begin{cases} \dfrac{\sqrt{\dfrac{L_{pp}}{g}} \sqrt[3]{k_{yy}}}{1.17} 0.05^{0.143} \omega & for \, Fn < 0.05 \\ \dfrac{\sqrt{\dfrac{L_{pp}}{g}} \sqrt[3]{k_{yy}}}{1.17} Fn^{0.143} \omega & for \, Fn \geq 0.05 \end{cases} \tag{B.14}$$

For $C_B \leq 0.75$

$$b_1 = \begin{cases} 11.0 & for \, \bar{\omega} < 1 \\ -8.5 & elsewhere \end{cases} \tag{B.15}$$

$$d_1 = \begin{cases} 14.0 & for \, \bar{\omega} < 1 \\ -566\left(\dfrac{L_{pp}}{B}\right)^{-2.66} * 6 & elsewhere \end{cases} \tag{B.16}$$

For $C_B > 0.75$

$$b_1 = \begin{cases} 11.0 & for \, \bar{\omega} < 1 \\ -8.5 & elsewhere \end{cases} \tag{B.17}$$

$$d_1 = \begin{cases} 566\left(\dfrac{L}{B}\right)^{-2.66} & for \, \bar{\omega} < 1 \\ -566\left(\dfrac{L_{pp}}{B}\right)^{-2.66} * 6 & elsewhere \end{cases} \tag{B.18}$$

Appendix C Calculation Of AR Due To Wind

AR due to wind is calculated according to IMO guidelines and ITTC guidelines as following:

$$AR_{winds} = \frac{1}{2} \rho_\alpha A_T C_{Dwind} V_{rel}^2 \qquad (C.1)$$

ρ_α : Air density 1.226 (kg/m^3)

A_T: Projected transverse area above the designated load condition

C_{Dwind}: Drag coefficient due to wind

Vrel: Relative wind speed

$$Vrel = U_{wind} + U_{ship} \qquad (C.2)$$

The drag coefficient is calculated as following (IMO MEPC.1 Circ. 796):

$$C_{Dwind} = 0.922 - 0.507 \frac{A_L}{L_{OA} B} - 1.162 \frac{C}{L_{OA}} \qquad (C.3)$$

Where:

A_L : Projected lateral area above the designated load condition

L_{OA}: Length overall

B: Beam of ship

C: Distance from the midship section to the center of the projected lateral area (A_L); a positive value of C means that the center of the projected lateral area is located ahead of the midship section

Appendix D Calculation Of AR Due To Fouling

According to Willsher (2001), increase in resistance due to fouling can be calculated as following:

$$\Delta R / R = 0.044 \left[(k_2 / L)^{1/3} - (k_1 / L)^{1/3} \right] / C_T \tag{D.1}$$

where:

- L is L_{BP}

- k_1 is initial roughness in μm

- k_2 is final roughness in μm

The other symbols are defined in nomenclature.

C_T can be approximated (Willsher, 2001):

$$C_T = 0.018 L^{-1/3} \tag{D.2}$$

So the increase in resistance can be approximated as

$$\Delta R / R = 0.044 \left[(k_2 / L)^{1/3} - (k_1 / L)^{1/3} \right] / C_T = 0.044 \left[(k_2 / L)^{1/3} - (k_1 / L)^{1/3} \right] / 0.018 L^{-1/3}$$
$$0.044 / 0.018 \left[(k_2^{1/3} - k_1^{1/3}) \right] = 2.4444 \left[(k_2^{1/3} - k_1^{1/3}) \right]$$

$$\tag{D.3}$$

The roughness for new building is 120μm (International Marine Coatings, 2004). According to Willsher (2001), for traditional antifoulings the increase in roughness is 40 μm/year, so in 5 years the increase in roughness will be 200μm, so the final roughness will be 320 μm.

By applying E.3, the increase in calm water resistance in 5 years will be 4.6 or roughly 5%

Appendix E Criteria For Minimum Propulsion Power In Adverse Conditions

According to MEPC 68/WP.9-Annex 6 the required minimum propulsion power for tankers is calculated as :

$$MCR_{min} = 0.0652 * DWT + 5960.2 \quad [kW] \tag{E.1}$$

By using the way developed by V.Shigunov (2015) during SHOPERA project the minimum required power is defined by taking the maximum of the following:

1 Position-Keeping in Extreme Seaway

$$MCR_{req} = r \frac{n_{MCR}^2 K_{Q0} D_p^3}{\sqrt{K_{T0}} \sqrt{1-t}} \sqrt{(0.5 \rho_A A_T v_W^2 + 83 L_{pp} C_B^{1.5} h_s^2)} \quad [kW] \tag{E.2}$$

where:

- h_s : Significant wave height [m]
- L_{pp}: Length between perpendiculars [m]
- C_B: Block coefficient
- A_T: Transverse projected windage area [m^2]
- D_p: Propeller diameter [m]
- t: Thrust deduction
- K_{T0}: Thrust coefficient at bollard pull
- K_{Q0}: Torque coefficient at bollard pull
- n_{MCR}: Rotation speed at MCR [s^{-1}]
- v_W: Wind speed, where wind speed is estimated as:
$$v_W = 4.636 h_s^{0.7} \tag{E.3}$$
- r is empirical constant (r=220)

2 Propulsion Capacity in Coastal Areas

$$MCR_{req} = p \frac{n_{MCR}^2 K_{Q0} D_p^3}{\sqrt{K_{T0}} \sqrt{1-t}} \sqrt{(0.5 C_F \rho U^2 S + 0.5 \rho_A A_T (U + v_W)^2 + 83 L_{pp} C_B^{1.5} h_s^2 (1 + \sqrt{Fr}))} \quad [kW]$$

$$\tag{E.4}$$

where:

- C_F: Coefficient of frictional resistance according to ITTC-1957 friction formula
- ρ: Sea water density [kg/m^3]
- U: Ships speed [m/s]
- S: Wetted surface of ship [m^2]
- Fr: Froude number
- v_W: Wind speed, where wind speed is estimated as:

$$v_W = 3.2_s \qquad \text{(E.5)}$$

- p is empirical constant (r=200)

All the other symbols are defined as in position-keeping in extreme seaway.

3 Steering Capacity in Coastal Areas

3.1 Söding-ONR model:

$$MCR_{req} = d_1 \, coeff_1 \, h_s \quad [kW] \qquad \text{(E.6)}$$

3.2 Söding-Brix model:

$$MCR_{req} = q_2 \, coeff_1 \, h_s \sqrt{Ap/(C_L A_R^s)} \quad [kW] \qquad \text{(E.7)}$$

where:

$$coeff_1 = n_{MCR}^2 \, D_p^3 \sqrt{(8 \, \rho_A A_L + C_B^{1.5} L_{pp}^{2.13})} \qquad \text{(E.8)}$$

- d_1 is empirical constant (d_1=7.5)
- q_2 is empirical constant (q_2=8.0)
- A_p: Propeller area [m^2]
- C_L: Maximum rudder lift coefficient
- A_R^S: Rudder in propeller race [m^2]

Appendix F Pearson's Product-Moment Correlation Coefficient

The Pearson's product-moment correlation coefficient or simply Pearson's correlation coefficient is a statistical measure of the strength of a linear relationship between two variables X and Y, giving a value between +1 and -1 inclusive, where 1 is total positive correlation, 0 is no correlation, and -1 is total negative correlation. (Sedgwick, 2012).

The formula for Pearson's correlation coefficient is as following:

$$r = \frac{C_{XY}}{\sqrt{C_{xx}C_{yy}}} = \frac{C_{XY}}{\sigma_X \sigma_Y} \tag{F.1}$$

$$\bar{x} = \frac{1}{N} \sum_i x_i \tag{F.2}$$

$$\bar{y} = \frac{1}{N} \sum_i y_i \tag{F.3}$$

$$C_{XY} = \frac{1}{N-1} \sum_i (x_i - \bar{x})(y_i - \bar{y}) \tag{F.4}$$

$$C_{XX} = \sigma_X^2 = \frac{1}{N-1} \sum_i (x_i - \bar{x})^2 \tag{F.5}$$

$$C_{YY} = \sigma_Y^2 = \frac{1}{N-1} \sum_i (y_i - \bar{y})^2 \tag{F.6}$$

where xi, yi are two sets of data of variables X and Y and N is number of data points in each set of data.

The proper use of Pearson' correlation coefficient requires the following data assumptions (Statstutor, 2015):

- Interval or ratio level
- linearly related
- bivariate normally distributed

The first one is satisfied, since all the measurements are ratio level data sets, like most of the measurements in physical and engineering science. The second assumption is checked by observing the relationship between variables in graphs. The last assumption is not satisfied by data sets of design variables, since Sobol functions create uniformly distributed design variables. However the results here are used for descriptive statistics, or in other words, to provide simple summary about the samples and not to learn about population, as in inferential statistics. That's why distributional assumption can be neglected. That's also a proposal of NCSS in PASS documentation for use of Pearson's correlation coefficient (NCSS, 2015).

The calculation of Pearson's correlation coefficient is sensitive to size of sample. In Table F.1 it can be seen that, if two data sets are not correlated, limits within which 80% of sample Pearson's correlation coefficients will fall, decreases with sample size.

Table F.1: Limits within which 80% of sample Pearson's correlation coefficient will fall, when the true correlation is 0 (Graham, 2015)

Sample Size	80% limits for r
5	-0.69 to +0.69
15	-0.35 to +0.35
25	-0.26 to +0.26
50	-0.18 to +0.18
100	-0.13 to +0.13
200	-0.09to +0.09

Correlation can be verbally characterized according to Evans (1996) as:
- 0.00-0.19 "very weak"
- 0.20-.39 "weak"
- 0.40-0.59 "moderate"
- 0.60-0.79 "strong"
- 0.80-1.00 "very strong"

Also depending on the sign of Pearson's coefficient it is characterized as positive or negative. For example a correlation value of 0.42 would be a "moderate positive correlation".

According to Arsham (1994): "To express the accuracy of the estimates of population characteristics, one must also compute the standard errors of the estimates. These are measures of accuracy that determine the possible errors arising from the fact that the estimates are based on random samples from the entire population, and not on a complete population census. "

The standard error of a correlation coefficient is computed as following:

$$SE_r = \frac{\sqrt{1-r^2}}{\sqrt{N-2}}$$

(F.7)

Where r is Pearson's correlation coefficient and N is sample size.

So the calculated Pearson's correlation coefficient is expressed as following:

$$r \pm SE_r$$

Appendix G Last Generation Of Optimization

Table G.1: Results for R_{AWR} in head waves.

	Parameter for leadge bow	Waterline entrance angle	Flare angle parameter	Dx for 3rd and 4th control point of waterline	Dy for 3rd control point of waterline	RAWR [N]
Nsga2_05_des0287	0.9186389	51.458152	0.080645762	-9.8022431	0.82087434	273965.97
Nsga2_05_des0288	0.92796216	50.508125	0.32942992	-9.9166857	0.15877012	263494.27
Nsga2_05_des0289	0.93426413	50.469368	0.32964248	-9.9176013	0.068909743	262218.48
Nsga2_05_des0290	0.92643626	51.037919	0.32942992	-9.7992676	0.45967803	267805.69
Nsga2_05_des0291	0.93430991	50.517891	0.20723934	-9.9192035	0.15877012	263555.8
Nsga2_05_des0292	0.93377584	51.038224	0.32939956	-2.0677501	0.1314107	309472.17
Nsga2_05_des0293	0.91276417	50.520333	0.32967285	-9.8020142	0.096299687	264597.03
Nsga2_05_des0294	0.93382162	50.412909	0.32942992	-9.5676356	0.12755016	264207.58
Nsga2_05_des0295	0.93424887	50.937819	-0.66534234	-9.7992676	0.1509575	280671.57
Nsga2_05_des0296	0.89768826	50.208438	-0.043700771	-9.9146258	0.18916609	267480.84
Nsga2_05_des0297	0.92645151	51.408713	0.06515938	-9.9315633	0.84620432	272022.84
Nsga2_05_des0298	0.89671168	51.081865	0.31388281	-9.9292744	0.21260395	267478.37
Nsga2_05_des0299	0.90647745	51.409018	0.95374365	-9.8020142	0.28285649	267657.25
Nsga2_05_des0300	0.96942092	51.077592	0.20708751	-9.916228	0.81324483	268360.4
Nsga2_05_des0301	0.91233692	50.184024	0.46935393	-9.7690547	0.42476539	266764.93
Nsga2_05_des0302	0.99975586	50.520638	0.33134295	-7.894255	0.065003433	267895.33
Nsga2_05_des0303	0.91227588	50.76997	0.71835065	-9.5676356	0.42659648	268434.72
Nsga2_05_des0304	0.99681086	50.471504	0.32942992	-9.8834974	0.19807736	259823.35
Nsga2_05_des0305	0.92796216	50.940871	0.32942992	-9.9439231	0.19502556	264604.93
Nsga2_05_des0306	0.92790112	52.268406	0.32942992	-9.4156558	0.066971847	269118.91
Nsga2_05_des0307	0.90647745	50.476387	0.32942992	-9.9182879	0.19417105	265630.68
Nsga2_05_des0308	0.99955749	50.488594	0.34497704	-9.7690547	0.40877394	261978.00
Nsga2_05_des0309	0.93430991	51.062943	0.70474693	-9.9164569	0.17463951	263375.43
Nsga2_05_des0310	0.99632258	50.530709	0.32942992	-9.9448386	0.23793393	260026.2
Nsga2_05_des0311	0.90696574	51.020218	0.71859358	-9.7663081	0.88558785	272470.46
Nsga2_05_des0312	0.42648966	50.468757	0.32942992	-9.9164569	0.17439536	285380.4
Nsga2_05_des0313	0.93621729	50.161135	0.45584131	-9.916228	0.90882734	268245.32
Nsga2_05_des0314	0.97534142	51.077287	0.32939956	-6.0487526	0.81525902	286585.61
Nsga2_05_des0315	0.93430991	50.469062	0.45404974	-9.9146258	0.15877012	262570.1
Nsga2_05_des0316	0.93426413	51.143206	0.083074998	-9.8022431	0.81696803	271716.88
Nsga2_05_des0317	0.90647745	50.456855	0.32942992	-9.8020142	0.29848173	267022.39
Nsga2_05_des0318	0.92840467	50.161135	0.45584131	-9.916228	0.56897841	265794.82
Nsga2_05_des0319	0.92791638	50.471809	0.32939956	-9.9166857	0.42438392	265678.85

Table G.2: Results for R$_{AWR}$ (20°).

	Parameter for leadge bow	Waterline entrance angle	Flare angle parameter	Dx for 3rd and 4th control point of waterline	Dy for 3rd control point of waterline	RAWR [kN]
Nsga2_04_des0287	0.99273671	50.7953	0.3149456	-8.5214008	0.20764477	310.40495
Nsga2_04_des0288	0.91276417	50.661021	0.82994369	-9.9757382	0.1912871	308.18978
Nsga2_04_des0289	0.98699931	60.661173	0.44302708	-8.5726711	0.082703899	320.72089
Nsga2_04_des0290	0.99284352	50.800183	0.48547799	-9.9922179	0.48914321	306.63939
Nsga2_04_des0291	0.98492409	50.222782	0.22142	-9.9313344	0.19006638	304.52982
Nsga2_04_des0292	0.9850309	50.833143	0.48620676	-9.9913024	0.48719005	306.38135
Nsga2_04_des0293	0.74285496	50.973526	0.22069123	-9.9272145	0.44226749	321.78154
Nsga2_04_des0294	0.96112001	50.06775	0.066191806	-9.988098	0.21570153	307.10855
Nsga2_04_des0295	0.98492409	52.223545	0.47041672	-9.978027	0.45764858	308.64052
Nsga2_04_des0296	0.96942092	51.423972	0.23016526	-9.9913024	0.43225757	309.81161
Nsga2_04_des0297	0.99273671	50.06775	0.22069123	-9.6209659	0.19008164	305.7203
Nsga2_04_des0298	0.9693904	60.661784	0.23016526	-9.7367819	0.20764477	319.06053
Nsga2_04_des0299	0.96942092	50.740368	0.23016526	-9.8539712	0.23889525	307.74611
Nsga2_04_des0300	0.9918822	50.643931	0.22166293	-9.9766537	0.31531243	306.32959
Nsga2_04_des0301	0.9918822	50.662242	0.22044831	-9.9709316	0.44031434	307.28542
Nsga2_04_des0302	0.97723354	53.176928	0.68686168	-9.9862669	0.18835737	309.05309
Nsga2_04_des0303	0.90691997	51.013809	0.48790723	-9.8539712	0.20788891	311.04675
Nsga2_04_des0304	0.99285878	51.316548	0.47041672	-9.9858091	0.20788891	305.61263
Nsga2_04_des0305	0.96929885	51.01503	0.22044831	-9.978027	0.20764477	308.13644
Nsga2_04_des0306	0.99285878	50.66041	0.44302708	-8.5442893	0.080689708	309.17628
Nsga2_04_des0307	0.98699931	50.988174	0.22166293	-9.9913024	0.44226749	307.38673
Nsga2_04_des0308	0.96942092	50.662242	0.2206305	-9.9711604	0.45789273	308.78691
Nsga2_04_des0309	0.9918822	50.956435	0.22166293	-9.9775692	0.19031052	305.98488
Nsga2_04_des0310	0.99969482	51.013809	0.09728603	-9.9711604	0.20788891	306.64815
Nsga2_04_des0311	0.96940566	50.800183	0.22433509	-9.9917601	0.20776684	307.68306
Nsga2_04_des0312	0.95336843	55.641566	0.81123857	-9.9725338	0.70594339	317.15951
Nsga2_04_des0313	0.9918822	50.663462	0.22166293	-9.9180591	0.45008011	307.55254
Nsga2_04_des0314	0.9918822	50.995499	0.22166293	-9.9766537	0.44031434	307.84296
Nsga2_04_des0315	0.86688029	50.643931	0.22166293	-9.9766537	0.44031434	315.70443
Nsga2_04_des0316	0.98455787	50.653696	0.38102083	-9.8159762	0.20788891	305.14525
Nsga2_04_des0317	0.96844434	51.01503	0.096071412	-9.9913024	0.21570153	308.29586
Nsga2_04_des0318	0.96942092	50.662242	0.22044831	-9.9711604	0.20593576	307.52156
Nsga2_04_des0319	0.9918822	50.662242	0.22044831	-9.9709316	0.44226749	307.29947

Table G.3: Results for R$_{AWR}$ (45°).

	Parameter for leadge bow	Waterline entrance angle	Flare angle parameter	Dx for 3rd and 4th control point of waterline	Dy for 3rd control point of waterline	RAWR [kN]
Nsga2_03_des0287	0.91601434	51.424277	0.30040055	-9.3396658	0.29188983	366.90468
Nsga2_03_des0288	0.94407568	52.829938	0.44809812	-9.2169833	0.28383307	365.29558
Nsga2_03_des0289	0.9909514	50.047303	0.45198489	-9.5044633	0.28386358	362.70614
Nsga2_03_des0290	0.74094759	50.057069	0.44815885	-9.9214923	0.29948882	370.51105
Nsga2_03_des0291	0.96940566	50.009461	0.19202625	-9.0988785	0.25673304	365.62891
Nsga2_03_des0292	0.97143511	50.233768	0.64216373	-8.8688487	0.34656291	363.96492
Nsga2_03_des0293	0.9694667	52.577859	0.45587167	-8.5431449	0.41274128	365.34981
Nsga2_03_des0294	0.96894789	51.307088	0.22266499	-9.2169833	0.27235828	365.27112
Nsga2_03_des0295	0.97924773	53.310292	0.45587167	-8.5486381	0.28383307	363.60854
Nsga2_03_des0296	0.9931487	50.018006	0.20723934	-7.4005493	0.34633402	367.06442
Nsga2_03_des0297	0.94041352	52.548562	0.46364523	-7.582742	0.34657816	392.11539
Nsga2_03_des0298	0.98728923	50.057069	0.22266499	-9.2160678	0.77235065	365.59637
Nsga2_03_des0299	0.72802319	51.326619	0.2731931	-8.5493248	0.29187457	373.258
Nsga2_03_des0300	0.98692302	51.95285	0.067679713	-9.3900206	0.26063935	364.69506
Nsga2_03_des0301	0.98631266	50.232547	0.42489891	-8.3955138	0.29968719	364.12802
Nsga2_03_des0302	0.98728923	50.057069	0.21489143	-8.8352026	0.34657816	364.82499
Nsga2_03_des0303	0.98706035	50.233768	0.64240665	-9.2167544	0.8149691	363.65022
Nsga2_03_des0304	0.98701457	50.232853	0.21489143	-9.2233921	0.27235828	363.99993
Nsga2_03_des0305	0.97947662	51.307088	0.22266499	-9.2233921	0.36610971	364.85305
Nsga2_03_des0306	0.94401465	50.203555	0.2032311	-9.331426	0.28798352	366.25003
Nsga2_03_des0307	0.96948196	52.84947	0.43886702	-9.9713893	0.26820783	363.29655
Nsga2_03_des0308	0.96940566	50.019226	0.19202625	-9.333257	0.26845197	365.31227
Nsga2_03_des0309	0.98496986	50.222171	0.19205661	-9.8001831	0.27234302	363.33209
Nsga2_03_des0310	0.98631266	51.952544	0.30052201	-9.5161364	0.35437552	363.22589
Nsga2_03_des0311	0.93846036	52.504616	0.45599313	-9.3854429	0.28383307	364.33388
Nsga2_03_des0312	0.9694667	50.232853	0.22263462	-9.2133211	0.2723888	365.29792
Nsga2_03_des0313	0.85413901	53.924315	0.19205661	-6.0583658	0.27235828	403.41675
Nsga2_03_des0314	0.96942092	52.542153	0.20696605	-9.9482719	0.27197681	364.68629
Nsga2_03_des0315	0.97532616	50.351263	0.1915404	-9.4476997	0.33485924	365.75932
Nsga2_03_des0316	0.9694667	52.508278	0.19157076	-8.4882124	0.30360876	366.6106
Nsga2_03_des0317	0.97526513	50.361028	0.44812848	-9.9448386	0.2564889	362.78084
Nsga2_03_des0318	0.98496986	52.577859	0.19205661	-9.4806592	0.25282673	363.60568
Nsga2_03_des0319	0.9694667	50.232853	0.45587167	-8.3939117	0.2994583	365.81599

Table G.4: Results for total resistance.

	Parameter for leadge bow	Waterline entrance angle	Flare angle parameter	Dx for 3rd and 4th control point of waterline	Dy for 3rd control point of waterline	Total Resistance [kN]
Nsga2_04_des0287	0.88740368	50.169375	0.19928359	-9.3005264	0.34724956	2552.1136
Nsga2_04_des0288	0.88151369	50.520943	0.19773495	-9.2991531	0.49469749	2556.1123
Nsga2_04_des0289	0.78779278	50.169375	0.20851469	-9.3005264	0.34724956	2559.735
Nsga2_04_des0290	0.91865415	50.174258	0.19928359	-9.3005264	0.84725719	2557.3841
Nsga2_04_des0291	0.88838025	50.173953	0.013204089	-9.3005264	0.097062638	2549.5279
Nsga2_04_des0292	0.92060731	50.158999	0.39216495	-9.5056077	0.3510338	2549.0633
Nsga2_04_des0293	0.92106508	50.173953	0.20544778	-8.3630121	0.3472343	2558.3246
Nsga2_04_des0294	0.91087205	50.159304	0.43100237	-9.2977798	0.042542153	2546.7805
Nsga2_04_des0295	0.91102464	50.169375	0.2131606	-9.3005264	0.35506218	2551.4621
Nsga2_04_des0296	0.91105516	50.16907	0.08119234	-9.3060197	0.034729534	2548.0091
Nsga2_04_des0297	0.88935683	51.736477	0.30644327	-9.2996109	0.034729534	2555.8328
Nsga2_04_des0298	0.91862364	50.166629	0.20690532	-9.3005264	0.3472343	2551.3046
Nsga2_04_des0299	0.8820325	50.174258	0.2055996	-8.8390936	0.35115587	2555.9555
Nsga2_04_des0300	0.91912718	50.16907	0.18510292	-9.2991531	0.033752956	2547.4997
Nsga2_04_des0301	0.91276417	50.169375	0.72642786	-9.3078508	0.34724956	2549.8451
Nsga2_04_des0302	0.92059205	50.16907	0.20065003	-8.365301	0.034729534	2554.3649
Nsga2_04_des0303	0.91276417	50.173953	0.19913176	-9.3078508	0.037659266	2547.805
Nsga2_04_des0304	0.91862364	50.173953	0.20690532	-8.3703365	0.038635843	2554.4311
Nsga2_04_des0305	0.88151369	50.16907	0.19718837	-8.3987182	0.034729534	2555.342
Nsga2_04_des0306	0.92060731	50.173953	0.08119234	-9.3078508	0.097230488	2549.2261
Nsga2_04_des0307	0.92060731	50.174258	0.2055996	-6.4953079	0.28474861	2571.729
Nsga2_04_des0308	0.92057679	50.173953	0.20690532	-8.8390936	0.3472343	2554.7304
Nsga2_04_des0309	0.91914244	50.174258	0.2055996	-9.3078508	0.35115587	2551.328
Nsga2_04_des0310	0.91862364	50.208438	0.20052857	-9.2991531	0.28863966	2550.8146
Nsga2_04_des0311	0.66276036	52.517739	0.18370611	-8.3703365	0.041565576	2599.3561
Nsga2_04_des0312	0.91279469	50.213016	0.20061967	-9.3005264	0.34755474	2551.5749
Nsga2_04_des0313	0.88249027	50.16907	0.019003891	-9.3005264	0.038147555	2549.3577
Nsga2_04_des0314	0.87565423	50.213016	0.20544778	-9.3005264	0.11285573	2549.3262
Nsga2_04_des0315	0.91276417	50.208438	0.20065003	-9.2991531	0.41364157	2552.3943
Nsga2_04_des0316	0.92060731	50.174258	0.2055996	-8.3703365	0.34724956	2558.2829
Nsga2_04_des0317	0.91862364	50.173953	0.19913176	-9.3078508	0.038635843	2547.4753
Nsga2_04_des0318	0.92060731	50.174258	0.2055996	-9.3078508	0.34724956	2551.2387
Nsga2_04_des0319	0.92060731	51.424277	0.2055996	-9.3078508	0.35115587	2557.5166

Table G.5: Results for EEDI.

	Parameter for leadge bow	Waterline entrance angle	Flare angle parameter	Dx for 3rd and 4th control point of waterline	Dy for 3rd control point of waterline	EEDI ratio
Nsga2_03_des0287	0.99676509	52.068513	0.18777508	-9.8830396	0.25250629	0.87653131
Nsga2_03_des0288	0.84832532	51.433738	0.18182345	-8.8871595	0.5965362	0.88576444
Nsga2_03_des0289	0.99682612	50.818494	0.69402792	-9.7669947	0.36603342	0.87468733
Nsga2_03_des0290	0.97552453	50.305791	0.19542718	-8.4806592	0.48918898	0.87634637
Nsga2_03_des0291	0.98895247	50.183719	0.19542718	-8.8871595	0.86558328	0.87582072
Nsga2_03_des0292	0.7487602	51.521935	0.14274311	-9.8830396	0.4437171	0.8906495
Nsga2_03_des0293	0.99090562	50.027466	0.68916945	-8.8908217	0.47541009	0.87411267
Nsga2_03_des0294	0.99871824	50.164187	0.19639887	-8.8322271	0.86570535	0.87672131
Nsga2_03_des0295	0.97283894	50.266728	0.43640742	-8.8908217	0.11606012	0.8753882
Nsga2_03_des0296	0.93426413	50.164187	0.51511467	-8.9164569	0.94370947	0.87782108
Nsga2_03_des0297	0.99871824	51.511864	0.94174929	-9.7660792	0.94416724	0.87671269
Nsga2_03_des0298	0.99871824	50.183719	0.68916945	-8.8871595	0.44370184	0.87507954
Nsga2_03_des0299	0.98895247	50.183719	0.69293477	-8.8905928	0.44370184	0.87421722
Nsga2_03_des0300	0.99090562	50.213016	0.93391501	-8.8908217	0.44419013	0.87412751
Nsga2_03_des0301	0.98895247	50.177615	0.68904799	-8.8285649	0.86558328	0.87522043
Nsga2_03_des0302	0.99676509	50.193484	0.68904799	-8.8871595	0.44370184	0.87505058
Nsga2_03_des0303	0.99041733	50.25452	0.12935195	-9.7660792	0.47129015	0.87417831
Nsga2_03_des0304	0.99676509	50.183719	0.69305623	-8.8908217	0.44370184	0.87503086
Nsga2_03_des0305	0.99090562	50.164187	0.68904799	-8.8871595	0.86558328	0.87515261
Nsga2_03_des0306	0.99676509	50.208133	0.76508309	-8.9164569	0.94370947	0.87536252
Nsga2_03_des0307	0.99090562	51.746242	0.52191653	-8.8871595	0.60044251	0.87669999
Nsga2_03_des0308	0.99676509	50.193484	0.19639887	-9.0336461	0.48953994	0.87563334
Nsga2_03_des0309	0.9890135	50.300908	0.69269184	-8.8871595	0.86558328	0.87530289
Nsga2_03_des0310	0.99089036	51.434043	0.12950378	-8.9491875	0.44368658	0.87649225
Nsga2_03_des0311	0.99877928	50.183719	0.70240879	-9.8287938	0.44419013	0.87403122
Nsga2_03_des0312	0.99090562	51.770657	0.19178332	-8.8285649	0.44419013	0.87693746
Nsga2_03_des0313	0.99676509	50.176394	0.76678355	-9.8246738	0.59629206	0.87426106
Nsga2_03_des0314	0.99871824	50.183719	0.19603449	-9.8832685	0.85044633	0.87550482
Nsga2_03_des0315	0.99876402	51.443809	0.68519158	-9.7658503	0.47359426	0.8757542
Nsga2_03_des0316	0.99676509	50.16907	0.19542718	-8.8285649	0.36362249	0.87555885
Nsga2_03_des0317	0.99871824	50.193484	0.93452232	-8.8908217	0.86619364	0.87588317
Nsga2_03_des0318	0.98895247	50.206912	0.68516121	-8.8871595	0.86607156	0.87519338
Nsga2_03_des0319	0.99676509	50.193484	0.69293477	-8.8285649	0.86558328	0.87532555